UNIVERSITI TEKNOLOGI MARA

MOLECULAR INTERACTION STUDY OF DIMETHYL SULFOXIDE SOLVENT ON CELLULOSE AND POLYESTER DISSOLUTION FROM TEXTILE WASTE

NUR UMMUL WALIYYATULLAH
BINTI MUHAMMAD FAEZ TAN

MSc

July 2026

UNIVERSITI TEKNOLOGI MARA

MOLECULAR INTERACTION STUDY OF DIMETHYL SULFOXIDE SOLVENT ON CELLULOSE AND POLYESTER DISSOLUTION FROM TEXTILE WASTE

NUR UMMUL WALIYYATULLAH BINTI MUHAMMAD FAEZ TAN

Thesis submitted in fulfilment
of the requirements for the degree of
Master of Science
(Chemical Engineering)

Faculty of Chemical Engineering

July 2026

CONFIRMATION BY PANEL OF EXAMINERS

I certify that a Panel of Examiners has met on 18th June 2026 to conduct the final examination of Nur Ummul Waliyyatullah binti Muhammad Faez Tan on her Master of Science thesis thesis entitled "Molecular Interaction Study of Dimethyl Sulfoxide Solvent on Cellulose and Polyester Dissolution from Textile Waste" in accordance with Universiti Teknologi MARA Act 1976 (Akta173). The Panel of Examiners recommends that the student be awarded the relevant degree. The Panel of Examiners was as follows:

Atikah Kadri, PhD
Associate Professor
Faculty of Chemical Engineering
Universiti Teknologi MARA

Ahmad Ramli Rashidi, PhD
Senior Lecturer
Faculty of Chemical Engineering
Universiti Teknologi MARA
(Internal Examiner)

Nardiah Rizwana Jaafar, PhD
Senior Lecturer
Fakulti Kejuruteraan Kimia dan Kejuruteraan Tenaga
Universiti Teknologi Malaysia
(External Examiner)

PROFESSOR DR HJH ZURAEDA IBRAHIM
Dean
Institute of Postgraduates Studies
Universiti Teknologi MARA
Date: 9 July 2026

AUTHOR'S DECLARATION

I declare that the work in this thesis was carried out in accordance with the regulations of Universiti Teknologi MARA. It is original and is the result of my own work, unless otherwise indicated or acknowledged as referenced work. This thesis has not been submitted to any other academic institution or non-academic institution for any degree or qualification.

I hereby acknowledge that I have been supplied with the Academic Rules and Regulations for Postgraduate Studies at Universiti Teknologi MARA, which regulate the conduct of my study and research.

Name of Student	:	Nur Ummul Waliyyatullah binti Muhammad Faez Tan
Student ID. No.	:	2024451262
Programme	:	Master of Science (Chemical Engineering) – CEEH750
Faculty	:	Chemical Engineering
Thesis Title	:	Molecular Interaction Study of Dimethyl Sulfoxide Solvent on Cellulose and Polyester Dissolution from Textile Waste
Signature of Student	:	……..
Date	:	July 2026

ABSTRACT

Blended textile waste, such as polycotton (polyester and cotton), presents significant challenges to conventional textile recycling due to different physicochemical properties. Chemical recycling, particularly dissolution, is a method that highly promising strategy for selective fibre separation. However, most reported studies show that it highly depends on hazardous solvents and requires high energy input, which limits their environmental and economic feasibility. Since there are limited studies on the application of pure dimethyl sulfoxide (DMSO) as an alternative solvent for the selective dissolution of cotton from polycotton blends, marking this as a novel research area. Therefore, this study used an integrated computational and experimental framework to investigate the potential of using DMSO as a single solvent for fibre separation. Firstly, BIOVIA Material Studio 2023 were used to run molecular dynamics (MD) simulation to predict the intermolecular interactions between pure DMSO with cotton (cellulose) and polyester from textile waste. COMPASS force field was applied under NPT-NVT ensembles and paired with Andrensen-Berendsen thermostat to enable a reliable representation of molecular interaction. Next, the prediction was validated experimentally using a Taguchi L9 orthogonal array design for a precise result. Three main factors have been evaluated, which are temperature (50, 100, 150℃), concentration (4.5, 6.0, 7.5 mg/ml) and dissolution time (4, 6, 8 hours). The dissolution efficiency was evaluated using signal-to-noise (S/N) ratio analysis under the "larger the better" criterion and further assessed by analysis of variance (ANOVA). Lastly, the dissolved cotton was regenerated using water as an anti-solvent with a 1:10 ratio of cotton/DMSO to water method. Then, the quality of regenerated cotton and polyester fibre were analysed in terms of structural, thermal and morphological properties and compared to their respective pure fibres. Based on the results, MD simulation had predicted that cotton has stronger interactions with DMSO at 150℃ and 4.5mg/ml compared to polyester. These predictions were proven by the experimental process through dissolution. Based on the measured dissolution efficiency, cotton shows higher solubility in DMSO (~80%) compared to polyester (<20%). The final condition of Experiment E7 (150℃, 4.5 mg/ml, 8 hours) was the optimal combination in maximising dissolution performance of both cotton and polyester. In the meantime, S/N ratio and ANOVA analysis had confirmed that temperature is the most influential parameter affecting the dissolution process, as indicated by a p-value (<0.05) for both cotton (p=0.007) and polyester (p=0.043). These results show that solvent–polymer interactions and the dissolution performance of textile fibres in DMSO are significantly influenced by temperature. Finally, the characterisation shows result confirmed that both regenerated cotton and polyester fibres properties were similar to their respective pure fibres. For example, the FTIR spectrum exhibited a characteristic absorption band at 1427 cm^{-1} and 898 cm^{-1}. This peak is assigned to the crystalline regions of cellulose I and β-glycosidic linkages, typically related to the amorphous structure of cellulose, respectively. The calculated lateral order index (LOI) of the absorbance ratio A1427/A898 was 3.25. This value suggests a predominance of the cellulose II crystalline structure in the analysed sample. Overall, this study has proven the effectiveness of DMSO as a selective solvent for cotton separation from polycotton blends.

ACKNOWLEDGEMENT

In the name of Allah, the Most Merciful and Gracious. All praise is expressed to Allah, the King of all Kings, the Lord of the Worlds, and the Master of the Day of Judgment, and peace be upon Muhammad, His servant and messenger. Alhamdulillah.

First and foremost, I must acknowledge my limitless thanks to Allah, for the strength, health, wisdom, and stamina needed to complete this work were given by His kindness and mercy. Gratitude is expressed to Him for the gift of a loving family, dedicated supervisors, and supportive friends. Without it, this achievement would not have been possible.

The highest appreciation goes to my advisors, Dr Arbanah Muhammad, for her unwavering support and insightful critiques throughout my research journey. Her deep commitment to academic excellence and meticulous attention to detail have significantly shaped this dissertation. Sincere appreciation is extended to Ir. Dr Intan Suhada Azmi and Prof. Madya Ir. Dr Noor Fitrah Abu Bakar for their constructive feedback and essential suggestions that enhanced the quality of my work.

My appreciation goes to the Ministry of Higher Education through the Fundamental Research Grant Scheme (Grant No. FRGS/1/2024/TK09/UITM/02/15), managed by Universiti Teknologi MARA (600-RMC/FRGS 5/3 (118/2024) who provided the facilities and assistance during this. A heartfelt note of appreciation is also directed to the Faculty of Chemical Engineering, Universiti Teknologi MARA, Kampus Pasir Gudang. Their academic environment, technical assistance, and collegial spirit contributed meaningfully to the successful execution of this research.

I am also thankful for my best friends and the postgraduate community of UiTM Pasir Gudang, with meaningful moments, shared laughter, and encouragement when it seemed impossible to continue. The discussions and unwavering support from my peers at the university have enriched my research experience, making this journey not only possible but also enjoyable. Their presence and insights have been important in navigating the complexities of my research topic.

Finally, this thesis is dedicated to the loving memory of a beloved sister and to the family whose unwavering support has been a constant source of strength. My very dear late father (Muhammad Faez Tan) and mother ( ), this piece of victory is dedicated to both of you. Although you were unable to be here to see this accomplishment, it is dedicated to them with sincere appreciation and gratitude.

TABLE OF CONTENTS

LIST OF TABLES

LIST OF FIGURES

LIST OF ABBREVIATIONS

Abbreviations

ANOVA	Analysis of Variance
BE	Binding Energy
COMPASS	Condensed-phase Optimised Molecular Potential for Atomistic Simulation Studies
D	Diffusion Coefficient
DMSO	Dimethyl Sulfoxide
DSC	Differential Scanning Calorimetry
FTIR	Fourier-Transform Infrared Spectroscopy
IE	Interaction Energy
L9	Level 9
MD	Molecular Dynamic
MSD	Mean Square Displacement
PET	Polyethylene terephthalate or Polyester
RDF	Radial Distribution Function
ReC	Regenerated Cotton Fibre
ReM	Regenerated Cotton from Polycotton
S/N	Signal to Noise Ratio
SEM	Scanning Electron Microscopy
Tg	Glass Transition Temperature
XRD	X-ray Diffraction

CHAPTER 1
INTRODUCTION

1.1 Research Background

In the textile industry, polyester fibre contributes the most significant production, approximately 57%, while cotton contributes 28% [1]. This difference occurs because manufacturers widely use polyester in mass-produced clothing, as polyester does not easily break down. Current estimates on disposal of textile waste were 75% landfilled, 25% are recycled, and less than 1% are regenerated into new yarns, which highlights the lack of effective large-scale recycling systems [2]. The reliance on landfilling is attributed to the high cost and technological complexity of current textile recycling methods [3]. There are 2 common textile recycling which are mechanical and chemical recycling methods. Mechanical recycling has generally shown limited effectiveness when applied to blended textile materials. This limitation has led to growing interest in chemical recycling methods as alternative recovery routes. Solvent-based dissolution is a promising strategy for selective fibre separation while producing higher-quality regenerated fibres [4]. However, the process is mainly dependent on the hazardous solvents, requires higher energy, and demands high-quality polymer inputs [5].

To address this problem, the introduction of new solvent systems is needed, which can selectively interact with both synthetic and natural types of fibre without inducing degradation [6]. The selected solvent systems must exhibit minimal energy consumption, low toxicity, and recyclability. The suitable solvent system also needed to achieve a balanced combination of polarity, hydrogen-bonding capacity, and thermal stability. These properties are important to promote selective interactions and enable controlled dissolution behaviour. By understanding both fibre and solvent interaction behaviour, the development of safer and more efficient textile recycling methods can be achieved [7]. The effects of concentration, temperature, and dissolution time have been reported as significant factors that affect the dissolution behaviour of fibre and solvent [8]. As recorded by previous studies, most dissolution studies focus on the factors influencing solubility, including temperature, pressure, and dissolution time, to

achieve high yield and recovery [9]. However, the study was not conducted under optimised conditions.

There is a notable gap from previous studies regarding methodology dedicated to studying solvent interactions with recycled textiles. Hence, this research aimed to maximise the interaction between the fibre and solvent by investigating the fundamental mechanisms of molecular interactions [10]. The fundamental intermolecular forces must be systematically evaluated in order to clarify the polymer chain solvation and structural disruption. In this context, molecular dynamics (MD) simulation has been selected as a computational approach for providing a detailed description of the interaction mechanisms between recycled textile and selected solvents system [11]. MD simulation had the capabilities to facilitate the development of recycling strategies such as improving material recovery and process optimisation [12].

However, need to be noted that MD simulation outcomes require experimental validation to ensure its reliability and accuracy. The integration of computational modelling and optimization by experimental design allows the dissolution performance to be evaluated under controlled conditions. Analysis of variance (ANOVA) are a statistical tool that can determine the significance of operational factors, including temperature, solvent concentration, and dissolution time [13]. In the meantime, characterisation of regenerated fibres such as structural integrity and thermal stability is important to verify the material quality and reusability [14]. These analyses also enable the validation of predicted molecular interactions and provide a robust correlation between simulation and experimental observation on dissolution behaviour [15].

1.2 Problem Statement

The dissolution method is the most common in chemical recycling technologies. However, the process was challenging due to the different polymer characteristics [16]. It is because the dissolution process relies on hazardous solvents and requires high energy consumption to recycle, especially blended fabrics such as polycotton (mixture of polyester and cotton) [17], [18]. Currently, Dimethyl Sulfoxide (DMSO) is the most common chemical used as a co-solvent combined with Ionic Liquid (IL) such as 1-ethyl-3-methylimidazolium chloride ([EMIm]Cl) [19]. However, there are limited studies that use DMSO solvent as the main solvent in the dissolution process of cotton

and polyester. Hence, the prediction of molecular interaction between DMSO with cotton and polyester can be analyse by using Molecular Dynamics (MD) simulation. This can be done by analysing the complex intermolecular interactions, including hydrogen bonding, dipole–dipole forces, van der Waals interactions, and chain entanglement effects.

On the other hand, the molecular mobility, solvent diffusivity, and mass transfer equilibrium were influenced by variations in temperature, polymer concentration, and dissolution time. Poor optimisation can lead to poor dissolution, polymer degradation, and excessive energy consumption. Therefore, a structured optimisation strategy is needed to determine the optimum dissolution parameters that maximises efficiency while preventing polymer degradation and minimise operational cost. To solve this problem, the Taguchi L9 orthogonal array was used in this study to allow simultaneous comparison of 3 parameters (with 3 levels) within 9 experiments. This method validated the dissolution effectiveness by using the Signal-to-Noise (S/N) ratio with "larger-the-better" criterion and analysis of variance (ANOVA) [20]. In the context of polymer dissolution optimisation, higher S/N ratios indicate that the selected combination of parameters can continuously enhance dissolution performance while reducing resistance, such as inconsistent mixing or other noise factors [21].

Although the aim of the study is to produce high dissolution efficiency of recycled cotton and polyester textiles, the physical and chemical transformations of the polymer need to be analysed. Noted that the quality of regenerated fibre cannot be verified without a full evaluation that includes structural, thermal, and morphological analysis. Accordingly, systematic characterisation after dissolution is necessary to ensure process reliability, high mechanical performance, and durability of regenerated fibre. At this point, no published study has used this integrated modelling with experimental to study the dissolution process of cotton and polyester in pure DMSO.

1.3 Research Objective

The objectives of this study are:

a) To investigate the molecular interactions of cellulose and polyester with DMSO solvent through molecular dynamics simulations.

b) To identify the optimised dissolution parameters (temperature, concentration, and dissolution time) of cotton and polyester in the DMSO solvent.
c) To evaluate the physical and chemical structural transformations of dissolved and regenerated fibres that occur after dissolution in DMSO solvent.

1.4 Scope of Study

This study aims to explore the dissolution behaviour of recycled textile, specifically cotton and polyester, in dimethyl sulfoxide (DMSO). This is carried out by using a combination of computational simulations and laboratory experiments to provide a clearer observation into the molecular interactions involved in dissolution and improve recycling textile recovery methods. Firstly, the evaluation on the molecular-level interactions between cellulose and polyester polymers with DMSO using molecular dynamics (MD) simulations. In MD simulation, the recycled fibre was renamed as their repeating unit to avoid confusion. Hence, instead of being named as recycled cotton and polyester fibre, it will be represented by cellulose and polyethylene terephthalate (PET), respectively. All simulations were conducted using BIOVIA Materials Studio 2023 as it enabled the construction, optimisation, and dynamic analysis of polymer-solvent systems. The Amorphous Cell module was used to construct and pack the polymer chains and solvent molecules in a simulation box, while the Forcite module was applied for geometry optimisation and molecular dynamics simulation. The simulations were performed using the COMPASS force field, which is well-established for modelling polymeric systems due to its accuracy in representing both inter- and intramolecular interactions. To reflect experimental dissolution conditions, simulations were run under two thermodynamic ensembles: NVT (constant volume and temperature) and NPT (constant pressure and temperature), both incorporating Andersen thermostat and barostat to control system dynamics. A variety of simulation temperatures of 50℃, 100℃, and 150℃ and polymer concentrations of 4.5mg/ml, 6.0mg/ml and 7.5mg/ml were selected to represent experimental thermal conditions during dissolution. The number of repeating units will be adjusted according to different conditions.

Next, a systematic method based on the Taguchi L9 orthogonal array were implemented to validate the prediction of polymer-solvent behaviour. The efficiency of polyester and cotton fibres dissolve in DMSO is evaluated with three main factors, which are temperature (50, 100, and 150°C), polymer concentration (4.5, 6.0, and 7.5 mg/ml), and dissolution time (4, 6, and 8 hours). The factor levels were carefully chosen based on preliminary study results to ensure that the selected ranges were both practical and relevant to the dissolution process. The data were analysed using analysis of variance (ANOVA) to compare different levels at a confidence level of $p < 0.05$, with all tests carried out in Statistical Package for the Social Sciences (SPSS). The dissolution trial was repeated three times to ensure reliable results. The validation test was also performed under the best conditions selected to confirm the accuracy. As part of the sample preparation, a decolourisation step was introduced using 0.6 M sodium hypochlorite (NaOCl) to remove dye from fibre sample. One limitation has been highlighted during decolourisation step, where the synthetic residues might not fully be removed. This may cause the low purity of regenerated fibre in blended textile systems.

Finally, this study focused on the chemical integrity, thermal behaviour, morphology, and crystallinity of the regenerated fibre. UV–Vis and FTIR spectroscopy were applied to verify the preservation of functional groups and arrangement of chemical structures after high-temperature dissolution. Thermal transitions and material purity of the regenerated solid fibres were evaluated using TGA and DSC. Additionally, SEM was employed to investigate surface morphology, while XRD was used to determine changes in crystallinity. These techniques collectively provide a comprehensive understanding of the regeneration effectiveness. However, this study does not include mechanical property testing or long-term stability assessments, which may be necessary for evaluating the fibre's end-use performance in real-world applications.

1.5 Significance Contributions of the Study

The contributions of this study are:

a) Provide an explanation of the molecular interaction mechanism between cellulose and polyester with DMSO solvent through molecular dynamic

simulations. Analysis of intermolecular interactions such as hydrogen bonding, dipole–dipole interactions, and solvation behaviour, allowed the clarification of atomic scale dissolution mechanism.

b) Present the optimised dissolution parameters, including temperature, concentration, and dissolution time of cotton and polyester in the DMSO solvent. Statistical evaluation, such as ANOVA, were help in determining the significance and contribution of each factor.

c) The comparison on characteristic of regenerated cellulose and polyester was highlighted, including structural, thermal, and morphological. Changes in crystallinity, molecular arrangement, and functional group integrity were determining the rearranging of polymer chains and changes in thermal stability during dissolution and regeneration after the dissolution in DMSO solvent.

CHAPTER 2
LITERATURE REVIEW

2.1 Textile Waste Overview

The "Fast Fashion" trend was characterised by high-volume production, trend-driven variety, rapid market turnover, and affordability [22], [23]. Since the population has grown, this trend has led to a sharp increase in global fibre use and textile waste generation [24]. According to the Materials Market Report 2024 (September Edition) by Textile Exchange, worldwide fibre production had risen by 7% from 116 million tonnes (MT) in 2023 to 124 MT in 2024 [25]. It is also estimated that global textile production will further expand from 140 MT in 2025 to 169 MT by 2030 [1]. This statistic indicates that the global average fibre consumption has increased significantly, rising from 8.3 kg/person in 2024 to 16.2 kg/person in 2025. Parallel to this escalation, global textile waste will increase from 92 MT in 2024 to 134 MT in 2025, showing that waste generation nearly keeps pace with production growth [1].

As mentioned in chapter 1, cotton-based fibre was the second most contributing to textile waste. Cotton is a natural cellulosic fibre obtained from the seed hairs of plants belonging to the *Gossypium genus* [26]. The primary component of pure cotton cellulose is approximately $C_6H_{10}O_5$, forming linear chains of β-(1→4)-linked D-glucopyranose units that aggregate into semi-crystalline microfibrils through extensive intra and intermolecular hydrogen bonding [27]. Abundant cellulose hydroxyl groups (-OH) enable covalent fixation of reactive dyes and accommodate durable press, antimicrobial, and other functional finishes [27]. Figure 2.1(a) shows the chemical structure of cotton (cellulose). Cotton provides air permeability and high moisture sorption where it enables thermos-physiological comfort in clothing [28]. Strength derives from secondary-wall crystallinity and microfibril orientation, while moisture alters hydrogen-bond topology and can raise wet strength relative to dry for scoured/bleached lint [29]. In comparison, polyester-based textiles are estimated to make up roughly 57% of this waste, consistent with their market dominance and slow degradation in the environment. Polyester fibre, also known as polyethylene

terephthalate (PET), is a thermoplastic polymer commonly used in clothing and technical textiles [30].

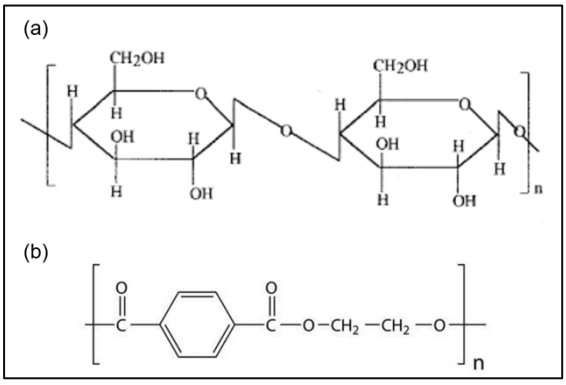

Figure 2.1 Chemical Structure of (a) Cotton (Cellulose) and (b) Polyethylene Terephthalate (PET)

Figure 2.1(b) shows an aromatic-aliphatic structure with ester linkages (-COO). Polyester was produced by the polycondensation of terephthalic acid or dimethyl terephthalate with ethylene glycol. This molecular arrangement results in a semi-crystalline morphology, contributing to its high tensile strength, solvent resistance, and thermal stability [31]. Due to these characteristics, polyester offers advantages such as rapid drying, resistance to stains and excellent compatibility with natural fibres like cotton. These allow the manufacturers to combine durability and ease of care with softness and aesthetic versatility [32], [33].

Nowadays, blended fibre from cotton and polyester (polycotton) is typically produced in 65:35 or 50:50 polyester to cotton ratios, depending on the desired performance characteristics [34]. The combination was designed to integrate the moisture absorption and breathability from cotton with the wrinkle resistance from polyester. As a result, polycotton fabrics offer improved durability while maintaining the comfort properties. Recent reviews on textile waste management have identified that polycotton is a significant contribution in post-consumer textile waste [35], [36], [37]. According to Future Market Insights, the global polycotton fabric market was valued at USD 468.9 million in 2025 and is projected to reach USD 618.1 million by 2035 [38]. However, the chemical and thermal incompatibility of its components makes recycling polycotton extremely difficult.

Mechanical recycling often reduces the cotton fibre length and the mechanical integrity. This limits its suitability for high-performance textile applications. In parallel,

polyester is highly prone to thermal deformation, especially when it is exposed to high temperatures [39]. These limitations have increased attention toward chemical recycling routes. However, chemical recycling presents its own challenges. Natural fibre usually recycles via hydrolysis to break down the polymer structure. Meanwhile, polyester requires glycolysis or ammonolysis under controlled conditions to recover its monomer [40], [41]. These different processes limit the effectiveness of separation and recovery for both materials. As a result, polycotton recycling remains inefficient, highlighting the critical need for selective separation techniques, efficient solvent systems to achieve long-term fibre recovery.

2.2 Textile Recycling Overview

In textile industries, mechanical recycling, such as shredding or carding, has fibres recovered by spinning into yarns or used as nonwoven materials [42]. However, mechanical recycling usually downgrades the quality of recovered materials such as fibre length, and mechanical strength compared to virgin fibres [43]. In addition, the presence of blended fibres makes the separation process more challenging as it reduces the purity of the recycled material [44]. As a result, mechanically recycled fibres are often downcycled into products with lower functional such as insulation materials and mattress stuffing [45]. This highlights the limitation of mechanical recycling to increase the recycling circularity (closed-loop system) in the textile industry [46], [47], [48]. Hence, researchers have turned to alternative recycling approaches, solvent-based methods, which aim to regenerate cellulose and synthetic polymers separately.

Chemical recycling has the potential to produce higher-quality fibres. However, the widespread application of this method has been constrained by the dependence on hazardous solvents, high energy cost, and the technical difficulties involved in handling blended textiles [49], [50]. Economically, chemical recycling is often less cost-effective than producing virgin fibres due to high operational and infrastructure costs [51]. Market demand for recycled textiles remains low, driven by concerns over quality and pricing expectations [52]. Textile chemical recycling technologies can be categorised into three approaches based on their interaction with the polymer chain. The first category consists of gasification and pyrolysis. These processes involved high-temperature thermal energy to break down the polymer structure completely. The second category of methods employed a more complex strategy, aiming for controlled

chemical depolymerisation to produce monomers or oligomers that can re-polymerise. These include ammonolysis, glycolysis, enzymatic hydrolysis, and the hydrothermal method. Finally, the last category was dissolution, which it directly addresses the core challenge of polymer separation and recovery. Table 2.1 presents a comparative overview of various chemical textile recycling technologies, highlighting their respective advantages and limitations.

Based on each category limitation, there are clear differences that are observed for preserving the value of textile fibre. In thermochemical processes (category 1), the polymer backbone is destroyed under very high energy input. These cause a low circularity of textile recycling since the originality of the polymer cannot be recovered [53], [54], [55], [56]. In contrast, chemical depolymerisation (category 2) cleaves the polymer chains into monomers under high conditions. Although it is favourable for synthetic textile, the process is not suitable for heterogeneous material feedstock and limits its stability [50], [57], [58], [59]. Due to the limitations by the previous recycling categories which are high energy consumption, high operating condition, and applicability restricted to specific textile waste, increasing attention has been directed toward Category 3 (Dissolution). Unlike thermochemical and depolymerisation approaches, dissolution had promising in polymer backbone preservation and can operate in a lower energy process. The selectivity of solubility also allows the separation of blended textile which enhances the process efficiency without causing significant chemical degradation. In addition, the dissolved polymer can be regenerated directly into fibre which enables the closed-loop recycling textile [60].

However, despite dissolution being advantage in chemical textile recycling, there are notable disadvantages. Various solvents have been studied to dissolve cotton and polyester without degrading the quality [61]. Examples of solvents used to dissolve cotton and extract cellulose include LiCl/DMAc solution, H_2SO_4 aqueous solution, and NaOH/urea aqueous solution [62]. Green solvents such as ionic liquids have favored to natural based materials such as cotton. However, the separation of cotton from polyester was difficult due to the high viscosity of IL [63]. The study reported by Wu et al. [64] mentioned that sulfone-based solvent was the most suitable co-solvent for the dissolution process, particularly for cotton-based textile. However, the question had raised as the ratio of sulfone-based solvent were higher than IL as the main solvent. This shows that sulfone solvent can be the main solvent in the dissolution process without any additional solvent.

Table 2.1
The Type of Chemical Textile Recycling, Advantages, and Limitations of Chemical Textile Recycling

Category	Type of Chemical Textile Recycling	Advantages	Limitations	Percentage (%)	Ref
1	Gasification	• Capable of processing blended textiles.	• Operate at high temperature and pressure. • Low selectivity.	~70	[54]
	Pyrolysis	• Applicable to various kinds of raw fibre materials.	• High temperature reaction process. • High energy consumption.	80	[56]
2	Ammonolysis	• Applicable to nitrogen-containing polymers only.	• Requires a high temperature and pressure. • Involves toxic chemical such as Ammonia.	~90	[65]
	Enzymatic Hydrolysis	• Lower energy requirement.	• Limited to specific materials like Rayon, and Hemp.	~75	[48]
	Glycolysis	• Low energy consumption compared to pyrolysis.	• Selective toward BHET monomer. • Required catalyst.	85	[66]
	Hydrothermal	• Applicable to heterogenous materials. • Water was used as reaction medium and reactants.	• Required high temperature. • Longer reaction time. • Low selectivity for heterogenous material	~99	[67], [68], [69]
3	Dissolution	• Applicable to both natural and synthetic fibre materials. • High selectivity (depend on solvent used).	• Used hazardous solvent such as Dimethylformamide (DMF) • High costs in developing a highly efficient recycling system.	~99	[60], [62]

2.3 Molecular Dynamics (MD) Simulation Overview

Molecular Dynamics (MD) simulation allows researchers to study materials' interaction with selected solvent systems at the atomic level using Newton's laws of motion [70]. Through MD simulations, the observation of the materials behaviour such as their structure, stability, and molecular mobilities are difficult to capture through traditional experiments. Over decades, MD has developed from a simple method for accurate predictions to a reliable approach for explaining solvation mechanisms. Nowadays, advanced computing and machine learning promote MD simulation to be widely used by integrating with experiments to relate the theoretical models with real-world applications [71]. Modern advances, such as GPU acceleration and parallel simulation methods, have enabled the study of molecular systems over microsecond timescales. However, there is a notable gap in research where the MD simulation only applied for validation data instead of predicting dissolution behaviour. Table 2.2 summarise the systematic review of the dissolution of polymer in MD simulation.

Notably, most reported studies show that MD simulation is often used to validate experimental results rather than to predict them. This practice limits the method's full potential in studying dissolution processes. MD simulation was designed to investigate the atomic-level interactions of molecules before laboratory work begins [72]. Miyata et. al mentioned that MD simulation allows researchers to examine the materials' solubility behaviour without using real material and allow to reduce the experimental cost. Hence, this method broadens the experimental design space, which enables the upscale process from atomic-scale data to larger-scale observations by averaging molecular trajectories. This advantage allows researchers to estimate measurable quantities, such as dissolution rates and activation energies. Since dissolution method affected by different parameters, MD simulation is the most suitable approach in reducing experimental cost for instance type of solvent, range of temperature and concentrations. Overall, based on Miyata et al findings, this justifies the predictive approach taken in this thesis. However, despite its advantages, there are a few parameters that need to be selected to accurately represent the real-life dissolution process through simulation. This setup involves selecting suitable software, force fields, ensemble, and thermostat control. Each selected parameters were directly affected the simulation's ability to accurately represent the physical conditions and reveal the mechanism of polymer-solvent interactions.

Table 2.2
Summary of Previous Study (2019 to 2025) of Validation Dissolution Polymer using MD Simulations

Author	Year	Type of Polymer	Solvent	Operating Temperature	Software	Ref
Deng et al.	2025	PET	DMI	453.15 K	GROMACS	[73]
Guo et al.	2025	Cotton	N/A	300 - 2000 K	LAMMPS	[74]
Bagherjeri et al.	2024	Denim waste (100% cotton)	NMMO	380 K	GROMACS	[75]
Cao et al.	2024	Cellulose	Phosphate-based IL and water	343 K	GROMACS	[76]
Ci et al.	2024	Cellulose	[DBUH]Lev/co-solvents* *DMSO, DMF, DMAc, DMI	348 K	GROMACS	[77]
Long et al.	2024	Cellulose	Ionic Liquids (ILs)	373.15 K	GROMACS	[78]
Wu et al.	2024	Poly-cotton	Ionic Liquids (ILs)	323 K	GROMACS	[79]
Zhong-Johnson et al.	2024	PET	Water	300 K	GROMACS	[80]
Orlando et al.	2023	PET	Water	303 - 423 K	GROMACS	[81]
Pang et al.	2023	Cellulose I, II, III (allomorphs)	Water	350 K (CG), 300 K (AA)	GROMACS	[82]
Zheng et al.	2023	PET	Ethylene Glycol with [Cho][OAc] (catalyst)	300 - 450 K	GROMACS	[83]
Yamamoto et al.	2022	PE	N/A	350 - 440 K	LAMMPS	[84]
Zhang et al.	2019	PolyUrea-Formaldehyde	SiO2 nanoparticles	298 K	Materials Studio	[85]

2.3.1 Software Selection for Molecular Dynamics

Molecular dynamics (MD) simulation software provides a computational approach for examining the motion and interactions of atoms and molecules over time. The method operates by applying Newton's laws of motion to calculate atomic trajectories and structural changes within a defined system [86], [87]. However, every MD software employs different numerical algorithms, potential energy models, and integration methods, which collectively influence the accuracy, computational efficiency, and applicability of the simulation outcomes [88]. Consequently, the selection of appropriate software must consider the nature of the chemical system, the scale of the simulation, and the type of analysis required to ensure accuracy and reliability [89]. BIOVIA Materials Studio (MS), GROMACS, and LAMMPS were common software that were used in modelling molecular interactions, as summarised in Table 2.3.

Table 2.3
Focus Study of Each Software in Molecular Interaction Analysis

Software	Focus Study	Ref
BIOVIA Materials Studio	• Material property prediction • Molecular modelling and simulation • Multiscale modelling • Customisation and analysis tools	[90], [91]
GROMACS (Groningen Machine for Chemical Simulations)	• High performance but long simulation time • Focusing on large biomolecules and polymers chain. • Commonly used for energy minimisation and analysing interaction energies.	[78], [92]
LAMMPS (Large-scale Atomic/Molecular Massively Parallel Simulator)	• Large-scale simulations. • Wide application range including polymers, biomolecules, metals, and mesoscale materials.	[93]

A comparative analysis by Sumit Sharma [91] highlights notable differences among MS, LAMMPS, and GROMACS in MD simulations of polymer–matrix composites, as well as their broader application to polymer–solvent interaction

modelling. The main objective involves constructing composite structures such as polymer chains embedded with fillers or solvated systems while also predicting mechanical and thermal properties and visualising molecular interactions. The study highlights that MS provides an integrated modelling environment that combines molecular mechanics, quantum mechanics, and mesoscale simulation within a user-friendly graphical interface. Its capability to link modules such as Forcite (classical MD), Dmol³ (Density Functional Theory, DFT), and Mesocite (coarse-grained modelling) enables seamless transitions across computational scales from electronic to atomistic and mesoscale levels [94]. Moreover, the availability of force fields such as Condensed phase Optimised Molecular Potential for Atomistic Simulation Studies (COMPASS) allows the accurate representation of polymer flexibility, solvent polarity, and cohesive energy density [91]. Since MS software usually applied COMPASS force field, hence effective for characterising molecular mobility and dissolution thermodynamics in complex organic systems. This feature makes it particularly effective for detailed investigations of polymer–solvent systems.

In contrast, GROMACS is widely recognised for its effectiveness in studying problems that involve long simulation times, large molecules, and multiple runs that are necessary [92]. Its optimised computational design provides strong performance and stability during extended simulations. GROMACS efficiently handles biological macromolecules and polymeric systems using advanced electrostatic methods, such as the Particle Mesh Ewald (PME), and constraint algorithms (such as Linear Constraint Solver (LINCS)), which help maintain energy balance throughout the simulation [95]. Although GROMACS offers computational efficiency and scalability, it is usually optimised for biomolecular and aqueous environments [96]. Modelling complex polymer–filler or composite systems often requires external structure-generation tools or additional workflow integration [97]. Hence, the application on heterogeneous polymer–solvent systems, careful customisation of the force field is typically required to achieve reliable, realistic results.

Eventually, LAMMPS (Large-scale Atomic/Molecular Massively Parallel Simulator) is a software that is suitable for both reactive and non-reactive simulations. Its support for numerous interatomic potentials, such as ReaxFF. Hence, it allows for the representation of complex model processes such as bond formation, crosslinking, and molecular degradation [98]. This adaptability makes LAMMPS particularly useful for examining inorganic composites, nanomaterials, and large heterogeneous systems

[99]. However, its reliance on text-based input and extensive scripting can make it less accessible for studies that emphasise structural visualisation and post-simulation analysis, especially for polymer–solvent systems [71]. However, LAMMPS requires advanced scripting skills, such as knowledge of Python or C++, and careful interpretation of simulation outputs [100].

Together, BIOVIA Materials Studio provide an integrative platform that for studying polymer-solvent system such as dissolution textile through multi-scale modelling environment and advanced visualisation features. Zhang et al mentioned that the integration of quantum and classical modelling, extensive force-field database, and customisable analysis modules enables a reliable representation of both inter- and intra-molecular interactions. Hence, it supporting accurate predictions of dissolution behaviour and material performance at the molecular scale. Overall, BIOVIA Materials Studio is the most suitable choice for this study as following the justification of Zhang et al.'s study [85].

2.3.2 Selection of Force Field

In molecular dynamics (MD) simulations, the interactions between atoms and molecules can be defined mathematically by a force field [101]. The force field serves as the mathematical framework that defines the potential energy surface governing atomic motion and intermolecular interactions [102]. Previous studies had highlighted that the accuracy of MD simulations depends critically on the reliability of the potential energy (U_{total}), which describes the balance of bonded and non-bonded interactions as a function of atomic positions, particularly for polymer–solvent systems [66-70]. The general functional form of a force field is expressed as Eqn. 2.1 [107]:

$$E_{total} = E_b + E_\theta + E_\varphi + E_{vdw} + E_{ele} + E_{cross} \quad (2.1)$$

Where Etotal is the total energy, Eb is the bond stretching energy, and Eθ is the angle bending energy. Eφ is dihedral torsion energy, Evdw is van der Waals interaction energy, Eele is electrostatic interaction energy, and Ecross is cross-term interaction energy. In polymer–solvent systems, dissolution and solvation behaviour is mainly influenced by non-bonded interactions, such as hydrogen bonding, dipole–dipole

interactions, and dispersion forces [108]. At the same time, the flexibility of the polymer's molecular backbone influences how the chains move and adjust within the solvent. Since the reliability of simulation results depends significantly on the choice of force field, the appropriate one must be carefully selected before proceeding with the simulation. Several force fields have been developed and optimised for different classes of materials, such as organic molecules, polymers, biomolecules, and inorganic systems. Table 2.3 shows the type of force field commonly used for polymer-solvent interaction in MD simulation.

In condensed-phase polymer systems, transferable and polarisable all-atom force fields such as Condensed-phase Optimised Molecular Potential for Atomistic Simulation Studies (COMPASS) and Polymer Consistent Force Field (PCFF) are preferred for polymer-solvent interaction studies because they incorporate cross-coupling terms (bond–bond, bond–angle, torsion–torsion) and reproduce condensed-phase experimental data, including densities, compressibility, and heats of vaporisation [109]. In contrast, simpler non-polarisable force fields such as Dreiding or Universal, while computationally efficient, often neglect higher-order interactions and polarisation effects that are essential for describing hydrogen bonding and solvent-induced conformational changes [110]. Thus, the inclusion of cross terms and accurate electrostatics significantly enhances the realism of polymer–solvent models, where solvent penetration and chain relaxation occur simultaneously at atomic and mesoscopic scales. Each force field is defined by its mathematical form and underlying theoretical assumptions. Dreiding and PCFF employ harmonic potentials for bonded interactions and a 12-6 Lennard–Jones potential for van der Waals forces. Meanwhile, PCFF and COMPASS employ more complex forms, like the 9-6 Lennard-Jones, to better simulate complex interactions at short range. Both models can be expressed by Eqn. 2.2 and 2.3 respectively:

$$E_{vdw_{12-6}} = D_0 \left[\left(\frac{r_0}{r}\right)^{12} - 2\left(\frac{r_0}{r}\right)^{6} \right] \tag{2.2}$$

$$E_{vdw_{9-6}} = \varepsilon \left[\left(\frac{r_0}{r}\right)^{9} - 3\left(\frac{r_0}{r}\right)^{6} \right] \tag{2.3}$$

Where D0 is the well depth (kcal/mol), corresponding to the minimum of the potential well. r0 is the equilibrium interatomic separation where potential energy is

minimal (Å), r is the instantaneous distance between atom centres (Å), and ε=D0/2 is the depth of the potential well. Electrostatic interactions are computed using Ewald summation or particle–mesh techniques, with charges derived either from quantum mechanical electrostatic potential fitting (as in COMPASS) or empirical assignment (as in PCFF). COMPASS ensures accurate representation of polarisation and dispersion effects, particularly crucial in heterogeneous environments like polymer–solvent interfaces.

Thus, COMPASS force field offers significant advantages by showing its high level of parameterisation to represent both organic and inorganic systems [111]. This force field had included with detailed parameters to describe bond stretching, angle bending, torsional rotation, and non-bonded interactions. This enables an accurate representation of the complex intermolecular forces involved in dissolution processes [112]. In contrast, the Dreiding force field is known as a general-purpose molecular modelling that offer simplicity and broad applicability. It employs transferable parameters which suitable for a wide range of molecular systems [113]. Although Dreiding offers less precision than COMPASS, it provides significant computational efficiency and is often used for preliminary studies or rapid evaluations of molecular interactions [114].

At the same time, PCFF force field also offers broad transferability across the periodic table. This is especially useful for systems containing that more complex or rare elements, including organometallics and certain inorganic compounds. Although PCFF was less accurate than COMPASS in simulating polymers or biomaterials, it remains advantageous for modelling chemically diverse systems where versatility is prioritised over specificity [115]. Considering the computational efficiency, Dreiding and UFF are often preferred for large-scale exploratory simulations due to their simplicity, though this comes at the cost of reduced thermodynamic accuracy [116]. Although various simulation software such as LAMMPS and GROMACS can implement these force fields, their reliability ultimately depends on the quality of the selected parameters [117]. Among these options, COMPASS stands out for integrating ab initio accuracy with condensed-phase calibration, molecular flexibility, solvation energetics, and polymer–solvent compatibility. COMPASS offers the required resolution and reliability for dissolution studies where hydrogen bonding, van der Waals attraction, and segmental relaxation dominate molecular behaviour. Its incorporation of cross-term coupling, the 9–6 potential form, and precise charge distribution ensures

realistic modelling of polymer–solvent interactions [118], [119]. Consequently, COMPASS enables accurate predictions of structural and dynamic properties, such as radial distribution functions, mean-square displacements, and cohesive energy density.

Based on its theoretical formulation, parameterisation strategy, and empirical validation, COMPASS is identified as the most appropriate force field for molecular dynamics simulations of polymer–solvent systems. Its dual validation against quantum mechanical data and experimental condensed-phase properties provides both physical accuracy and predictive reliability, making it particularly suitable for studying the molecular mechanisms underlying polymer dissolution, solvent penetration, and structural reorganisation at the atomic level [120]. Researchers can better understand the characteristics and functionality of polymers by selecting a force field that is suited to the polymer system and study goals. This allows them to capture molecular-level situations.

2.3.3 Selection of Ensembles

In molecular dynamics simulations, an ensemble is characterised by designated thermodynamic variables that control the behaviour of temperature, pressure, and energy throughout the simulation [121]. The primary ensembles in MD are the microcanonical (NVE), isothermal–isobaric (NPT) and canonical (NVT) ensembles. Each corresponds to different experimental conditions and computational objectives. In the microcanonical ensemble (NVE), the particle number (N), volume (V), and total energy (E) are constant. The system evolves under Newton’s equation of motion without external coupling to a thermostat or barostat, making it suitable for energy-conserving systems after equilibration [122]. However, polymer–solvent systems are strictly influence by temperature, concentration, and pressure, making NVE less appropriate for this study [123]. The isothermal–isobaric ensemble (NPT) maintains the number of particles (N), pressure (P), and temperature (T) by using a barostat to regulate pressure and a thermostat to control temperature, allowing the system's volume to fluctuate [124]. Meanwhile, the canonical ensemble (NVT) maintains a fixed number of particles (N), volume (V), and temperature (T) using a thermostat to maintain temperature. This making it more suitable for analysing systems with fixed density [125]. Hence, each ensemble is ideal for simulating real-world phenomena such as polymer swelling, pressure-dependent phase transitions, and density changes during

polymer-solvent interactions [126]. However, the order of ensemble pairing such as NPT, NVT, NVT-NPT or NPT-NVT need to be determined first before proceed to MD simulation.

A study by Zheng et al. [127] highlights that the importance of ensemble selection, specifically the NPT and NVT ensembles, is emphasised for achieving accurate and reliable molecular dynamics (MD) simulations. The use of NPT (constant number of particles, pressure, and temperature) and NVT (constant number of particles, volume, and temperature) ensembles was important in achieving equilibrium and analysing the structural behaviour of PET under different solvent conditions. The NPT ensemble was applied during the initial equilibration phase to allow the system adjust both pressure and temperature [72]. This step was important for ensuring the system was in optimum condition with accurate chemical properties. Then, the MD simulation was run under the NVT ensemble to analyse molecular interactions and structural changes under different temperatures. This enabled the simulation to accurately calculate the thermodynamic properties such as diffusion coefficients and mean-squared displacement (MSD) [128].

The study of calcite-organic interactions in water by Rukuan Chai et al. [129], he highlights that the NVT ensemble helped stabilise the calcite-organic molecule-water system. Meanwhile the NPT ensemble allowed the simulation to capture pressure-dependent dissolution behaviour. The simulations were carried out under different ensembles to evaluate the effects of the ensemble on the system dynamics. Overall, NPT ensures the simulation models mimic realistic conditions by allowing volume fluctuations and stabilising pressure. In contrast, the NVT maintains a fixed volume, facilitating detailed exploration of intermolecular forces and thermal stability within confined systems [130]. Hence, the combination of NPT-NVT ensemble provides comprehensive findings into molecular interactions and structural adaptations under various conditions.

In a study by Zheng et al. [70] also mentioned that the integration of NVT and NPT ensembles is significant in MD simulations for accurately representing interaction dynamics and process phases under regulated thermodynamic settings. The application of NPT-NVT ensembles enables the accuracy, stability, and physical relevance of molecular dynamics simulations across various material systems such as metals, non-metals, and polymers [131]. Based on comparison with other previous studies, NPT-NVT ensembles were the most suitable pair in simulating the interaction process that

involves either polymer-solvent systems or mineral-organic interfaces [132], [133], [134]. Hence, regardless of the type of molecular composition (rigid crystalline minerals or flexible polymer chains), the application of NPT-NVT ensembles ensures that the simulation results are both reliable and representative of real-world behaviour.

However, the selection of thermostat and barostat also important to maintain the accuracy and stability of NPT and NVT ensembles in MD simulations [102]. This is because both can control the algorithms which directly influences thermodynamic properties such as temperature, pressure, density, and molecular diffusion. Another study by Xujun Li et al. [111] highlighted the importance of the selection thermostat and barostat for each ensemble. To analyse polymer dissolution in solvent, both temperature and pressure required regulation. It is because, the polymer–solvent systems are highly heterogeneous. Since, the properties of the material are different, the suitable thermostat will enable the simulation to regulate and run in a steady temperature system. As a result, the simulation system was stable and produced consistent molecular motion and solvation interactions, and solubility measurements. At the same time, the barostat maintains precise pressure conditions that mimic actual polymer breakdown conditions include solvent diffusion and polymer solvation. A better knowledge of polymer-solvent interactions and the optimisation of conditions for effective dissolution are made possible by the combination of these controls, which create an environment that closely reflects real-world dissolution.

Thus, maintaining consistent thermal and pressure conditions is particularly important. Through these controls, the simulated system can reproduce realistic ensemble behaviour. The NPT ensemble introduces a pressure control mechanism in addition to temperature control, ensuring that both temperature and pressure fluctuate naturally around target values. Pressure (P) in MD is generally calculated using the Eqn. 2.4 [135]:

$$P = \frac{Nk_BT}{V} + \frac{1}{3V}\sum_i r_i \cdot f_i \tag{2.4}$$

where V is the instantaneous simulation box volume, r_i is the position vector, f_i is the atomic force and k_B is Boltzmann's constant. Meanwhile in the NVT ensemble, the temperature regulation is essential to maintain the accurate distribution of kinetic energy

that corresponds to the target temperature. The thermostat ensures that the average kinetic energy is satisfied by calculating using Eqn. 2.5 [135]:

$$\langle K \rangle = \frac{3}{2} N k_B T_0 \tag{2.5}$$

where K is kinetic energy and k_B is Boltzmann's constant. Table 2.4 shows the comparison of Andersen, Berensen, Nosé–Hoover, and Langevin as Thermostat and Table 2.5 shows the comparison of Andersen, Berensen, Nosé–Hoover, and Parrinello–Rahman as Barostat.

Table 2.4
The Comparison of Andersen, Berensen, Nosé–Hoover, and Langevin as Thermostat

Thermostat	**Andersen**	**Berendsen**	**Nosé–Hoover**	**Langevin**
Control Mechanism	Stochastic collisions between atoms and a virtual heat bath; random velocity reassignment according to the Maxwell–Boltzmann distribution.	Velocity scaling based on a relaxation time constant toward target temperature (T0).	Deterministic coupling of system to a heat bath using an extended Hamiltonian with fictitious variable for scaling.	Applies friction and random forces to simulate Brownian motion and maintain target temperature.
Application in MD	NPT or NVT equilibration stages for polymer–solvent systems	Widely used for NVT production runs or pre-equilibration	NPT or NVT with long simulations for precise thermodynamic averages	Biomolecular and polymer–solvent systems.
Reference	[72]	[136]	[137]	[138]

Table 2.5
The Comparison of Andersen, Berensen, Nosé–Hoover, and Parrinello–Rahman as Barostat.

Barostat	**Andersen**	**Berendsen**	**Nosé–Hoover**	**Parrinello–Rahman**
Control Mechanism	Couple system volume to external pressure by rescaling coordinates and velocities based on a "piston" mass.	Smooth scaling of box dimensions toward target pressure with relaxation constant (τP).	Combines Nosé–Hoover thermostat with barostat for deterministic constant (P, T) conditions.	Dynamically couples pressure tensor to box matrix allowing anisotropic cell fluctuations.

Barostat	Andersen	Berendsen	Nosé–Hoover	Parrinello–Rahman
Application in MD	NPT equilibration phase for polymer–solvent mixtures	Pre-equilibration of liquids and polymers under constant pressure	Long and stable NPT runs for homogeneous bulk systems	High-precision NPT production runs for crystalline and layered materials
Reference	[72]	[139]	[140]	[141]

Therefore, the NPT (Andersen)–NVT (Berendsen) ensemble combination is selected as the optimal configuration for molecular dynamics simulation of polymer–solvent interactions [142]. Berendsen barostat provides smooth, continuous temperature regulation with minimal perturbation, while preserving the accuracy of dynamic observables such as diffusion coefficient and radial distribution function (RDF). Thus, for the current simulation of polymer–solvent interactions, the NPT (Andersen) ensemble during equilibration followed by the NVT (Berendsen) ensemble during production provides the optimal balance between thermodynamic accuracy, numerical stability, and physical realism.

2.4 Thermodynamic Properties Analysis

The prediction on the chemical structural and molecular dynamic behaviour of polymers in different solvent environments can be evaluated by thermodynamics properties. Key parameters such as binding energy (BE), interaction energy (IE), mean square displacement (MSD), and glass transition temperature (Tg) can indicate the efficacy of swelling, dissolution, and other applications [16], [143]. Analysing these factors enables a more detailed understanding of how solvents interact with polymers, influencing properties that support processing efficiency, temperature optimisation, and compatibility. This knowledge is fundamental to advancing sustainable and efficient materials processing technologies.

2.4.1 Binding Energy (BE) and Interaction Energy (IE)

Binding energy (BE) and interaction energy (IE) were common properties that used in molecular modelling evaluation. Both were used to analyse the strength of intra

and intermolecular interaction in polymer-solvent system. BE refers to the energy difference between two different system (combined and individually) of polymer and solvent [144]. A higher BE indicates a stronger internal bond due to strong hydrogen bonding and π-π stacking. This shows the increases of the energy barrier for solvent penetration and chain separation, which reduces the dissolution rate. In contrast, a lower BE indicates lower polymer-polymer bonding, allowing solvent access to polymer chains and disrupting intermolecular connections disentangle the polymer chain [145]. A higher positive BE indicates stronger polymer–solvent interactions and generally suggests better dissolution capability, but the interpretation should always be made compare to other solvents or conditions studied. Meanwhile, IE represents the total energy resulting from non-bonded interactions (like Van der Waals forces and electrostatic forces) between them [146]. A more negative IE value indicates a stronger attractive and greater compatibility. Vice versa, the larger the value (more positive) shows weaker interactions and lower affinity.

A study by Zhang et al. [147] mentioned the theory behind binding energy in simulation. The thermodynamic principle where energy required to separate atoms or molecules from a solid structure (binding energy) directly impacts dissolution. Higher binding energy generally correlates with lower dissolution rates, as it requires more energy to dislodge molecules from the surface [148]. A study by Bering et al. [149] also supports this claim. As mentioned in his study, MD simulations showed that cellulose bundles with fewer chains dissolved more easily because of their lower interchain binding energy. By strengthening hydrogen bonds, the co-solvents NaOH and urea also reduced the IE between cellulose chains, allowing for the successful separation of individual cellulose chains [149].

In conclusion, the potential energy differences are used to evaluate the interaction or binding energy between bonded and separated structures at crystal or fibril surfaces. These energies are calculated in a suitable force field that isolates the contributions from van der Waals and electrostatic interactions. The calculated energy of the system is analysed afterwards, combined with dynamic characteristics like self-diffusion calculated from mean-squared displacement and solvent solubility evaluations like coordination numbers and radial distribution functions [150]. All the analyses were evaluated together to explain how well the solvent interacts with the material.

2.4.2 Glass Transition Temperature (Tg)

Glass Transition Temperature (Tg) is a critical temperature point where the materials can be existed in a glassy, rigid state and state. Jadhav et al. [151] study highlights the importance of Tg in enhancing the dissolution, bioavailability, and physical stability of drug molecules. Their findings indicate that Tg significantly influences drug solubility and stability due to their disordered configurations. In relation to the dissolution process of a polymer, Tg is crucial as it determines the molecular mobility within a polymer, impacting its interaction with solvents. Tg is highly dependent on the molecular weight of the polymer. For example, an increase in molecular weight decreases chain-end concentration, which reduces the free volume at the end-group regions and raises Tg [152]. Modifications to the end groups can also affect the molecular weight dependency of Tg, with stronger end-group interactions or reduced chain-end concentrations (in lower molecular weight polymers) resulting in higher Tg [153]. Hence, bulky and inflexible side groups in the molecular structure restrict mobility, leading to an increase in Tg.

In the meantime, a glassy state of polymers can be related with slower dissolution rates if the operation temperature (T0) lower than Tg. This is because it reduced chain mobility and lower free volume. Conversely, when polymers are in a rubbery state (T0>Tg), they exhibit higher dissolution rates. This is attributed to increased free volume and greater chain flexibility, which facilitate the solvent's ability to penetrate and interact with the polymer matrix.

Ren et al. [154] conducted MD simulations on cellulose in mixed DMSO-ionic liquid environments. They observed that the disruption of interchain hydrogen bonding decreased the cohesive energy density and shifted Tg downward by approximately 30–50 K relative to the dry cellulose reference. Another study by Xie et al. [155] shows that Poly-N-vinylcarbazole demonstrates increased Tg due to the substitution of the bulky carbazole group. Moreover, chemical cross-linking had limited the molecular mobility and reduced free volume, thereby elevating Tg. Cross-linking introduces a rigid network that restricts the flexibility of the polymer chains, resulting in enhanced thermal and mechanical stability [156].

In conclusion, polymer chains are trapped in deep potential-energy wells, restricting their motion and reducing atomic vibrations at temperature below Tg [157]. As the temperature approaches Tg, the polymer gains enough thermal energy to

overcome rotational and translational barriers along its backbone. Finally, when the temperature exceeds Tg, the polymer transitions into a more dynamic state by cooperative segmental motion and greater free volume, which enhances solvent accessibility and accelerates dissolution [156]. Therefore, this change leads to more frequent dihedral angle transitions, increased chain flexibility, and higher mean-squared displacements (MSD) and diffusion coefficients (D) [158].

2.4.3 Mean Square Displacement (MSD)

In MD simulations, Tg has significantly related with the mobility of polymer chains. It is because the fundamental change in polymer dynamic, which could be influenced by the intermolecular interactions [159]. Mean Square Displacement (MSD) provides valuable information on the diffusivity of molecules over time. This indicates the movement of polymer chains or solvent molecules within the system. The slope of MSD curve shows various type of diffusion behavior [157]. Figure 2.4 illustrates the transition, while Table 2.6 shows the type of MSD slope and diffusion behavior. [160]

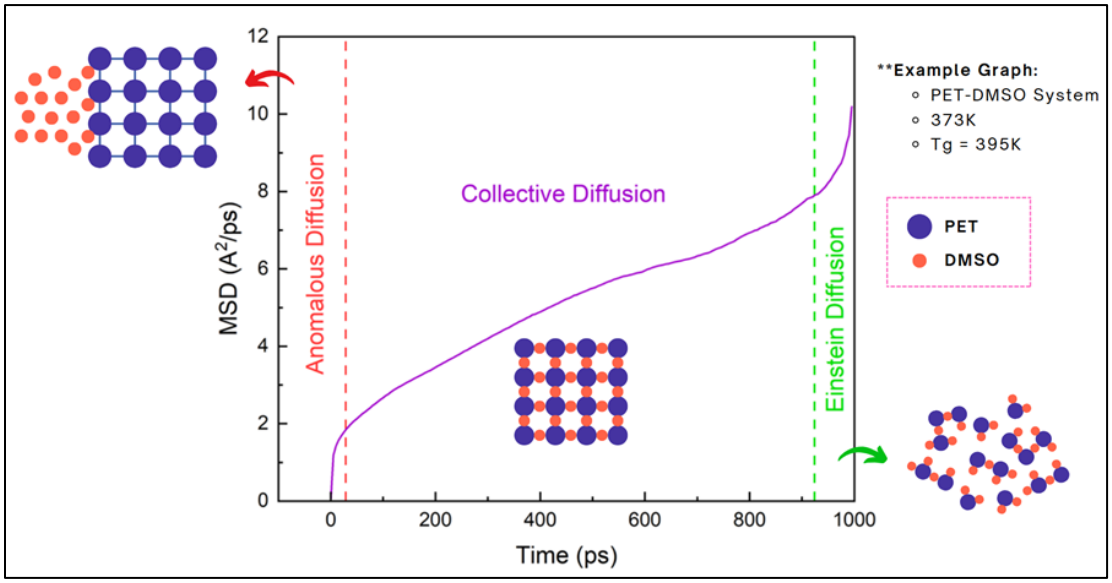

Figure 2.2 Transition Diffusion Behavior During MD Simulation. Illustration only.

Table 2.6
Type of Glass Transition Temperature, Mean Square Displacement Slope and Diffusion Behavior.

Temperature	Polymer State	MSD Slope	Diffusion Type	Ref
T < Tg	Glassy	Subdiffusive or restricted	Anomalous	[161]
T ≈ Tg	Transition Zone	Gradual increase in slope	Collective (Case II)	[12]
T > Tg	Rubbery	Linear	Normal (Fickian)	[158]

Next, collective diffusion or known as Case II diffusion describe the movement of groups of particles responding to concentration gradients or external perturbations. Marked by a sharp solvent front advancing at a constant velocity, separating swollen and unswollen regions within the polymer. Typically observed in transition zone of polymers near their glass transition temperature (Tg) [12]. Finally, the Fickian (Normal) diffusion were following Fick's Law with Stokes – Einstein relation as shown in Eqn. 2.6 [158]:

$$D = \frac{k_b T}{6\pi\eta R} \tag{2.6}$$

Based on the literature discussed above, MD simulation has been widely used to replicate the real-life polymer-solvent interaction. This method enables the observation of molecular behaviour such as diffusion and solvation. Previous study had shown the that MD simulation usually being validation tools which enable it to represent the interactions under various conditions effectively. However, MD simulation evaluation was limited to temperature and concentration only. Hence, the integrated computational and experimental method need to be applied in order to ensure the reliability of overall performance. As the author known, there are lack of investigations from previous studies that use this reliable method on the prediction of polymer-solvent interaction. Overall, MD simulation can be considered as reliable method in predicting of interaction of polymer-solvent system as it can provide accurate findings into how polymer chins respond to solvent environment.

2.5 DMSO as an Alternative Solvent in Dissolution

The dissolution of textile polymers, especially blended fibers like cotton-polyester, continues to be one of the biggest challenges to the development of textile recycling systems. The potential of dissolution processes in recycling applications is highlighted by the promised high efficiencies of this contemporary approach [60]. However, there are notable disadvantages. There are various solvents have been study to dissolve cotton and polyester without in degrade the quality [61]. Table 2.7 shows the xamples of solvents used to dissolve cotton including LiCl/DMAc solution, H_2SO_4 aqueous solution, and NaOH/urea aqueous solution [62]. Conversely, polyester is soluble in popular aprotic solvents such as N,N-dimethylformamide (DMF), N,N-dimethylacetamide (DMAc), dimethyl sulfoxide (DMSO), γ-valerolactone (GVL), dihydrolevoglucosenone (Cyrene), and N-methyl-2-pyrrolidone (NMP) [162]. Unfortunately, the application of toxic chemicals in textile recycling is frequently connected with serious consequences, particularly their toxicity. To address this issue, green solvents should be introduced for textile recycling [163].

Table 2.7
Comparative Textile, Solvent Systems and Dissolution Parameters

Study (Year)	Textile Involve	Solvent Type	Temperature (°C)	Efficiency (%)	Ref
Zhou et al. (2021)	Cotton	NaOH/urea	0–10	~95	[164]
Zhou et al. (2021)	Cotton	H_2SO_4	25–40	~92	[164]
Zhou et al. (2021)	Cotton	LiCl/DMAc	80	~70	[164]
Zhang et al. (2025)	Cotton	[AMIM]Cl + DMSO	110	85–90	[165]
Chang et al. (2023)	Cotton/ Polyester	[Bmim]Cl	100–110	~88	[166]
Ferreira Knihs et al. (2024)	Cotton/ Polyester	[EMIM]Cl	110–130	80–90	[167]
Jungbluth et al. (2025)	Cotton/ Polyester	DBU/DMSO/CO_2	40	~95	[168]
Villar et al. (2024)	Cotton/ Polyester	Alkaline hydrolysis	60–80	~80	[169]

Despite efforts to incorporate green solvents, there are a few factors that directly influence the dissolution rates. In the real situation, the recycled waste is heterogeneous material such as polyester and cotton blended. The significant different properties of material need to be considered to ensure the quality of regenerated fiber were preserved [63]. Therefore, a highly selected new solvent that can dissolve both cotton and polyester selectively with optimal condition should be introduced. Previous study research by Yan et al. revealed that cellulose undergoes dissolution with a lower activation energy requirement (14.81 kcal/mol) in comparison to polyester (21.46 kcal/mol). This difference accounts for the preferential dissolution of cellulose under the given experimental conditions (temperature, concentration and dissolution time) [170]. This statement is supported by the findings of Zhang et al., who revealed that the dissolution process was significantly influenced by temperature, concentration and dissolution time. This is because, the parameters involve directly in breaking the intra- and intermolecular hydrogen bonds, which allows individual polymer chains to separate [64].

Dimethyl Sulfoxide (DMSO) is one of high recommended sulfone-based solvents for the dissolution process. It is recyclable, which minimises solvent waste and reduces the environmental footprint during disposal [168]. Based on DMSO properties, DMSO is a very good alternative to replace hazardous chemicals. It is because DMSO is chemically inert with respect to many solutes, ensuring that it does not readily participate in unwanted side reactions during dissolution processes [171]. DMSO is highly polar with low toxicity and thus can be used at high temperatures [172]. The potential of DMSO as a solvent is further highlighted by its chemical stability and thermal stability up to 190°C, but it breaks down at higher temperatures to release compounds containing sulfur [173]. The molecular structure of DMSO enhances its ability to change and adapt to the environment.

DMSO's amphiphilic nature (as shown in Figure 2.3) consists of both polar (sulfoxide) and nonpolar (methyl) groups, enabling the interaction of both polar and nonpolar components commonly found in recycled textiles [174]. The oxygen atom in the sulfoxide group (S=O) is highly electronegative and can form hydrogen bonds or dipole-dipole interactions. Meanwhile, the two methyl groups ($-CH_3$) will interact with nonpolar chains of polymer via Van der Waals forces [175]. DMSO can act as both a hydrogen bond donor and acceptor due to its electron-rich oxygen atom and the slightly

acidic hydrogen on the methyl group. This dual functionality allows DMSO to form strong intermolecular interactions with solutes [176].

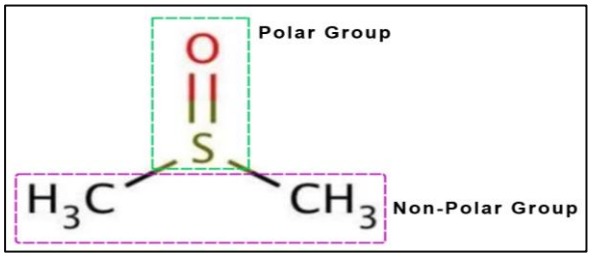

Figure 2.3 Chemical Structure with Polar and Non-polar Groups of DMSO

Moreover, the polarity of polyester and cellulose is important in their respective interactions with DMSO. Cellulose (cotton), as shown in Figure 2.4(a), contains a greater number of polar regions due to its hydroxyl (-OH) functional groups, which facilitate strong interactions with polar solvents such as DMSO [177]. These interactions promote polymer swelling during dissolution, provided they are sufficiently strong to overcome the intermolecular forces that hold the polymer structure together. [178]. Conversely, Figure 2.4(b) polyester possesses a greater proportion of non-polar regions, which results in weak interactions with polar solvents. Consequently, polyester exhibits limited or no swelling and does not dissolve readily in DMSO [179]. Thus, DMSO is capable of swelling or dissolving many types of polymers, including both natural (cotton) and synthetic (polyester) fibres, making it a versatile solvent in polymer processing and textile recycling applications [180]. However, the reliability of the interaction of both cotton (cellulose) and polyester with pure DMSO needs to be evaluated since there are no investigations from previous studies, as the author known.

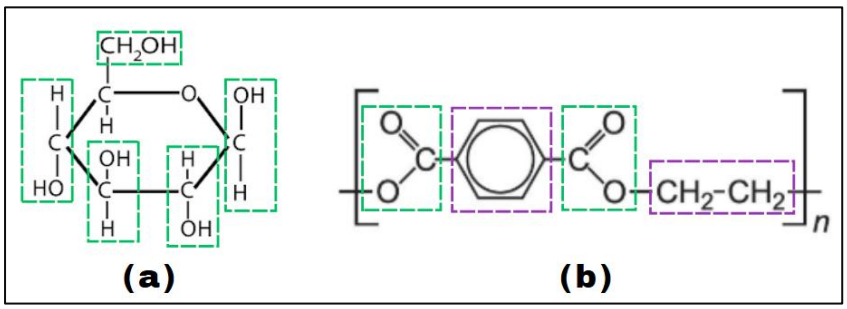

Figure 2.4 Chemical Structure of (a) Cellulose (b) Polyester (Green Box is Polar Region and Purple Box is Non-polar Region)

2.6 Regeneration Via Anti-Solvent Method

DMSO has considerable potential to increase the selective dissolution of cotton fiber without causing significant chemical degradation. Targeted regeneration techniques can be used to regenerate cotton fibers while maintaining their structural and functional integrity. In the regeneration of cotton, water serves as an antisolvent, inducing the precipitation of dissolved cotton chains through disruption of solvent-cellulose interactions. This promotes the intermolecular hydrogen bonding between hydroxyl groups. This method was suitable for environmentally friendly dissolution systems, due to its simplicity, nontoxicity, and compatibility with green chemistry principles. Table 2.8 shows the previous study from 2016 untill 2025 consistently demonstrate that water is an effective and environmentally benign anti-solvent for cellulose regeneration from various cotton-derived sources, including waste-colored fabrics, textile waste, and post-consumer cotton.

Table 2.8
Previous studies (2016 – 2025) On Cellulose Regeneration Using Water as an Anti-Solvent

Study By	Year	Cellulose Source	Dissolution Solvent System	Regeneration Method	Key Findings/Properties of Regenerated Cellulose	Ref
Zhang et al.	2025	Waste coloured cotton fabric	Ionic liquid 1-allyl-3-methylimidazole chloride ([AMIM]Cl) or zinc chloride (ZnCl2) aqueous solutions	Immersion in distilled water for solidification	Regenerated cellulose films (from IL system) showed superior mechanical properties (139.6 MPa fracture strength) and transparency	[181]
Barbosa de Brito et al.	2025	Textile cotton waste	Imidazolium-based ionic liquids (ILs) and DMSO	Water coagulation bath	Regenerated fibers showed structural changes from Cellulose I to amorphous or Cellulose II.	[182]
Du et al.	2024	Cellulose	Sulfuric acid treatment (followed by dissolution)	Regeneration in water	Regenerated cellulose exhibited Cellulose II crystal type Average particle size, and crystallinity were highest when regenerated in water compared to methanol or ethanol.	[183]
Juan Francisco Delgado et al.	2023	Filter paper	7 wt% NaOH/12 wt% urea aqueous solution	Regeneration with distilled water	Complete Cellulose I to Cellulose II transition Hot pressing significantly enhanced stiffness and strength.	[184]
Zhang et al.	2020	Cellulose	Ionic Liquids (BMIMCl, EMIMDEP) and N-methylmorpholine N-oxide (NMMO·H2O)	Dry-jet wet spinning into water	Coagulated gels in water showed different appearances (transparent, translucent, opaque) correlating with void structure and fiber properties.	[185]
Liu et al.	2019	Post-consumer cotton waste	Alkaline/urea aqueous solution and Ionic liquid (IL) 1-ethyl-3-methylimidazolium chloride ([EMIM]Cl)	Regeneration in water	Regenerated films from IL showed good mechanical properties.	[186]
Hauru et al.	2016	Cellulose	Ionic Liquids (NMMO·H_2O,OAc, [emim]OAc,OAc)	Dry-jet wet spinning into water	Water hydrates the ionic liquid and regenerates cellulose Rheological properties of dopes and diffusion constants of water/IL influence spinnability and fiber formation.	[187]

A notable trend is the increasing reliance on ionic liquids (ILs) such as [EMIM]Cl and NMMO, often coupled with aqueous or alkaline co-solvents, to achieve efficient cellulose dissolution prior to regeneration [19]. Regeneration in water not only induces the transformation of cellulose I to the thermodynamically more stable cellulose II crystalline structure but also enables the formation of films and fibers with tailored mechanical and morphological properties [188]. For example, regenerated cellulose films produced by immersion in distilled water after IL dissolution exhibited enhanced fracture strength and transparency, underscoring water's ability to promote uniform precipitation and reduce residual solvent contamination. Additionally, coagulation in water has been shown to generate fibers with controlled porosity and improved spinnability, attributes crucial for advanced textile and composite applications.

Previous research has consistently shown that the addition of water triggers rapid coagulation and precipitation of cellulose, converting it from a solvated amorphous phase into a semi-crystalline regenerated form[189]. During this process, the hydration of cellulose hydroxyl groups restores intra- and intermolecular hydrogen bonding, which supports the formation of Cellulose II. The outcome largely depends on the regeneration rate and the miscibility between the solvent and antisolvent[190]. This transformation from native Cellulose I to regenerated Cellulose II has been widely reported, for instance, by Juan Francisco Delgado et al. [184] and Zhang et al. [191], who demonstrated that water's high polarity and protic nature promote crystalline rearrangement during precipitation.

Meanwhile at the molecular level, water functions both as a precipitant and as a structural mediator. The replacement of solvent molecules by water reorients cellulose hydroxyl groups from a parallel to an antiparallel configuration, leading to the formation of the Cellulose II structure [192]. The frequent observation of this polymorphic conversion (Cellulose I → Cellulose II) across multiple studies highlights the thermodynamic stability of the hydrated cellulose lattice. In addition, rheological investigations by Hauru et al. [187] revealed that water–cellulose interactions strongly affect the spinnability, viscosity, and diffusion behavior of cellulose dopes. This influence fiber uniformity and solution stability during dry-jet wet spinning. Overall, the body of evidence strongly supports water as a versatile, sustainable anti-solvent capable of producing regenerated cellulose with properties comparable or superior to those achieved using conventional approaches.

CHAPTER 3
RESEARCH METHODOLOGY

3.1 Introduction

In Chapter 3, the methodologies will be separated into three sections. First, the details of the computational setup for the Molecular Dynamics (MD) simulations, which predict the interaction between cotton (cellulose) and polyester (PET) in the presence of DMSO. Next, the simulation predictions will be validated using a Taguchi-based Design of Experiments (DOE) to optimise the dissolution parameters and evaluate their significance on the dissolution efficiency. Finally, the fibre regeneration process will be performed, followed by comprehensive characterisation analyses of the regenerated fibres to examine their structural, morphological, and thermal properties after regeneration.

3.2 Materials

The interaction between polymer and solvent was predicted using Materials Studio software (2023), developed by BIOVIA Dassault Systèmes that designated with 64 cores and 128 GB memory. Recycled cotton and polyester fabrics were obtained from the local market and decolourised using a 6% sodium hypochlorite (NaOCl, Chemiz) solution. The dissolution process was carried out using dimethyl sulfoxide (DMSO, 99.9%, Chemiz), and the fibres were regenerated using distilled water. All chemicals were used without purification and purchased from BT Science Sdn Bhd (Selangor, Malaysia).

3.3 Research Framework

Figure 3.1 illustrates a systematic research framework designed to address the research objectives in this study. The framework was structured based on three core objectives which are integrate a fundamental computational modelling, robust optimisation by experiment, and comprehensive characteristic validation. This

approach begins with the investigation of the molecular interactions of cotton (cellulose) and polyester (PET) with dimethyl methyl (DMSO) solvent through Molecular Dynamics (MD) simulations. Next, the result analysis from MD simulation was used to guide an optimise dissolution parameters of cellulose and PET in the DMSO solvent by evaluate their significance on the dissolution efficiency. Finally, the fibre regeneration process was carried out, followed by comprehensive characterisation of the regenerated fibres to evaluate their structural, morphological, and thermal properties. This comprehensive approach ensures the research focuses on achieving a practical, well-defined result.

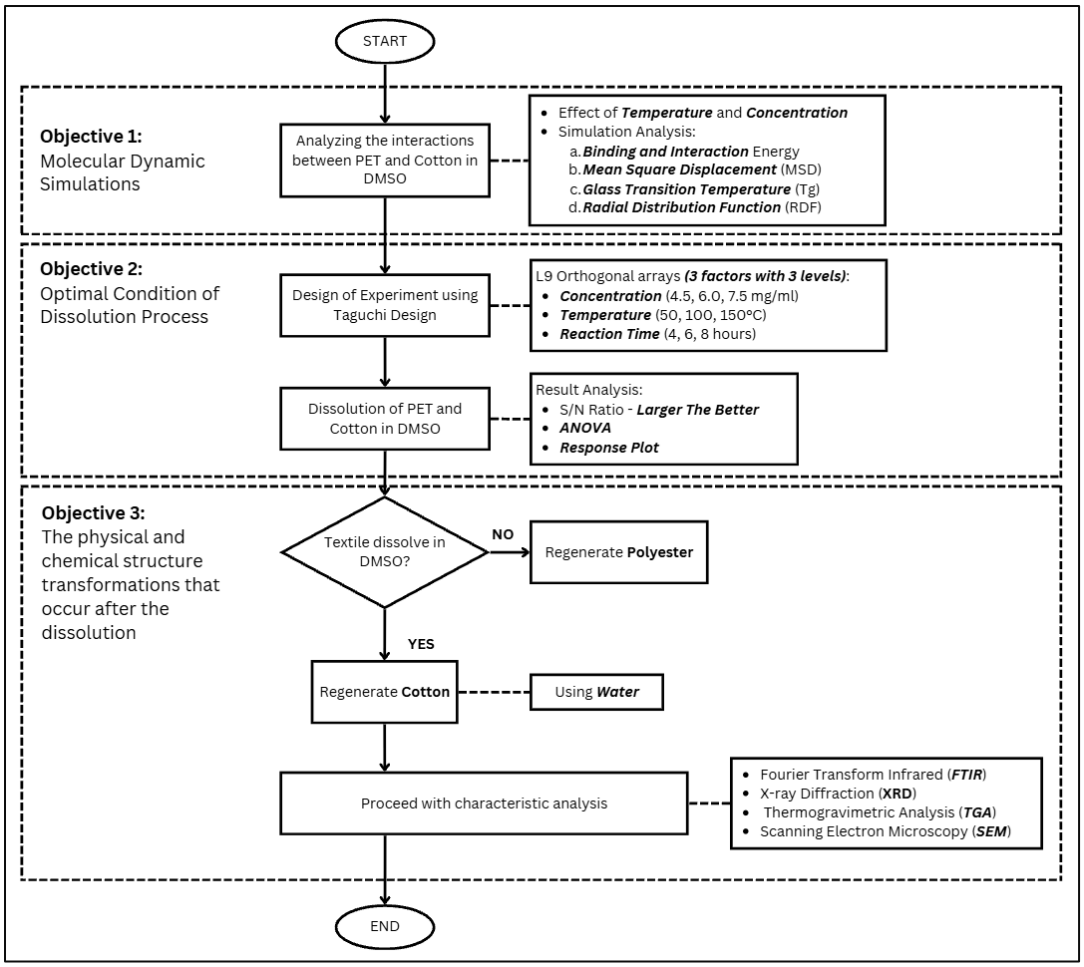

Figure 3.1 Research Framework for Molecular Interaction Study of Eco-Friendly Dimethyl Sulfone Solvent on the Enhancement of Cellulose and Polyester Recovery from Recycled Textiles Study

3.4 Molecular Dynamics Simulation

In this study, molecular dynamics (MD) simulation was used to understand the interaction of fibres with the DMSO solvent. Then, the evaluation of interaction polymer-solvent system were enable the prediction of the system's behaviour in detail. In this section, only the influence of temperature and concentration. To obtain reliable results, careful setup and control of the simulation conditions were carried out.

3.4.1 Simulation Setup

Figure 3.2 presents the overall workflow for constructing and initialising the molecular dynamics (MD) simulation system. Firstly, the molecular structures of polyethylene terephthalate (PET), cellulose, and dimethyl sulfoxide (DMSO) monomers were imported from the Cambridge Structural Database (CSD) into Materials Studio for model preparation (Figure 3.2(a)). Polyethylene terephthalate (PET) was modelled using its repeating ethylene terephthalate unit, derived from the condensation of ethylene glycol and terephthalic acid [31]. Each repeat segment comprises an aromatic terephthalate ring, responsible for π–π stacking interactions and dipolar stabilisation, together with an aliphatic ethylene spacer that imparts conformational flexibility and facilitates rotational motion along the polymer backbone [30].

Meanwhile, the cellulose component was represented by the β-(1,4) glucose repeating unit, which constitutes the fundamental structural motif of the polymer. Cellulose is a linear homopolymer of β-D-glucopyranose residues covalently linked through β-(1,4) glycosidic bonds, forming an extended chain stabilised by an extensive network of intra- and intermolecular hydrogen bonds [193]. This hydroxyl-rich configuration gives rise to the high crystallinity and mechanical rigidity characteristic of cotton fibres [194]. This structural representation captures the essential physicochemical features governing the intermolecular interactions and chain mobility of the PET and cellulose with DMSO system investigated in the simulation.

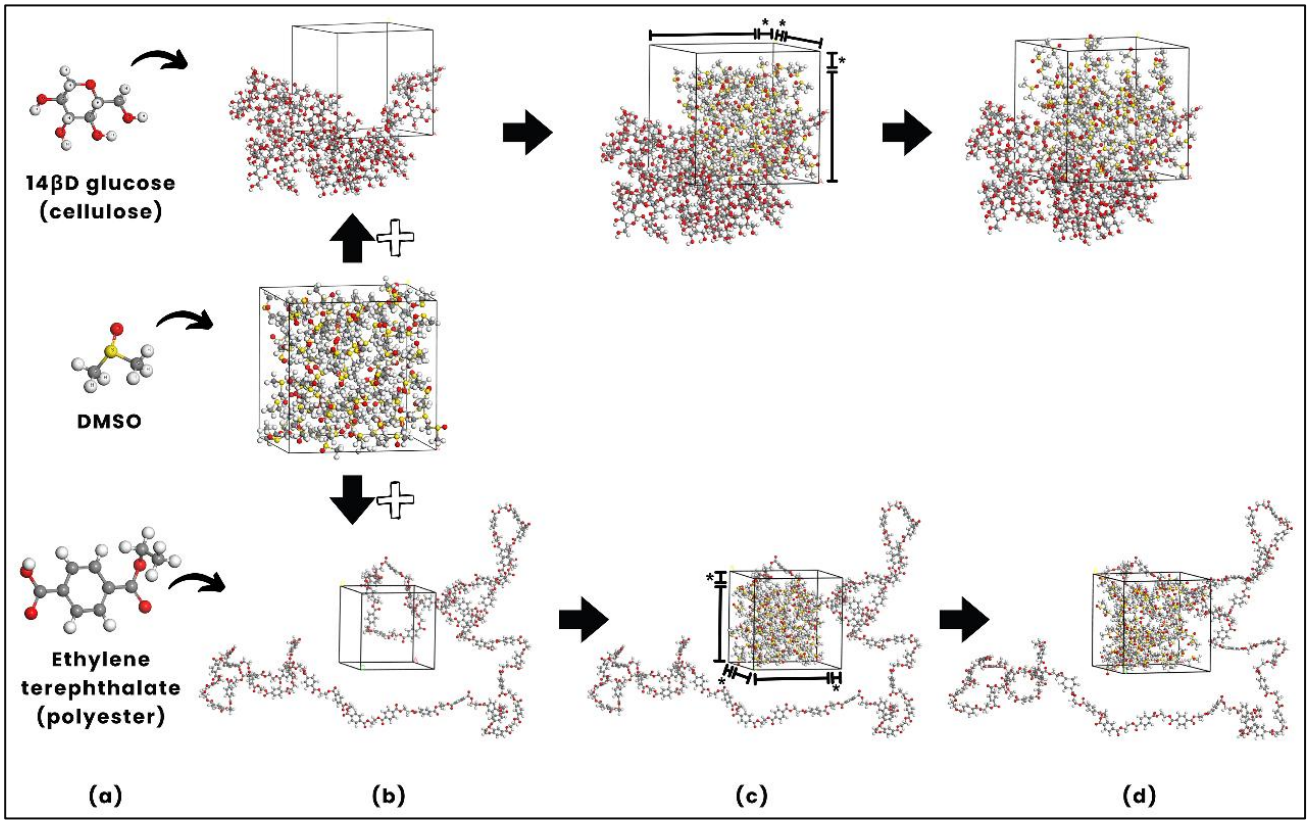

Figure 3.2 The Example of MD Simulation Procedural Setup for Cotton/DMSO.

(a) The Monomers of cotton and DMSO were imported from CSD, (b) A single chain of 50 repeating unit cotton and respective DMSO molecules were built in a separate cell and the energy of each cell were optimised (c) Combined the molecules into a cell with a tolerance distance of 3.0Å (*) from the original cell size and (d) The system's energy were minimised before proceed to MD simulation. All grey atom is the carbon, white atom is the hydrogen, red atom signifies the oxygen and yellow atom is the sulfur.

Next, a single molecular chain of polyester (ethylene terephthalate) and cellulose (14β-D-glucose) was then built based on their respective repeating units (based on Table 3.1) using the "Random Copolymer" tool with a cell size of 23 $Å^3$ (Figure 3.2(b)). A chain length of 50 repeating units was selected as the reference model, corresponding to a polymer concentration of 7.5 mg/ml. The selection of a chain length of 50 repeating units (RUs) in molecular dynamics (MD) simulations represents a deliberate balance between computational feasibility and physical representativeness of the polymer chain's behaviour in solution. This selection ensures that the simulated polymer captures the important interaction characteristics such as molecular weight polymers. This will be maintaining the simulation times and system sizes within the limits of available computational resources [127].

Table 3.1
The Basic Parameters of the Polymer and the Combined Polymer/DMSO System.

System	Concentration (mg/ml)	$N_{PET/Cellulose}$	N_{DMSO}	Density (g/cm^3)	Volume ($V/Å^3$)	Cell Size ($Å^3$)
PET/DMSO	N/A	50	0	1.330	11999	23
	4.5	30	121	1.340	21952	27
	6.0	40	121	1.619	19683	27
	7.5	50	121	1.722	19683	27
Cellulose/DMSO	N/A	50	0	1.140	13465	23
	4.5	30	104	1.072	23395	27
	6.0	40	104	1.370	19683	27
	7.5	50	104	1.465	19683	27

In the pure PET system and the pure cellulose system, the weight fraction of DMSO was set to 0 because no solvent molecules were included in these reference simulations. These systems served as baselines to evaluate the inherent structural density, volume, and molecular packing behaviour of the pure polymers in the absence of solvent effects. Consequently, only the polymer component contributed to the total system mass, yielding a DMSO weight fraction of zero. This size has been commonly adopted in polymer–solvent simulations to ensure adequate configurational sampling of intra- and intermolecular dynamics without excessive computational cost [127]. The

final volume and density of pure PET and Cotton (Cellulose) are also shown after the optimisation. The system was valid if only the density of the PET system is 1.330 g/cm^3, which is comparable to the amorphous PET polymer's experimental density (1.330 g/cm^3) [127]. In contrast, the density of the cellulose system is 1.140 g/cm3, which is close to the amorphous cellulose polymer that was measured by experimental density of (1.140 g/cm^3) [195]. The comparison between simulated and experimental data confirms the validity of the optimisation method and the reliability of the computational methods and parameters used in this study.

Each Polymer/DMSO system was simulated under various conditions, with temperatures (323, 373, and 423 K) and polymer concentrations (4.5, 6.0, and 7.5 mg/ml). On the evaluation of temperature effects, the polymer concentration was maintained at 7.5 mg/ml, equivalent to 50 repeating units [127]. On the other hand, for the influence of concentration study, the temperature was fixed at 423K to maintain consistent thermal conditions during the analysis. To vary the polymer concentration, the number of repeating units (N) of each polymer chain was modified. This was achieved by scaling the initial chain length of 50 repeating units according to the ratio of polymer solubility in DMSO at different concentrations, as described in Eqn. 3.1.

$$N_{adjusted} = N_{initial} \times \frac{C_{desired}}{C_{reference}} \tag{3.1}$$

The number of DMSO molecules (N_{DMSO}) was automatically generated by the molecular modelling software based on the predefined concentration, target density, and simulation cell dimensions. This automated computation ensured that the solvent content was consistent with the desired polymer weight fraction and that the periodic cell contained an appropriate solvent environment for molecular relaxation and diffusion analysis. Further steps, all the cell systems were optimised using Forcite Geometry Optimisation tools with the Smart Minimiser algorithm. After that, the polymer chains were combined with DMSO molecules in a 27 Å^3 simulation box (cell), with a tolerance distance of 3.0 Å (*) from the original cell size (Figure 3.2(c)) and generated through the Amorphous Cell module at room temperature [127]. Then, the system energy was optimised by using Forcite Energy Minimisation tools to obtain a more stable structure (Figure 3.2(d)). The thermostat (Andersen) and Barostat (Berendsen) were used to control the temperature and pressure, respectively. In this

study, the COMPASS force field was selected to perform the high-precision calculations throughout the molecular dynamics simulations by calculating the total energy of the system using the following Eqn. 3.2 [196]:

$$E_{total} = E_b + E_\theta + E_\varphi + E_\chi + E_{cross} + E_{ele} + E_{vdw} \quad (3.2)$$

Where E_{total} is the total energy, E_b is bond stretching energy, and E_θ is angle bending energy. E_φ is dihedral torsion energy, E_χ is out-of-plane energy, E_{cross} is cross term interaction energy, E_{ele} is electrostatic interaction energy, and E_{vdw} is van der Waals interaction energy. The COMPASS force field was selected due to its parameterisation for a wide range of organic, polymeric, and condensed-phase systems, enabling accurate representation of covalent bonding, non-bonded van der Waals interactions, and electrostatic effects within polymer–solvent environments. Hence, COMPASS can accurately capture hydrogen bonding, dipole–dipole interactions, and torsional flexibility within the PET/DMSO and Cellulose/DMSO systems. Finally, COMPASS had been selected as force field since it the most suitable for polar solvents systems such as DMSO and polymers rich in oxygen-containing functional groups (–C=O, –OH) [197].

3.4.2 Thermodynamics Properties Analysis

In this work, molecular dynamics (MD) simulations were employed to investigate the thermodynamics properties, including binding energy (BE), interaction energy (IE), glass transition temperature (Tg), and mean square displacement (MSD). By employing this method, the study offered consistent and reliable results of the thermodynamic and kinetic behaviour of the polymer-solvent system.

3.4.2.1 Binding Energy (BE) and Interaction Energy (IE)

The binding energy between the polymer matrix and the solvent molecules was calculated to quantify the strength of intermolecular interactions. Accordingly, throughout the molecular dynamics simulations, the binding energy and interaction

energy of the system will be applied as expressed by the following Eqn. (3.3) and (3.4) [127]:

$$E_{Binding} = -E_{Interaction} \tag{3.3}$$

Where the interaction energy was determined by subtracting the total energies of the isolated components from the total energy of the composite system:

$$E_{Interaction} = E_{Total} - \left(E_{Polymer} + E_{Solvent}\right) \tag{3.4}$$

The calculation was performed using the Forcite module with a COMPASS force field, and the simulation cell was optimised prior to energy evaluation. Energy minimisation was carried out employing the Smart Minimiser algorithm until the convergence criteria were satisfied (energy tolerance: 1×10^{-4} kcal/mol, force tolerance: 0.005 kcal/mol/Å).

3.4.2.2 Mean Square Displacement (MSD)

MSD analysis was performed to assess the mobility of the molecules within the simulation cell. The simulations were conducted under the NPT-NVT ensemble for a duration of 1ns. MSD was calculated using the trajectory analysis module based on the mobility of polymer chains and can be measured by Eqn 3.5:

$$MSD = \langle |r_i(t) - r_i(0)|^2 \rangle \tag{3.5}$$

Where $r_i(t)$ is the coordinates of the atom at time t, $r_i(0)$ is the initial position of atoms in the system, and the angle bracket is the statistical average value of the time of the system under study. MSD quantifies the average distance travelled by molecules or atoms over time, reflecting molecular mobility within a material [127]. Next, the diffusivity of molecules can be calculated using the diffusion coefficient, D, where the Eistein's relation for Brownian motion will be applied in Eqn. 3.6:

$$D = \lim_{t\to\infty}\left(\frac{\langle|r_i(t)-r_i(0)|^2\rangle}{6t}\right) \quad (3.6)$$

The slope of the linear of the MSD versus time curve was determined through linear regression. The diffusion coefficient was reported as the average over all relevant atoms or molecules. All results were compared across different simulation conditions to understand the influence of temperature and composition.

3.4.2.3 Glass Transition Temperature (Tg)

In molecular dynamics (MD) simulations, the estimation of glass transition temperature (Tg) requires a systematic procedure, as outlined by previous studies [198]. Firstly, MD simulations are conducted across a range of temperatures, typically between 200 K and 500 K for polymer systems [152]. The calculated specific volume of the system obtained at each temperature. Then, calculated specific volume were plot against temperature. Linear regression is applied to the data to produce two best-fit lines representing the temperature regions below and above the transition. The point at which these two lines intersect is identified as Tg the of the system.

3.5 Dissolution of Recycled Textile

The dissolution of recycled textiles goes through several important steps to prepare the fibre material before it can be regenerated. The process usually starts with removing any remaining colour from the fabric to ensure that the sample is clean. After that, the experimental conditions are optimised using the Taguchi method to determine the most effective settings. Once these steps are completed, the material is then proceeded to the dissolution process, where the textile fibres are dissolved in the selected solvent for further analysis and regeneration.

3.5.1 Decolourisation

Based on the preliminary study conducted before, the recycled fabric sample were shredded into small pieces (5mm x 5mm) to increase the surface area, thereby enhancing the efficiency of the decolourisation process. A solution of 12.4 ml of 6%

sodium hypochlorite (NaOCl) was diluted with distilled water to obtain 20 ml of 0.6 M NaOCl, which was used for the batch decolourisation treatment. An ultrasonic bath tank was filled with an adequate amount of water, and 20 ml of diluted NaOCl solution. The ultrasonic bath was then heated to 50°C using the degas mode to remove air bubbles that might have interfered with the decolourisation process. Once the desired temperature was reached, 300mg/20ml of each type of fabric sample was placed into separate beakers containing the NaOCl solution. The ultrasonic frequency was set to 80 kHz at sweep mode to ensure uniform exposure of the textiles to the chemical treatment. The fabric samples were fully submerged in the solution and undergo the decolourisation process for 60 minutes. After that, the fabric samples were carefully removed from the NaOCl solution and immediately immersed in distilled water for 5 minutes. This step was for removing any residue of the NaOCl solution. Then, the samples were subjected to wet blending using a high-speed blender for mechanical size reduction into smaller fibrous sample. The slurry then dried in an oven at 100°C for 2 hours to remove any remaining moisture. Once completely dried, the samples were dry blending using a laboratory-scale grinder to further reduce the particle size, ultimately producing a fine shredded fibre [199]. Figure 3.3 shows the transformation of both cotton and PET fibre after the decolourisation process.

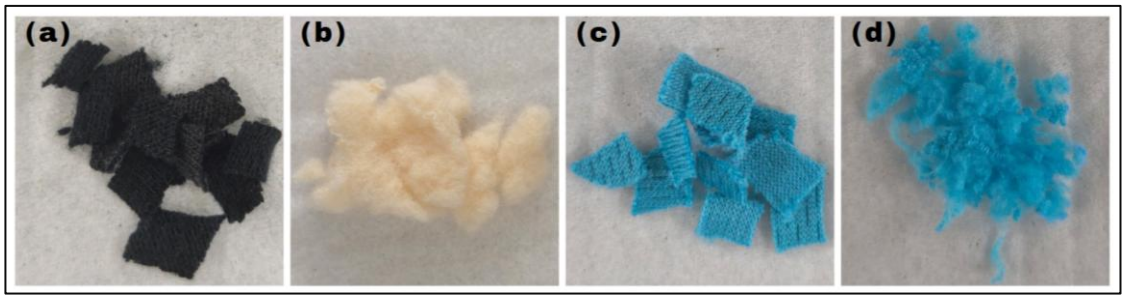

Figure 3.3 (a) Cotton Before, (b) Cotton After, (c) PET Before, (d) PET After Decolourisation Process Using 0.6M NaOCl

3.5.2 Dissolution

Table 3.4 shows the mass of each treated sample for the different concentrations tested. Each sample was carefully weighed and placed in 10 ml of DMSO at its assigned temperature, then left to dissolve for 24 hours. To ensure consistent and reliable results, every experiment was repeated three times. After the dissolution step, the mixtures were

filtered using standard filter paper to separate any remaining solid fibres from the solvent. The undissolved fibres were collected and dried in an oven at 150 °C for 2 hours to remove any leftover moisture. Figure 3.4 illustrates the dissolution process step using DMSO.

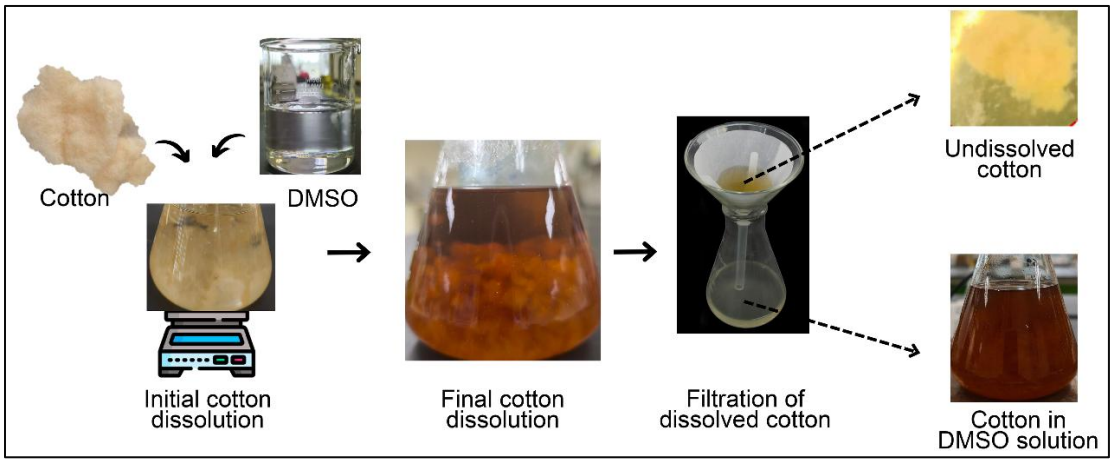

Figure 3.4 Dissolution Process Step using DMSO (Example experiment of 4.5mg/ml Cotton/DMSO)

Table 3.2
Mass of Treated Sample for Each Experiment.

Exp No.	Concentration (mg/ml)	Mass of Treated Sample (mg)
E1	4.5	45
E2	6.0	60
E3	7.5	75
E4	4.5	45
E5	6.0	60
E6	7.5	75
E7	4.5	45
E8	6.0	60
E9	7.5	75

Finally, the average dissolution percentage from the three trials was calculated and used for further analysis. The percentage of dissolution, D (%), was determined by the following Eqn. 3.7 to validate the dissolving of cotton and polyester in DMSO solvent [194]:

$$Dissolution\ (\%) = \frac{Initial\ Weight\ (mg) - Final\ Weight\ (mg)}{Initial\ Weight\ (mg)} \times 100\% \quad (3.7)$$

3.5.3 Taguchi L9 Orthogonal Array Design

Table 3.5 involves the manipulation of three key parameters temperature, concentration, and reaction time with three-level factorial design, with temperature set at 50°C (Low), 100°C (Mid), and 150°C (High); concentration at 4.5 mg/ml (Low), 6.0 mg/ml (Mid), and 7.5 mg/ml (High); and contact time at 4 hours (Low), 6 hours (Mid), and 8 hours (High). These parameter levels were selected based on findings from preliminary experimental results to ensure relevance and operational feasibility within the dissolution process parameters.

Table 3.3
Factors and Levels Parameters for the Dissolution Process of Cotton and Polyester in DMSO.

Factors	Level 1	Level 2	Level 3
Temperature (°C)	50	100	150
Concentration (mg/ml)	4.5	6.0	7.5
Contact Time (Hours)	4	6	8

In this study, the Taguchi method, specifically the L9 orthogonal array, was employed as a statistical tool to systematically design the experiment involving the dissolution of textile materials under varying conditions of temperature (50, 100, 150°C), concentration (4.5, 6.0, 7.5 mg/ml), and dissolution time (4, 6, 8 hours). This approach significantly reduces the total experimental workload while maintaining the analytical precision required to distinguish the main and interaction effects between temperature, concentration, and reaction time. In the present investigation, the L9 orthogonal array was adopted to represent three factors at three levels each, thereby condensing 27 possible combinations into nine strategically distributed experimental runs (E1–E9), as listed in Table 3.6.

The Taguchi method is widely recognised as a reliable approach as it employs statistical evaluation, such as orthogonality and signal-to-noise (S/N) ratio analysis [200]. These principles enable the measurement of the stability and sensitivity of the process to changes in various conditions. This method was able to identify the influence

of each factor on the overall result of the experiment [201]. It also helps improve consistency of the result by analysing the effect of each factor to avoid bias from overlapping influences. This makes the Taguchi method useful for dissolution studies to determine the influencing factors such as temperature, polymer concentration, and dissolution time on the polymer–solvent interactions [202]. By applying this approach, the optimum conditions of the dissolution process can be achieved while minimise the experimental errors.

Table 3.4
L9 Taguchi Design Showing Different Combinations of Temperature, Concentration, and Reaction Time used to Study the Dissolution of Cotton and Polyester in DMSO.

Exp No.	Temperature (°C)	Concentration (mg/ml)	Contact Time (hrs)
E1	50	4.5	4
E2	50	6.0	6
E3	50	7.5	8
E4	100	4.5	6
E5	100	6.0	8
E6	100	7.5	4
E7	150	4.5	8
E8	150	6.0	4
E9	150	7.5	6

Next, the evaluation of dissolution effectiveness was validated using Signal-to-Noise (S/N) ratio under the "larger-the-better" criterion. It serves as a robustness metric in Taguchi design, aiming to maximise desired responses while minimising variability. In the context of polymer dissolution optimisation, the S/N ratio calculated using Eqn. 3.8 quantifies dissolution efficiency. Higher S/N ratios indicate process parameters that continuously enhance dissolution performance, such as a higher temperature or optimum solvent concentration, while reducing resistance to outside disruptions, such as inconsistent mixing or other noise factors [21].

$$\frac{S}{N}\ Ratio = \ -10\ \log_{10}\frac{1}{n}\sum_{i=1}^{n}\frac{1}{yi^2} \tag{3.8}$$

All the experimental procedures were conducted in triplicate to ensure their consistency, accuracy, and reliability. The process can be considered complete if the validation criteria are met the optimum condition in L9 parameters.

3.6 Characteristic Analysis of Regenerated Fibre

The regeneration of fibres was carried out to validate the preserve chemical structure of the components. In this section, the experimental framework was starting from pre-regeneration character analysis, regeneration process, and post-regeneration character analysis. This is to ensure procedural consistency and material compatibility throughout. Analytical methods such as spectroscopic, thermal, and morphological evaluations were employed to examine changes in the structural integrity and functional properties of the fibres.

3.6.1 Pre-Regenerated

The chemical integrity of the dissolved cotton in DMSO had been evaluated using UV-Vis spectrophotometry (UV1800, Shimadzu) and Fourier-Transform Infrared spectroscopy (FTIR, Bruker VERTEX 70) before proceed to the regeneration process. UV-Vis analysis was scanned from 300 to 700 nm at 1 nm intervals. This is for monitoring and identify any potential degradation products that might appear as new absorbance peaks or shifts within the UV-Visible range. Next, FTIR spectroscopy was performed at an average of 32 scans over the 400–4000 cm^{-1} range. The presence of characteristic functional groups associated with cellulose will detect. This combination analysis will provide evidence that the cotton remained chemically intact in the DMSO medium, with no formation degradation products even though the dissolution were at 150°C. Hence, this confirms the suitability of DMSO as a solvent for high-temperature dissolution studies involving natural cellulosic textiles without compromising their chemical structure.

3.6.2 Regeneration Process

The regeneration of cotton from cotton/DMSO solution using antisolvent precipitation. Water, being a strong non-solvent for cellulose but miscible with DMSO, was introduced to the polymer solution. This disrupts the solvation of cellulose chains by DMSO and precipitate into regenerated cotton fibres (ReC) [203]. The process is meticulously controlled to ensure high purity of the final product. The regeneration was carried out by adding deionised water at ambient temperature (25°C) with ratio of 10:1 water to Cotton/DMSO solution volume ratio [204]. Following precipitation, the ReC is left to coagulate for a minimum of 24 hours to allow for the initial diffusion of DMSO out of the cellulose matrix. Then, the precipitate cotton was extracted by using a separating funnel and then proceeded to a slow dry at 60°C overnight. Next, the dry ReC was washed using deionised water for a minimum of three washing cycles to remove any DMSO residues.

3.6.3 Post-Regenerated

The dried regenerated cotton fibres (ReC) were evaluated its thermal behaviour, morphology, and crystallinity using Thermogravimetric analysis (TGA), Scanning Electron Microscopy (SEM), and X-ray Diffraction (XRD). Thermogravimetric analysis (TGA 8000, Perkin Elmer, USA) was performed to analyze the thermal changes of regenerated fibre. About 10 mg of cotton was placed in the sample pans and heated from 25℃ to 700℃ with a heating rate of 10℃/min. Nitrogen was used as both a balance gas (flow rate of 10ml/min) and sweep gas (flow rate of 60ml/min). The TGA results were obtained at a heating temperature range of 105℃ to 700℃ [205].

Next, surface morphology of the regenerated fibre was examined using a Scanning Electron Microscope (JEOL JSM-IT200, Japan). Samples were sputter-coated with an approximately 5nm gold layer to enhance surface conductivity and imaging resolution. Observations were carried out at an accelerating voltage of 10 kV with magnifications series of 100, 500, and 1000 times. The SEM micrographs provided findings into the surface smoothness, fibrillar alignment, and the occurrence of pores or defects originating from the regeneration process. Morphological characteristics were further interpreted in conjunction with crystallinity data and DSC thermograms to determine structure–property relationships.

Finally, the crystalline structure and degree of crystallinity were determined using X-ray Diffraction (XRD) analysis performed on a diffractometer equipped with Cu Kα radiation (λ = 1.5406 Å). The diffraction patterns were analysed to identify characteristic cellulose peaks, and the crystallinity index (CrI) was calculated using the Segal method (Eqn. 3.9).

$$CrI = \frac{I_{002} - I_{am}}{I_{002}} \times 100\% \quad (3.9)$$

Where I_{002} is the intensity of the crystalline peak at 2θ ≈ 22.5°, and I_{am} is the intensity of the amorphous background at 2θ ≈ 18° with a step size of 0.02°, operating at 40 kV and 30 mA. The obtained diffractograms were analysed to identify characteristic cellulose reflections and to estimate the relative crystallinity index, which was subsequently correlated with the DSC thermal parameters and SEM morphological observations to provide a comprehensive assessment of the regenerated fibre structure.

CHAPTER 4
RESULTS AND DISCUSSION

4.1 Molecular Dynamics Simulation

In this study, MD simulation was used to predict the compatibility of polyester (PET) and cotton (cellulose) with DMSO. Both PET/DMSO and Cellulose/DMSO system were simulated at different temperature and concentration. Notably, before proceeding with the MD simulation, both systems must undergo energy minimization. Table 4.1 and 4.2 show the value of total energy (E_{Total}) before and after the energy optimisation using Forcite Energy Minimisation tools for each system. The decrease of E_{Total} of each system after energy minimisation steps shows that the systems are stable and ready for MD simulation. After the energy of the cell was reduced and the density of the system was confirmed, the MD simulation was proceeded using a combination of Canonical ensemble (NPT) and Isothermal–isobaric ensemble (NVT) with a total simulation time of 1 ns [206].

Table 4.1
The Total Energy Before and After Optimisation Steps for Each System at Different Temperatures (K).

System	Temperature (K)	E_{Total} Before (kcal/mol)	E_{Total} After (kcal/mol)
PET/DMSO	323	9.84×10^{11}	5,908
	375	6.13×10^{11}	7,437
	423	3.63×10^{11}	9,104
Cellulose/DMSO	323	120.33×10^{11}	3,832
	375	86.54×10^{11}	3,025
	423	23.95×10^{11}	-857

Table 4.2
The Total Energy Before and After Optimisation Steps for Each System at Different Concentrations (mg/ml).

System	Concentration (mg/ml)	ETotal Before (kcal/mol)	ETotal After (kcal/mol)
PET/DMSO	4.5	2.59×10^{11}	7,167
	6.0	3.10×10^{11}	8,834
	7.5	3.63×10^{11}	9,104
Cellulose/DMSO	4.5	9.86×10^{11}	-1172
	6.0	13.35×10^{11}	-1033
	7.5	23.95×10^{11}	-857

Figure 4.1 shows that the total energy remained stable throughout the simulation. This consistency indicates that the MD setup (force field, time step, total simulation time, thermostat/barostat algorithms, and ensemble) was appropriate [127]. Figure 4.1(a) shows how the system's temperature changes over time during the simulation. The temperature remains close to an average of approximately 420 K, with minor fluctuations of around ±30 K [207]. Since there is no apparent drift or continuous rise or fall in temperature, it indicates that the thermostat successfully maintained the target temperature and that the system reached thermal equilibrium [208].

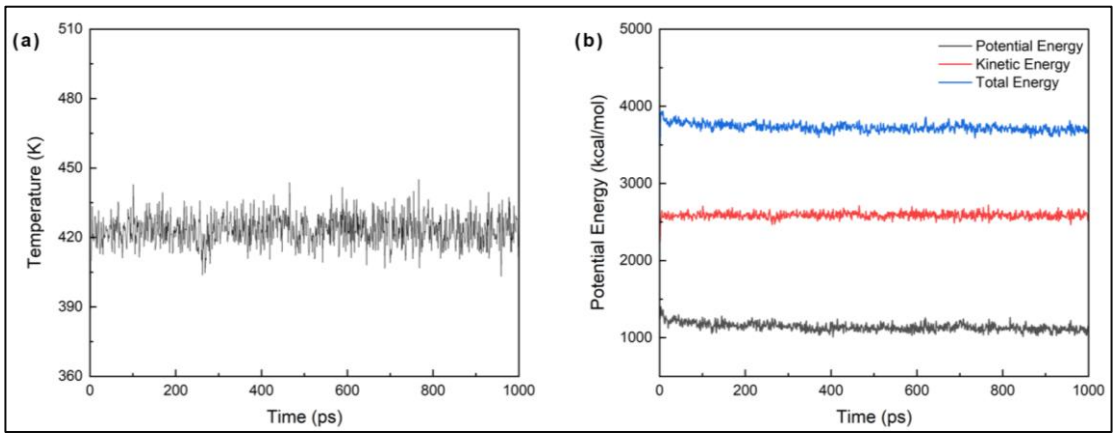

Figure 4.1 (a) Temperature Curve (b) Energy Curve of Equilibration System throughout the 1000 ps Trajectory.

Overall, the temperature pattern confirms that the system's kinetic energy is well balanced under the intended thermal condition. Meanwhile, in Figure 4.1(b), the graph shows that both potential energy (black) and kinetic energy (red) fluctuate slightly in a

random way but do not show any noticeable drift. Meanwhile, the total energy (blue) stays almost constant throughout the 1000 ps simulation period. This indicates that the algorithm method used maintains the energy conservation without any external energy build-up [209]. The stable potential energy shows that the system has achieved structural equilibrium, with no significant molecular rearrangements or solvent disturbances. At the same time, the steady total energy confirms that the simulation is numerically reliable and thermodynamically stable [210], [211]. Therefore, the system is well-equilibrated and ready for further analyses such as mean square displacement (MSD), diffusion coefficient (D), or binding and interaction energy evaluation.

4.1.1 Effect of Temperature

Table 4.3 visualised comparisons of the system configurations reveal that temperature-dependent had change the polymer compactness and chain conformation. At 323 K, both cellulose and PET restricted molecular motion and formed a compact structure. After simulation, both systems have a dense hydrogen-bonded network is maintained, showing minimal configurational change throughout the simulation [212]. This stability suggests strong interchain cohesion and limited solvent penetration. As the temperature increases to 373 K, a noticeable loosening of the cellulose chains occurs as the chains becoming less ordered and slightly swollen. This reflecting the partial disruption of hydrogen bonds by DMSO. In contrast, the PET chains do not undergo any significant conformational changes and remain relatively intact, suggesting that the intermolecular interactions within the PET matrix continue to dominate over the PET–DMSO interactions at this temperature [83]. Finally, at 423 K, the structural differences of both polymers system become obvious. Cellulose retains overall cohesion but shows a more open and less entangled arrangement. Additionally, PET exhibits substantial conformational rearrangement, characterized by increased chain separation, reduced packing density, and a more disordered morphology [133]. These structural changes indicate enhanced solvent accessibility and molecular mobility at elevated temperature, reflecting the progressive weakening of polymer–polymer interactions and the increased influence of polymer–solvent interactions [213].

Table 4.3
Comparison of Cellulose/DMSO and PET/DMSO System Before and After (time step = 1ns) MD Simulations at 323 K, 373 K, and 423 K.

Temp	Cellulose/DMSO		PET/DMSO	
	Before	After	Before	After
323K	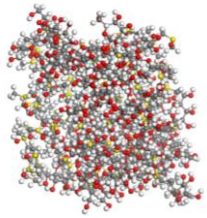	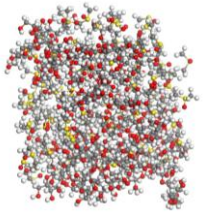	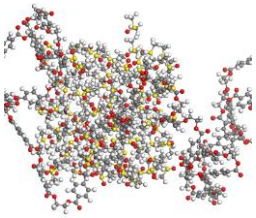	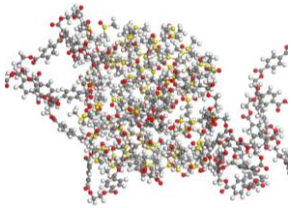
373K	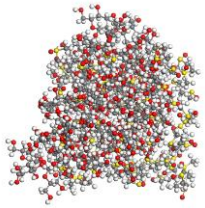	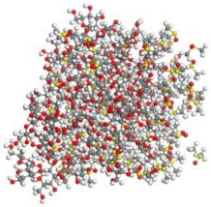	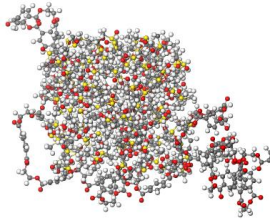	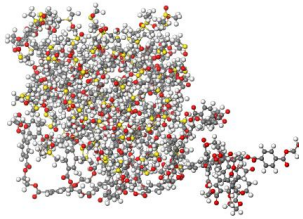
423K	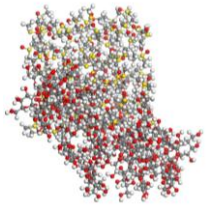	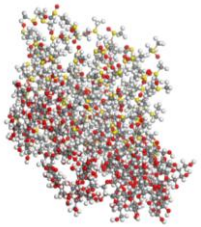	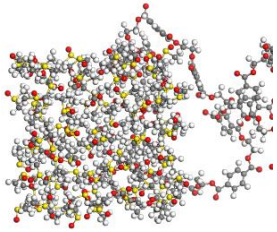	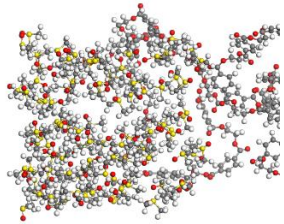

Figure 4.2 shows the hydrogen-bond interaction between the oxygen atom of DMSO (O_{DMSO}) and the hydrogen atom of cellulose ($H_{cellulose}$). This interaction shows DMSO as a strong hydrogen-bond acceptor, disrupting the native hydrogen-bond network in cellulose. The electron-rich oxygen in DMSO attracts the hydrogen of the hydroxyl group in cellulose, weakening the cellulose interchain hydrogen bonds [145]. As temperature increases, these $O_{DMSO}\cdots H_{cellulose}$ interactions become more dynamic, resulting in partial chain separation and improved solvent penetration.

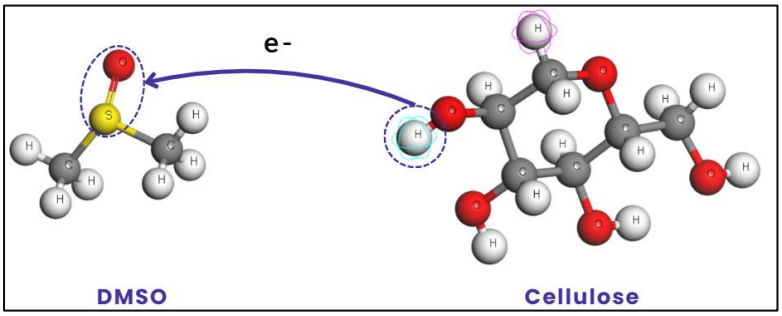

Figure 4.2 $O_{DMSO}\cdot H_{cellulose}$ Interaction in the Cellulose/DMSO System.

DMSO is a strong hydrogen-bond acceptor and interacts with cellulose's hydroxyl groups, reducing the internal bonding energy. This interaction causes swelling and partial chain separation, especially as the temperature increases. In Cellulose/DMSO systems, increasing temperature has enhanced glycosidic flexibility while decreasing hydrogen-bond lifetimes. This indicates that the configural structure was shifted from compact to swelling cellulose [214]. Overall, the result data indicate that DMSO's strong hydrogen-bond-accepting capacity plays an important role in reducing cellulose interactions and enabling dissolution.

4.1.1.1 Interaction Energy and Binding Energy

Notably, the indicator of polymer-solvent compatibility was comparing the interaction energy and binding energy of both systems. Once the polymer system been identified, the selection of favourable temperature was obtained. Based on the equation 3.3 (refer section 3.4.2.1), the lower interaction energy shows the weaker hydrogen bonding between polymer-polymer chain. In contrast, the higher binding energy indicates the stronger compatibility between the polymer and solvent. Figure 4.3 illustrates the interaction energy (Figure 4.3(a)) and binding energy (Figure 4.3(b))

between the polymers (PET and cellulose) and DMSO at different temperatures (323K, 373K, and 423K). The interaction energy in the PET/DMSO system forms a U-shaped trend, reaching its lowest point at 373K. This indicates that PET interacts most effective with DMSO at 373K, where the balance between molecular motion and intermolecular attraction appears to be most favourable. However, PET also exhibits a lower binding energy (less than –6,000 kcal/mol) compared to cellulose (more than –4,000 kcal/mol). Hence, the overall result indicates that cellulose was more favourable interaction compared to PET. A study by Huang et al. provides a mechanistic explanation for this phenomenon where the interaction between the polymer and the solvent becomes stronger than the cohesive forces within the polymer itself and between solvent molecules, causing the system to unexpectedly compact to each other instead of dispersing [215]. Research by Cheng et al. mentioned that the interaction energies also impact the diffusion of small molecules within polymer matrices. The study identified that solvent diffusion slowed down by larger interaction energies between the solvent and the polymer matrix. In such cases, solvent molecules promote chain compaction and potentially hinder complete dissolution [150]. This deviation from ideal mixing behaviour suggests the emergence of nanoscale heterogeneities or phase separation under certain thermal regimes.

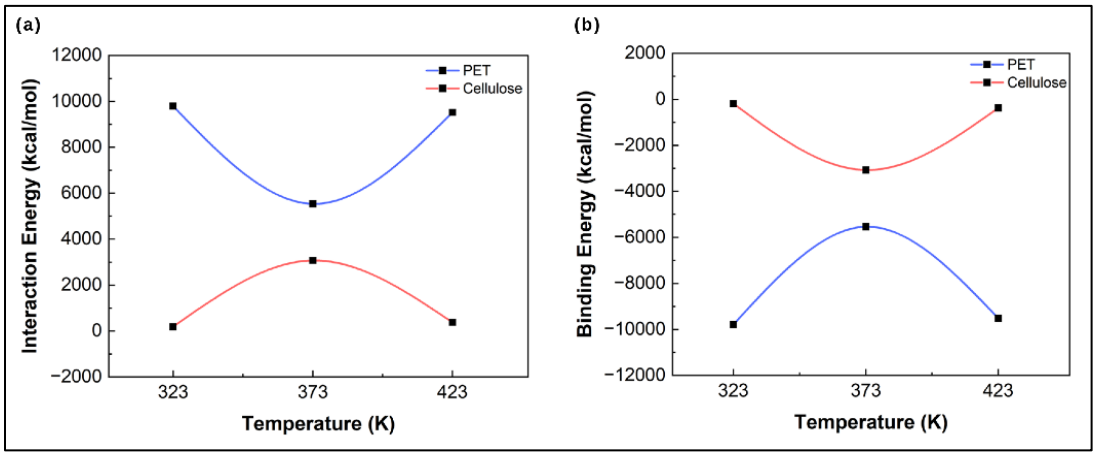

Figure 4.3 (a) Interaction Energy (b) Binding Energy for Cellulose/DMSO and PET/DMSO at 323K, 373K, 423K

In contrast, cellulose also shows a parabolic interaction energy and binding energy profile. However at both 323 K and 423 K temperatures, the interaction energy decreases, signifying reduced affinity likely due to limited mobility at low temperatures and solvent disengagement at high temperatures [158]. The binding energy of cellulose

also reveals the highest value were at 423K which represent the best solvation state due to many hydroxyl groups in cellulose that can form hydrogen bonds with DMSO, allowing continuous interaction even as temperature increases [216]. This behaviour supports a reversible and stable solvation process in DMSO. Wang et al. reported that such hydrogen bonding interactions are important in stabilising polymer-solvent complexes, especially in systems with polar backbones like cellulose [217]. In summary, the results indicate that cellulose exhibits greater compatibility with DMSO than PET, as evidenced by its higher binding energy. Due to the binding energy represent interactions between polymer chain and solvent which highlight the compatibility of polymer-solvent system. Hence, based on the findings of binding energy suggest stronger cellulose–DMSO intermolecular interactions at higher temperature (423K), which promote solvent penetration and facilitate the disruption of the extensive hydrogen-bonding network within the cellulose structure.

4.1.1.2 Glass Transition Temperature (Tg)

Figure 4.4 presents the specific volume versus temperature plots used to estimate the glass transition temperatures (Tg) of PET and cellulose, both in their pure and DMSO-solvated states. The Tg, identified at the intersection of dual linear regressions, indicates the onset of segmental chain mobility and polymer softening behaviour. Figure 4.4(a) shows that pure PET has a glass transition temperature (Tg) of about 421 K. When DMSO is introduced, the Tg decreases notably to around 395 K (Figure 4.4(c)). This reduction suggests that DMSO enhances chain flexibility through a plasticising effect. The solvent likely disrupts interchain interactions in the polyester matrix, weakening van der Waals forces and enabling greater molecular mobility. This observation aligns with earlier interaction energy results (Figure 4.3(a)), where PET showed reduced interaction strength with DMSO at elevated temperatures. At 373 K, the strong negative binding energy (Figure 4.3(b)) indicates that DMSO interacts favourably with the PET chains, creating a less restrictive molecular environment. This interaction reduces the energy barrier needed for chain movement, consistent with a plasticisation effect. In this process, DMSO molecules penetrate between the polymer chains, increasing the free volume and thereby lowering the glass transition temperature (Tg) [73].

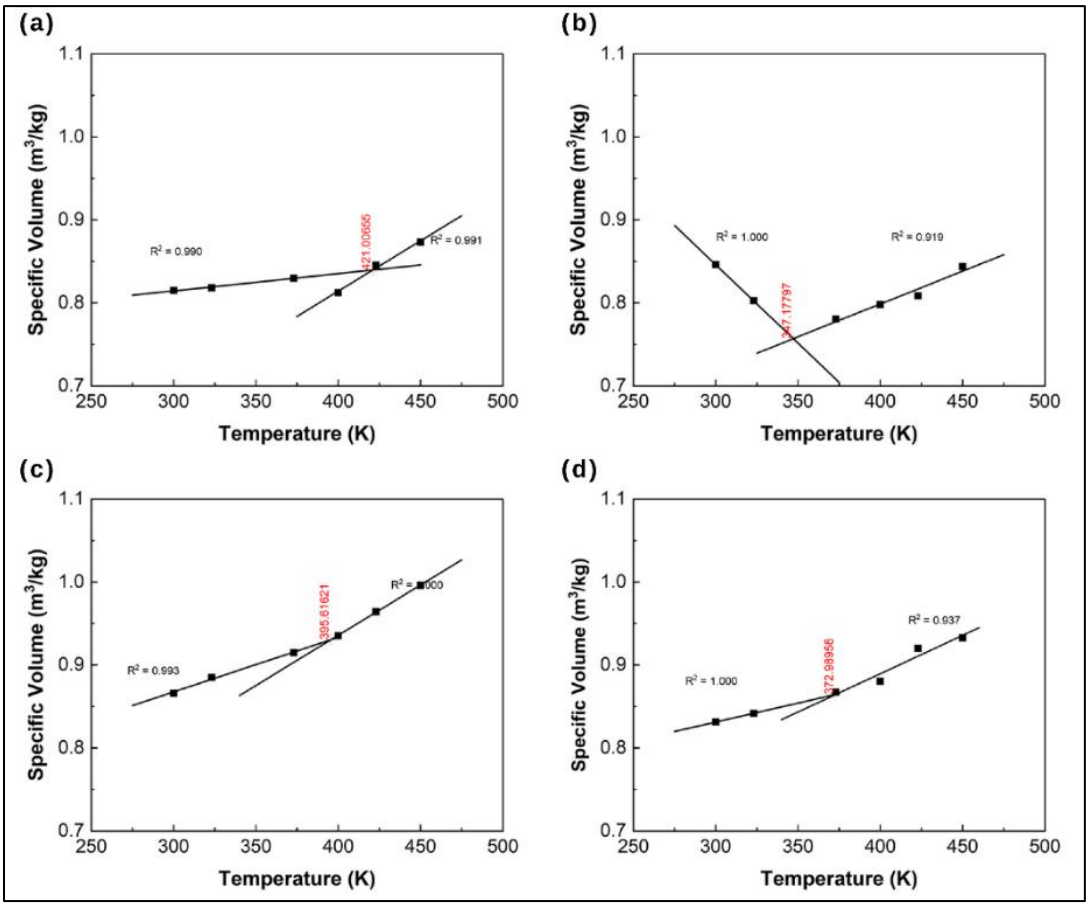

Figure 4.4 The Glass Transition Temperature (Tg) of (a) Pure PET (b) Pure Cellulose (c) PET/DMSO (d) Cellulose/DMSO

In contrast, cellulose demonstrates an opposite thermal response upon DMSO solvation. As shown in Figure 4.4(b), the Tg of pure cellulose is approximately 347 K, which increases to 372 K in the Cellulose/DMSO system (Figure 4.4(d)). This upward shift indicates a reduced segmental mobility and greater structural rigidity. The interaction energy results (Figure 4.3(a)) support this inference, which cellulose displays maximum polymer–solvent interaction strength at 373 K, consistent with enhanced hydrogen bonding networks between cellulose's hydroxyl groups and DMSO's sulfoxide moiety. Rather than plasticising, DMSO likely participates in the formation of strong intermolecular bridges, restricting molecular rearrangement and thereby elevating Tg [218]. This behaviour is further substantiated by the modest binding energy values (Figure 4.3(b)), which suggest moderate but persistent stabilisation of the polymer–solvent complex without the collapse or aggregation observed in PET. Such restriction in chain movement can be attributed to the intrinsic high molecular weight and linear rigidity of cellulose chains. According to Wu et al., polymers with longer chains and greater entanglement density exhibit elevated Tg due

to constrained segmental motion, a behaviour accentuated when such chains are further stabilised by strong solvent interactions [143].

The high R^2 values across all panels (ranging from 0.919 to 1.000) attest to the precision of the linear regressions applied to determine Tg, thus affirming the thermodynamic reliability of the simulation outputs [16]. These findings also emphasise the distinct solvation mechanisms between PET and cellulose. While DMSO reduces Tg in PET via plasticisation, it raises Tg in cellulose through associative hydrogen bonding and molecular stiffening. Together, these results provide the mechanism of solvent interactions that influence by the thermal and highlight the understanding of how solvent–polymer interactions.

4.1.1.3 Mean Squared Displacement (MSD) and Diffusion Coefficient (D)

Figure 4.5 illustrates the effect of temperature on the mean square displacement (MSD) of polymer chains in DMSO for PET (Figure 4.5(a)) and cellulose (Figure 4.5(b)). Meanwhile, Figure 4.6 presents the calculated diffusion coefficients derived from these MSD trajectories across a temperature range of 323 K to 423 K. In both systems, MSD values increase progressively with temperature, reflecting enhanced molecular motion at elevated thermal energy [219]. This is consistent with classical diffusion theory and confirms that temperature is a critical driver of polymer chain mobility. For PET/DMSO systems (Figure 4.5(a)), the MSD shows a subtle but progressive rise, with a modest acceleration near 423 K. In contrast, Cellulose/DMSO systems (Figure 4.5(b)) exhibit a more dramatic increase, particularly at higher temperatures, indicating significantly greater dynamic mobility.

These observations align well with the interaction energy and Tg analyses discussed previously. In PET, the interaction energy (Figure 4.3(a)) becomes less favourable with increasing temperature, and the binding energy (Figure 4.3(b)) is highly negative at 373 K, suggesting the formation of a tightly bound PET/DMSO complex. Such strong interactions restrict chain flexibility, limiting translational motion, and thus leading to a lower overall MSD and diffusion coefficient. This phenomenon is consistent with Li et al.'s study, who reported that stronger polymer–solvent interactions can reduce polymer diffusivity by anchoring chains in local potential wells [11]. Moreover, this behaviour is reflected in the PET's MSD curve (Figure 4.5(a)),

where the slope remains relatively shallow, and a diffusive regime is only marginally approached at 423 K.

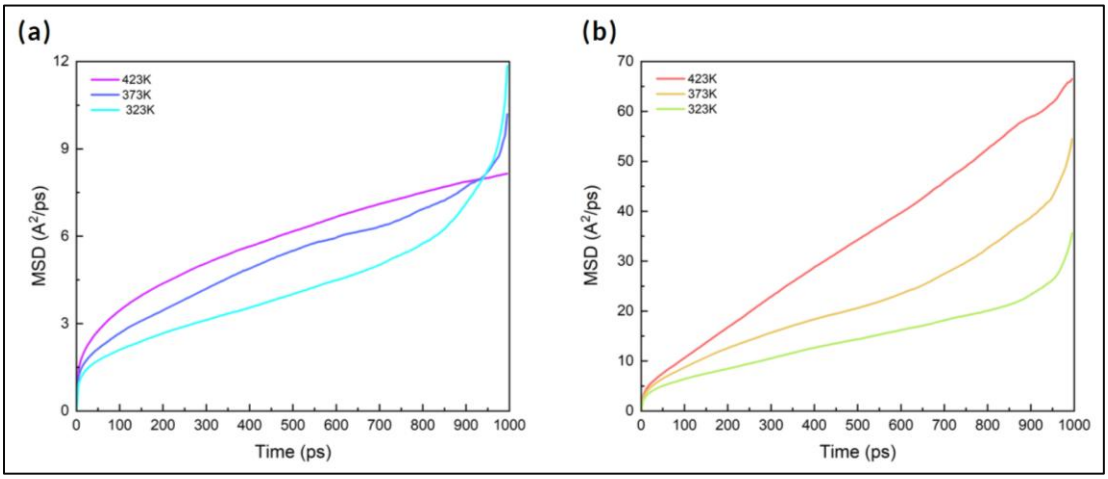

Figure 4.5 The MSD of (a) PET/DMSO (b) Cellulose/DMSO at 323K, 373K, 423K

Conversely, cellulose demonstrates much higher mobility and diffusion values at elevated temperatures, reaching a peak diffusion coefficient near 11 × 10^{-7} cm^2/s at 423 K (Figure 4.6). The corresponding MSD curves show a marked and steady increase with temperature, indicating the polymer chains progressively transition from a constrained to a diffusive state. These transitions, as explained by Hsu et al., are typically characterised by a plateau in the MSD followed by a sharp increase, suggesting the breakdown of local confinement and the onset of chain disentanglement [220]. In cellulose, this behaviour coincides with the temperature regime just above its glass transition (Tg = 372.990 K from Figure 4.4(d)), where segmental relaxation and swelling contribute to uncoiling and solvent-assisted dispersion. The radius of gyration and MSD analyses together validate this structural-to-diffusive transition mechanism, as noted in earlier studies [219].

The enhanced molecular mobility in Cellulose/DMSO systems can be attributed to DMSO's ability to form extensive hydrogen bonds with cellulose's numerous hydroxyl (-OH) groups [221]. This interaction facilitates the disruption of strong intra- and intermolecular hydrogen bonds native to cellulose's crystalline structure [43]. DMSO's sulfoxide group, with a highly electronegative oxygen atom, acts as an excellent hydrogen bond acceptor, enabling it to penetrate cellulose matrices and induce chain separation and swelling [173]. Consequently, higher mobility and diffusivity emerge not from weak interactions as seen with PET but from effective, reversible

interactions that promote dynamic solvation [222]. This is further supported by the moderate binding energies (Figure 4.3(b)) and optimal interaction energy at 373 K (Figure 4.3(a)), highlighting the balanced solvation effect that favours diffusion without over-stabilising the polymer-solvent complex.

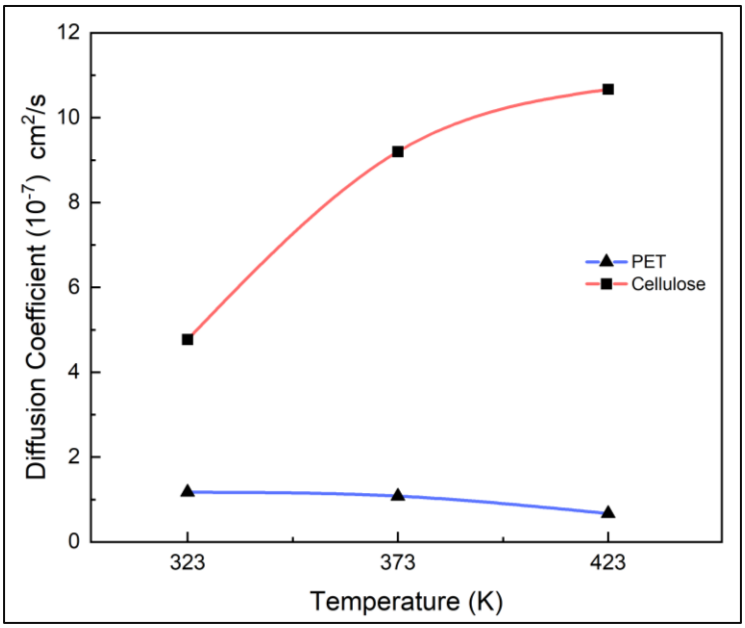

Figure 4.6 The Diffusion Coefficient (D) of PET and Cellulose with DMSO at Different Temperatures (323K, 373K, 423K).

In contrast, the PET/DMSO system exhibits significantly lower diffusion coefficients across all temperatures, remaining below 2×10^{-7} cm^2/s even at 423 K. This limited diffusivity is attributed to PET's relatively hydrophobic and aromatic structure, which hinders hydrogen bond formation with DMSO [179]. The stronger and increasingly negative binding energy observed in PET (Figure 4.3(b)) indicates a possible aggregation or chain collapse effect at intermediate temperatures, in line with Huang et al., further reducing molecular freedom. Consequently, even at temperatures near or above Tg (395 K in Figure 4.4(c)), PET chains exhibit minimal uncoiling, and solvent penetration remains kinetically and thermodynamically unfavourable.

Cellulose are expected to exhibit higher solubility due to favourable hydrogen bonding interactions, while polyester-rich systems may remain largely inert or aggregated under identical thermal and solvent conditions [223]. The disparity in diffusion behaviour between PET and cellulose directly correlates with their interaction energetics and transition temperatures, highlighting the importance of matching solvent systems not only with chemical functionality but also with thermophysical properties.

4.1.2 Effect of Concentration

This section investigates the effect of polymer concentration on the structural behaviour of Cellulose and PET in a DMSO solvent system under molecular dynamics (MD) simulations. The simulations were conducted at a constant temperature of 423 K with a time step of 1 ns, focusing on three different concentrations: 4.5, 6.0, and 7.5 mg/ml. The visual comparison of polymer structures before and after the simulation is presented in Table 4.4, highlighting changes in polymer configuration influenced by concentration.

4.1.2.1 Interaction Energy and Binding Energy

The results presented in Figure 4.7 illustrate the interaction energy (Figure 4.7(a)) and binding energy (Figure 4.7(b)) between the polymers (PET and cellulose) and DMSO at different concentrations (4.5, 6.0, 7.5 mg/ml). The interaction energy for PET significantly increases linearly as the concentration increases, indicating weaker polymer-solvent interactions. In this study, PET exhibited negative binding energy at lower concentrations, which became progressively less negative as the concentration increased, indicating a decline in the stability of the PET/DMSO complex at elevated polymer loadings. This trend is consistent with the hydrophobic nature of PET, which limits its interaction with DMSO, a polar aprotic solvent lacking hydrogen-bond donor capability. As PET concentration increases, solvent molecules become insufficient to solvate the hydrophobic PET chains effectively, promoting polymer-polymer associations.

Table 4.4
Comparison of Cellulose/DMSO and PET/DMSO System Before and (time step = 1ns) MD Simulations at 4.5, 6.0, 7.5 mg/ml.

Concentration	**Cellulose/DMSO**		**PET/DMSO**	
	Before	**After**	**Before**	**After**
30RU (4.5mg/ml)	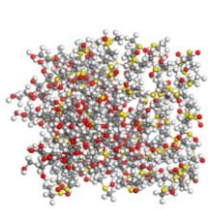	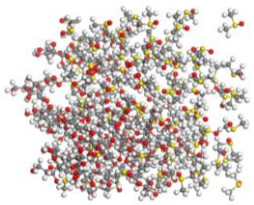	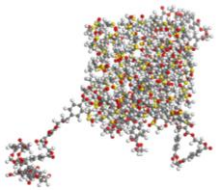	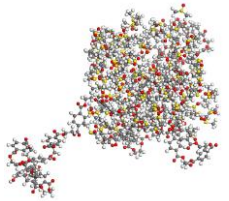
40RU (6.0mg/ml)	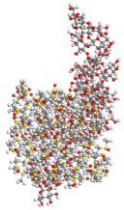	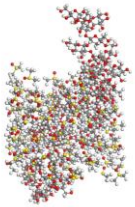	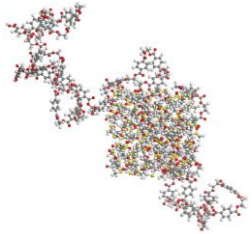	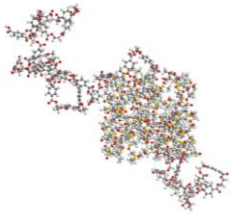
50RU (7.5mg/ml)	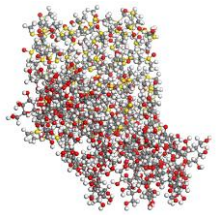	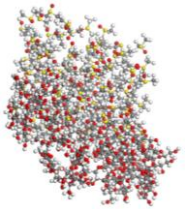	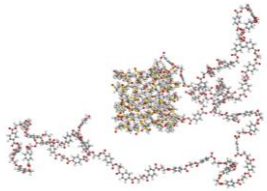	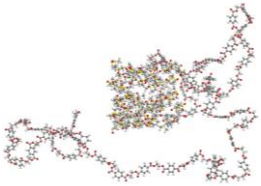

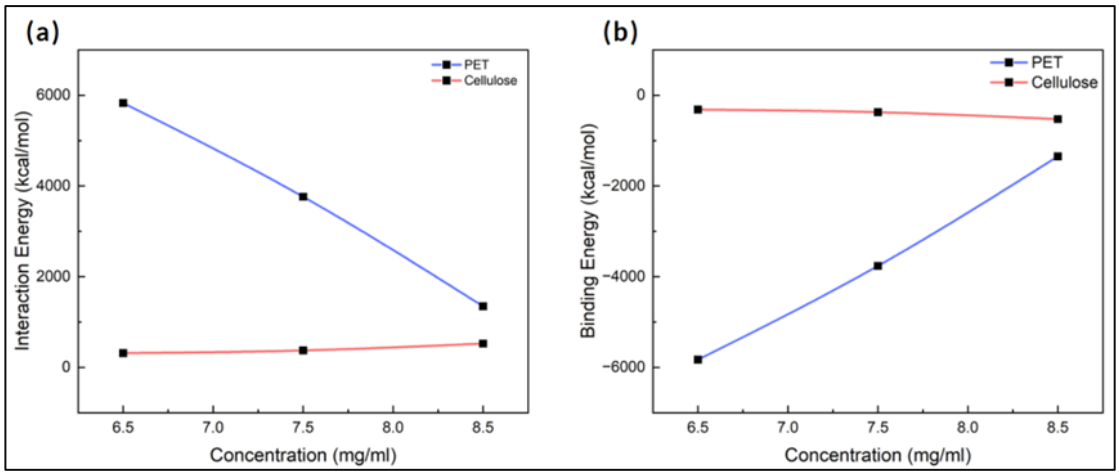

Figure 4.7 (a) Interaction Energy (b) Binding Energy for PET/DMSO and Cellulose/DMSO System At 4.5, 6.0, 7.5 mg/ml

This observation aligns with Cheng et al., who noted that higher interaction energies in polymer-solvent systems restrict solvent diffusion within polymer matrices by reducing solvent mobility and availability [150]. Huang et al. further observed that when polymer-solvent interactions surpass twice the strength of polymer-polymer and solvent-solvent interactions, unexpected polymer chain collapse and phase separation occur, attributed to solvent molecules acting as a 'glue' between polymer chains, triggering aggregation, and destabilising the system [215]. Polyester's structure (as in Figure 4.8) includes aromatic benzene rings, which increase the energy needed to break the molecular bonds and make it more resistant to dissolving, even though it contains ester functional groups (-C=O and -O-) that form weak hydrogen bonds with DMSO [224].

In contrast, for cellulose, the interaction energy also has a linear trend with a smaller range. This suggests that cellulose has the most favourable interactions with DMSO as the concentration decreases, enhancing its dissolution process. The binding energy shows less variation with temperature but remains less negative compared to PET. This is consistent with cellulose's hydrogen-bonding nature, as DMSO's ability to act as both a donor and acceptor allows for moderate binding. Wang et al. found that greater binding energies are most likely caused by the formation of hydrogen bonds, which strengthen the intermolecular interactions between the polymer and the solvent system [217]. Cellulose (cotton) is rich in hydroxyl groups, which serve as hydrogen bond donors and form strong hydrogen bonds with DMSO, thus enhancing its solubility [225], [226].

4.1.2.2 Mean Squared Displacement (MSD) and Diffusion Coefficient (D)

Figure 4.8 shows the effect of concentration on the Mean Square Displacement (MSD) of polymer-DMSO systems at 4.5, 6.0, and 7.5 mg/ml. The mean squared displacement (MSD) profiles of PET (Figure 4.8(a)) exhibit a clear concentration-dependent decline in molecular mobility. At the lowest concentration of 4.5 mg/ml, PET demonstrates the highest MSD over the 1 ns simulation period, indicating relatively unrestricted diffusive behaviour. As the concentration increases to 6.0 mg/ml and 7.5 mg/ml, a marked reduction in the slope and magnitude of the MSD curves is observed. This trend can be attributed to increased polymer–polymer interactions and chain entanglement at higher concentrations, which restrict segmental motion [214]. Moreover, the relatively modest increase in MSD with time, even at low concentrations, suggests that PET exhibits inherently limited dynamic freedom in DMSO. This is likely due to its semi-rigid aromatic backbone and fewer polar interaction sites, which reduce its compatibility with polar aprotic solvents like DMSO. The resulting low solvation efficiency limits PET's dispersibility and molecular motion in solution [227].

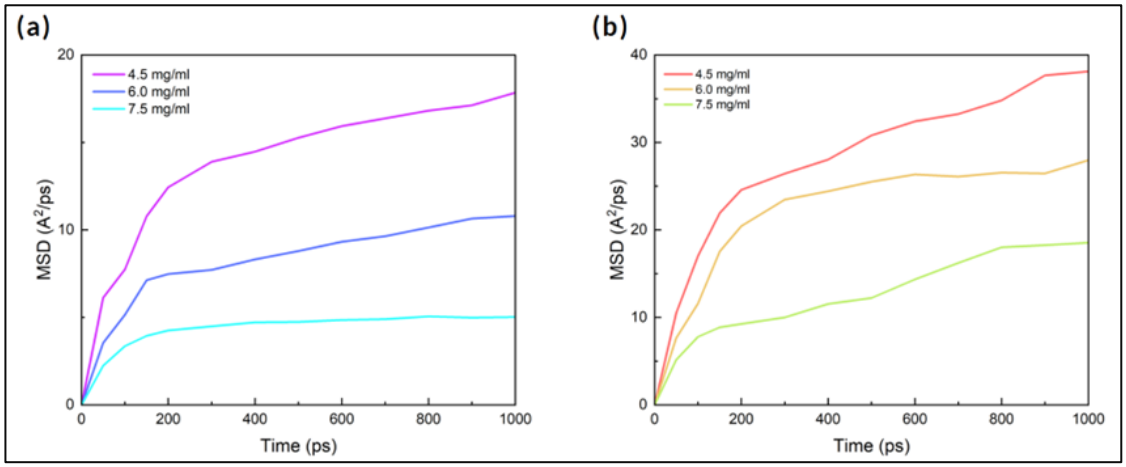

Figure 4.8 The MSD of (a) PET/DMSO (b) Cellulose/DMSO at 4.5, 6.0, 7.5 mg/ml

In contrast, the MSD results for cellulose (Figure 4.8(b)) indicate that it exhibits significantly higher molecular movement at all concentrations compared to PET. At 4.5 mg/ml, cellulose records the highest MSD value, reflecting its strong molecular motion and better interaction with the solvent. Even when the concentration increases to 6.0 and 7.5 mg/ml, cellulose still maintains relatively high MSD values, although a slight drop is observed. This pattern suggests that while higher concentrations slow down

diffusion, the effect is not as severe for cellulose [228]. The higher mobility of cellulose can be linked to its many hydroxyl groups, which form strong hydrogen bonds with the oxygen atoms in DMSO. These bonds help break the internal hydrogen bonds within cellulose, improving its interaction with the solvent and allowing the polymer chains to move more freely [229]. As a result, cellulose exhibits better compatibility with DMSO, resulting in greater flexibility and molecular diffusion compared to PET.

Figure 4.9 shows a series of time-lapse snapshots from the molecular dynamics simulation of the Cellulose/DMSO system at 0, 250, 500, 750, and 1000 ps. Over time, the DMSO molecules gradually move into the cellulose matrix, breaking the hydrogen bonds between cellulose chains and transforming the tightly packed polymer structure into a more relaxed, solvated state [102]. In the early stages (Figure 4.9 at 0–250 ps), the solvent starts to enter the cellulose clusters. By around 500–750 ps (Figure 4.9), the molecular movement becomes more active, leading to faster chain separation and stronger interactions with the solvent. The higher MSD value seen in the graph (Figure 4.8(b) – red line) indicates that the solvent penetrates more effectively, allowing the polymer chains to move more freely and reach dynamic equilibrium more quickly.

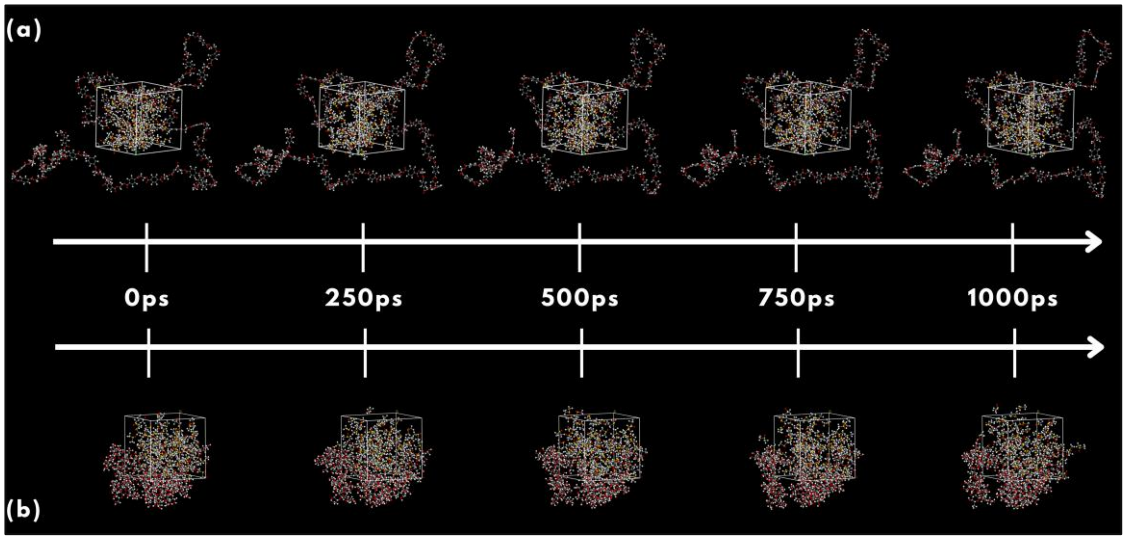

Figure 4.9 Time-lapse Snapshots of the Molecular Dynamics Simulation for the (a) PET/DMSO System (b) PET/DMSO System at 0, 250, 500, 750, and 1000 ps at 4.5mg/ml.

Meanwhile, Figure 4.10 shows the diffusion coefficient of a systematic decrease in diffusivity with increasing concentration for both PET and cellulose. However, cellulose consistently exhibits higher diffusion coefficients than PET at all concentrations, indicating superior solvation and lower resistance to molecular motion.

This trend suggests that the higher molecular motion observed in the MSD plots corresponds to greater diffusivity. The decline in diffusion at higher concentrations can be explained by the increase in system viscosity and the reduction of free space available for molecular movement, which together slow down the motion of the chain [230]. Overall, the results from both the MSD and diffusion analyses indicate that DMSO interacts more favourably with cellulose than with PET, resulting in improved molecular mobility and more efficient dissolution.

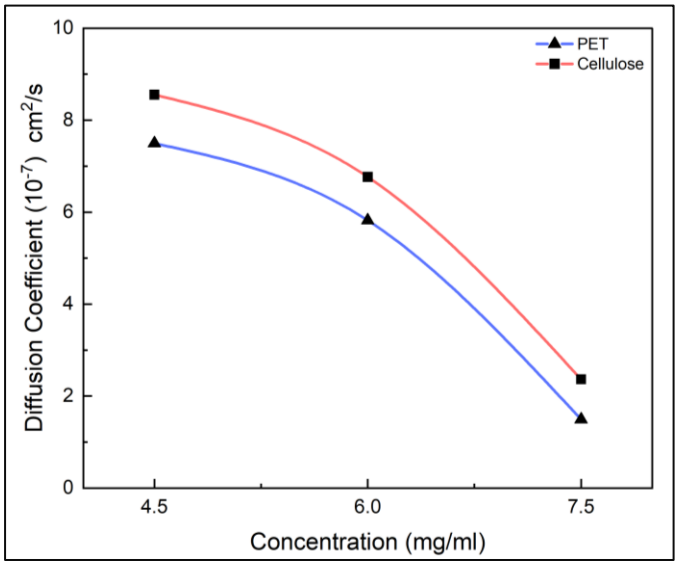

Figure 4.10 The Diffusion Coefficient (D) of PET/DMSO and Cellulose/DMSO at 4.5, 6.0, 7.5 mg/ml.

Cellulose is more hydrophilic than polyester, leading to stronger interactions with the polar DMSO solvent [179]. As a result, cotton-rich textile blends tend to dissolve more readily, often forming gels [154]. Notably, cellulose can be efficiently dissolved in DMSO while polyester remains undissolved, allowing for the separation and recovery of various fibre materials [179]. These results reinforce the differential solubility behaviour of cellulose and PET in DMSO, with cellulose demonstrating superior compatibility due to its hydrophilicity, while PET resists dissolution because of unfavourable thermodynamic interactions, particularly at higher polymer concentrations. DMSO, as a polar aprotic solvent, engages more effectively with the hydroxyl-rich cellulose via hydrogen bonding, particularly through its oxygen atom, thereby enhancing cellulose chain separation and mobility. PET, by contrast, interacts primarily through weaker dipole–dipole interactions between its ester functionalities and DMSO, resulting in limited disruption of its compact structure and thus lower

diffusivity. The nonlinear decline in diffusion coefficients further suggests complex solvation dynamics, including the influence of polymer entanglements, localised viscosity, and competition for solvent molecules. Overall, these results underscore the critical role of specific polymer–solvent interactions in governing the dynamic behaviour of polymer solutions.

4.1.2.3 Radial Distribution Function (RDF)

Based on the result above, it can be concluded that the highest interaction between cellulose and polyester with DMSO is at 4.5mg/ml and 423K. However, the result needs to be validated by analysing the possibilities of swelling or dissolution of polymers in DMSO. Figure 4.11 shows the radial distribution functions (RDF) of the PET/DMSO and Cellulose/DMSO. The peaks at 1.09 Å represents the intramolecular C–H covalent bonds stretching along the polymer backbones (glucoside/phenyl rings), serving as an internal calibration point for the structural models. [231].

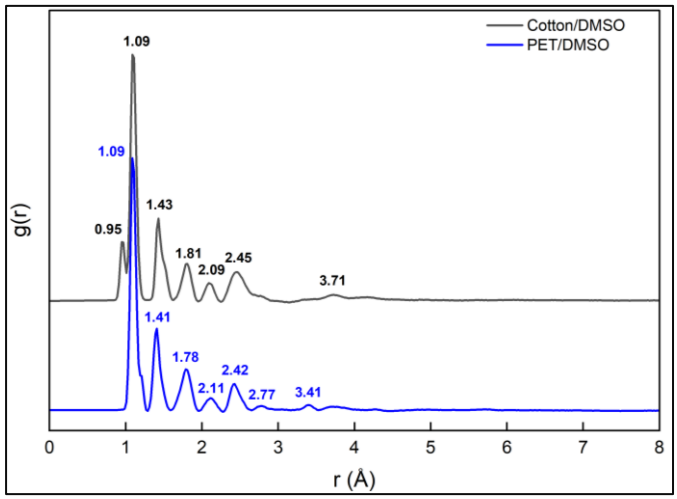

Figure 4.11 The Radial Distribution Functions (RDF) of the PET/DMSO and Cellulose/DMSO.

Table 4.5 presents the interpretation of important peak of Cellulose/DMSO in Figure 4.11. The sharp and intense peak near 0.95 Å indicates directly to the intramolecular of the cellulose's hydroxyl groups. This features confirms the abundance of available protic hydrogen donors [229]. Peak at 1.43 Å correspond to the primary skeletal covalent bonds. These indicate the C–C and C–O single bonds within the glucopyranose rings of cellulose. Finally, the small peak at 1.81 Å represents direct

structural evidence of intense intermolecular affinity. The hydroxyl protons of the cellulose chain are tightly coordinated by the oxygen (sulfoxide group) of the DMSO [212].

Table 4.5
The Interpretation of Important Peak of Cellulose/DMSO in Figure 4.11.

Peak (Å)	Interaction
0.95	Hydroxyl donor peak of O–H···O between cellulose hydroxyls and DMSO oxygen.
1.09	Intramolecular C–H covalent bonds stretching along the polymer backbones and glucoside.
1.43	The C–C and C–O single bonds within the glucopyranose rings of cellulose.
1.81	Intermolecular hydrogen bond peak between Cellulose (Hydroxyl) and DMSO (Sulfoxide), O–H···O=S.

Meanwhile, table 4.6 presents the interpretation of important peak of PET/DMSO in Figure 4.11. The RDF of the PET/DMSO system has similar peak at 1.09 Å. However, these peaks are notably representing the intramolecular C–H covalent bonds stretching of phenyl rings [232]. The peak at 1.43 Å were corresponding to the C–C aromatic and C=O ester linkages inherent to the PET backbone. Finally, the peaks between 1.78 are likely correlation to rigid intramolecular distances between non-bonded atoms and weak Van Der Waals dispersion forces (C–H···O) between the aromatic protons and the solvent [233].

Table 4.6
The Interpretation of Important Peak of PET/DMSO in Figure 4.11.

Peak (Å)	Interaction
1.09	Intramolecular C–H covalent bonds stretching along the phenyl rings.
1.41	The backbone covalent linkages (C–C aromatic and C=O ester linkages) bonds within the PET backbone.
1.78	Weak Van Der Waals dispersion forces of C–H···O interactions between the aromatic protons and the solvent.

Overall, the comparative RDF analysis highlight a thermodynamic contrast between the two polymer/solvent systems. The dissolution and swelling behavior of cellulose in DMSO is driven by highly specific, localized, and energetically favourable intermolecular hydrogen bonding networks (O–H···O=S). Conversely, the interaction

between PET and DMSO is characterized by a weaker macro-molecular dispersion force that lack long-range structural ordering. This justification was supported by Sangkhawasi et al. study where the behaviour of the weak first peak in RDF shows a slower diffusion of solvent into polymer [234]. This is caused by the weak hydrogen bond interaction between polymers and solvent. Thus, the weaker peaks indicate that PET mostly interacts with DMSO through dipole and van der Waals forces rather than strong hydrogen bonds. This clarifies that PET is less soluble and interacts with DMSO.

4.2 Dissolution of Cotton and Polyester

Figure 4.12 shows the dissolution percentages for each parameters combination of E1 – E9 (refer Table 3.6 in section 3.5.3). Based on the results in Figure 4.12(a) demonstrate that cotton achieved the highest dissolution percentage (79.27%) in E7 (150℃, 4.5 mg/ml, 8 hours) compared to polyester. This shows that cellulose has stronger chemical compatibility and molecular interaction with dimethyl sulfoxide (DMSO). The high solubility of cellulose can be related to numerous hydroxyl groups, which are easier to form hydrogen bonds with the polar sulfoxide groups in DMSO [218]. Thus, this process promotes chain disentanglement, swelling, and solvent penetration [190]. This mechanism shows that DMSO (alone or as a cosolvent) enhances cellulose solvation by engaging hydrogen-bond interactions and by lowering blend viscosity to accelerate mass transfer [154]. Previous study in molecular dynamic simulation by Roos et al. also shows that DMSO stabilises solvated cellulose chains by occupying hydrogen-bonding sites and by solvating ion pairs in IL/DMSO mixtures [229]. This solution weakens the cellulose–cellulose bonds and stabilises solvated chains, making dissolution thermodynamically and kinetically favourable in DMSO-rich blends [226]. In contrast, Figure 4.12(b) reveals that polyester dissolution remained below approximately 20%, highlighting the limited ability of DMSO to disrupt the strong intermolecular interactions within the polyester matrix. Polyester's hydrophobic and crystalline structure restricts solvent access and chain separation, requiring high temperatures even for the partial swelling [235].

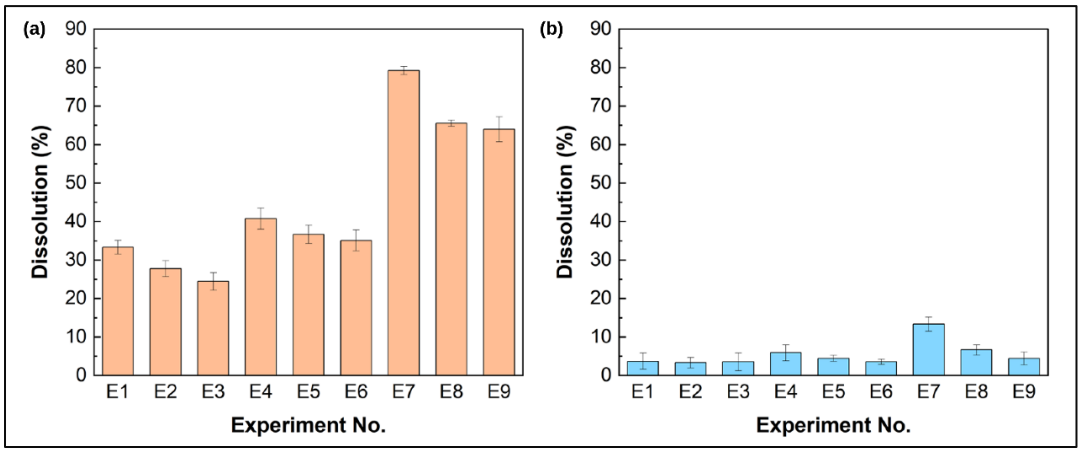

Figure 4.12 The Result of Varying Conditions on (a) Cotton (b) Polyester Dissolution in DMSO.

Polyester has a lower affinity for polar sulfoxide solvents because its repeating units are dominated by hydrophobic aromatic/ester segments and a paucity of hydrogen-bond donor sites [32], [236]. This chemical inertness and higher crystallinity limit solvent–polymer interactions and require substantially higher thermal input or chemically reactive conditions for comparable disruption [237]. This behaviour noted in surface-property and recycling reviews that characterise PET as relatively hydrophobic and solvent-resistant. Dimethyl sulfoxide (DMSO) acts as an effective co-solvent for cellulose because it can form hydrogen bonds with hydroxyl groups and reduce the overall viscosity of the solvent system [238]. This effect is especially evident in hydroxyl-rich and highly hydrophilic materials such as cellulose. The variation in solubility observed between the fibres is mainly related to differences in their molecular structures. This is supported by the dissolution efficiency results, which showed a significant difference between the two fibres when processed under the same E7 conditions (150 °C, 4.5 mg/ml, and 8 hours). The statistical validation using ANOVA and signal-to-noise (S/N) ratio analysis under the “larger-the-better” criterion supported the reliability of these findings.

Based on the response table (Table 4.7) and ANOVA analysis (Table 4.8), temperature is shown as the most significant parameter influencing fibre dissolution, though its effect is notably difference between cotton and polyester. For cotton, temperature contributed the largest factor of variance (SSTemp = 1.373, MSTemp = 0.687) and produced a very high F-value with a P-value less than 0.05 (F = 148.17, p = 0.007), indicating strong statistical significance. Meanwhile, polyester also shows that temperature contributed the largest factor of variance (SSTemp = 46.501, MSTemp = 23.250) and produced a very high F-value with a P-value less than 0.05 (F = 22.42, p =

0.043). This result aligns with findings that thermal energy promotes the breakdown of the extensive hydrogen-bonding network within cellulose, thereby enhancing molecular mobility. The increased chain movement allows the DMSO solvent to penetrate more effectively, leading to greater swelling and improved dissolution efficiency. This result was supported by Wu et al. [239], who found that increasing temperature increases dissolution, as shown in the experiment conducted over the temperature range. Hence, higher temperatures and longer times are required for its high dissolution. Futhermore, study by Yang et. al [63] found that limited dissolution occurred as the temperature decrease, and the structural breakdown in the residue was negligible. The lack of significant degradation is attributed to insufficient energy breaking the covalent bonds within the polyester structure.

Table 4.7
Response Table for S/N ratios (Larger is better) for Cotton and Polyester Sample

Cotton			
	Temperature (°C)	**Concentration (mg/ml)**	**Contact Time (Hrs)**
Level 1	30.50	31.03	30.70
Level 2	30.44	30.75	30.74
Level 3	31.30	30.46	30.80
Delta (Δ)	0.86	0.57	0.11
Rank	1	2	3
Polyester			
	Temperature (°C)	**Concentration (mg/ml)**	**Contact Time (Hrs)**
Level 1	10.95	15.91	12.12
Level 2	13.14	12.46	13.48
Level 3	16.48	12.19	14.96
Delta (Δ)	5.53	3.72	2.84
Rank	1	2	3

Next, concentration was identified as the second most influential parameter. The factor of variance (SSConc = 0.492, MSConc = 0.246) with F-values of 53.03 (p = 0.019) for cotton and factor of variance (SSConc = 25.831, MSConc = 12.916) with F-value of 12.45 (p = 0.074) for polyester. These findings are consistent with classical

mass-transfer and rheological principles, where increasing solid concentration raises the system's viscosity and promotes polymer–polymer interactions, thereby restricting solvent penetration and slowing dissolution [240]. In contrast, lower or moderate concentrations allow better solvent diffusion and facilitate more efficient solvation under the same thermal conditions. An increase in DMSO concentration also increases the solvent–solute interactions by providing additional polar sites capable of accepting hydrogen bonds from cellulose hydroxyl groups, improving dissolution efficiency.

Table 4.8
Analysis of Variance (ANOVA) for S/N Ratios (Cotton and Polyester Sample)

Cotton				
	SSk	**MSk**	**F-value**	**P-value**
Temperature (°C)	1.373	0.687	148.17	0.007
Concentration (mg/ml)	0.492	0.246	53.03	0.019
Contact Time (Hours)	0.017	0.009	1.86	0.349
Residual Error (SSE/MSE)	0.009	0.005		
Total (SST)	1.892			
Polyester				
	SSk	**MSk**	**F-value**	**P-value**
Temperature (°C)	46.501	23.250	22.42	0.043
Concentration (mg/ml)	25.831	12.916	12.45	0.074
Contact Time (Hours)	12.104	6.052	5.84	0.146
Residual Error (SSE/MSE)	2.074	1.037		
Total (SST)	86.510			

An experimental and modelling study by Ren et al. and Keppeler et al. reported precisely that solutions with lower solute concentrations or higher co-solvent fractions exhibit lower viscosity, which promotes chain disentanglement and speeds up fibre dissolution. This relationship helps explain the shorter time-to-clarity seen at reduced polymer concentrations, as lower intermolecular friction allows faster solvation and disruption of crystalline regions. The effect is particularly notable in cellulose and polyester systems dissolved in polar aprotic solvents such as DMSO, where improved

molecular transport and hydrogen-bond exchange accelerate the formation of uniform solutions [154], [228].

Lastly, according to the Taguchi S/N analysis and ANOVA, contact time statistically has a non-significant effect for both cotton (SSTime = 0.017, MSTime = 0.009, F = 1.86, p = 0.349) and polyester (SSTime = 12.104, MSTime = 6.052, F = 5.84, p = 0.146). The results suggest that once an appropriate balance between temperature and solvent accessibility is reached, the dissolution process begins to level off. This pattern is mainly governed by two related mechanisms [241]. First, thermal energy lowers the effective activation barrier for disruption of intra- and inter-chain hydrogen bonds in cellulose and increases solvent and chain mobility, which greatly accelerates the early stages of swelling and chain disentanglement. Second, the addition of a low-viscosity co-solvent such as DMSO reduces bulk viscosity and improves mass transport, allowing solvent molecules to reach and solvate fibre surfaces more quickly [241]. Beyond this point, extending the contact time mainly supports slower diffusion into tightly packed crystalline regions, which has little effect on the overall S/N ratio in the Taguchi analysis. Hawkins et al. also observed that prolonging dissolution beyond this stage yields minimal improvement. This trend supports previous kinetic findings that dissolution is governed by a time–temperature–composition relationship, where higher temperatures or greater co-solvent fractions can achieve comparable dissolution levels in a shorter duration than milder conditions over extended times [242].

Figure 4.13 presents the main effects plots for the S/N ratios, indicating that both cotton and polyester fibres dissolved most effectively at 150 °C, a concentration of 4.5 mg/ml, and a contact time of 8 hours. These results are consistent with the dissolution efficiency shown in Figure 4.12, where condition E7 (150 °C, 4.5 mg/ml, 8 hours) produced the highest dissolution for both fibre types. For both fibres, the S/N ratio increases notably with temperature, indicating that heat plays the most critical role in promoting dissolution. Lower fibre concentrations consistently result in higher S/N values, suggesting that reduced viscosity and improved solvent accessibility at 4.5 mg/ml enhance dissolution behaviour. Although contact time exerts a weaker influence, the best performance still occurs after 8 hours, implying that extended exposure allows greater solvent diffusion and molecular relaxation.

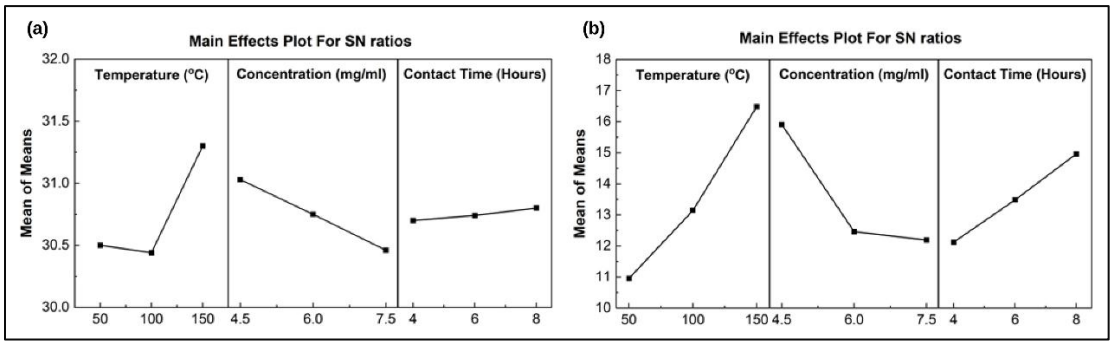

Figure 4.13 Main Effect Plot for S/N Ratios for (a) Cotton and (b) Polyester.

In summary, the combination of high temperature, low concentration, and sufficient contact time provides the most favourable conditions for fibre dissolution in DMSO. Cotton responds more effectively due to its hydrophilic structure, while polyester shows a smaller improvement because of its hydrophobic and crystalline characteristics. In summary, the Taguchi analysis demonstrates that dissolution in DMSO increases with temperature, decreases under high polymer concentrations, and is only slightly affected by contact time. The low residual errors and consistent parameter rankings confirm the reliability of the Taguchi L9–ANOVA method in determining dominant factors.

4.3 Regeneration Process and Characteristic Analysis

From the previous section, E7 (150°C, 4.5 mg/ml, 8 hours), was previously identified as achieving the highest dissolution efficiency for cotton. Therefore, these cotton samples had been chosen for the regeneration process. In this section, the result of the regeneration process will be shown, starting from pre-regeneration character analysis, which evaluates the structural and chemical integrity of the dissolve fibre. All analytical methods, including spectroscopic, thermal, and morphological evaluations, were employed to assess the effectiveness of regeneration and to examine changes in the structural integrity and functional properties of the fibres.

4.3.1 Pre-Regeneration

In this step, UV–Visible spectroscopy and Fourier Transform Infrared Spectroscopy (FTIR) was utilised to confirm that the polymer chains remained

chemically intact and assess whether any significant chemical modifications occurred during the high-temperature dissolution process.

4.3.1.1 UV-Vis

Figure 4.14 displays the UV-Vis absorbance spectra of (a) cellulose and (b) PET dissolved in DMSO at various concentrations, within the wavelength range of 300–800 nm. Both systems exhibit the expected trend of higher absorbance intensities at lower wavelengths (300–400 nm), tapering off toward the visible region. For the Cellulose/DMSO system in Figure 4.14(a), a progressive increase in absorbance is observed with increasing cellulose concentration, particularly in the 300–400 nm region. Importantly, no distinct absorbance peaks attributable to degradation products such as furfural derivatives or carbonyl-containing fragments were detected across the scanned range, even though the dissolution was conducted at an elevated temperature of 150°C. This indicates that the cellulose chains remain chemically intact under the applied conditions, with dissolution occurring primarily via solvation and physical disintegration rather than thermal degradation.

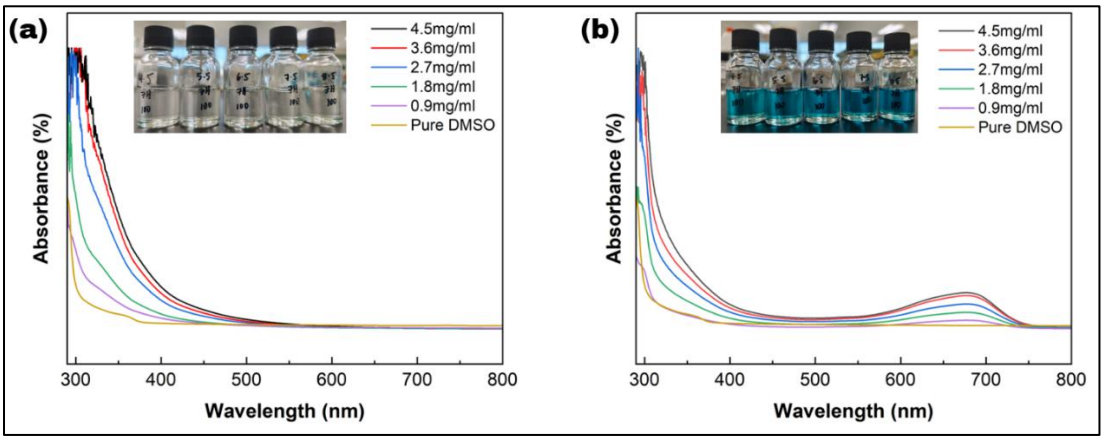

Figure 4.14 UV-Vis's Absorbance Spectra of (a) Cellulose and (b) PET Dissolved in DMSO

In contrast, the PET/DMSO system shown in Figure 4.14(b) exhibited lower absorbance intensities compared to cellulose, confirming a lower extent of dissolution under identical conditions. Notably, a minor hump around 650–700 nm appears at higher concentrations, possibly resulting from colloidal dispersion phenomena or light scattering by semi-crystalline PET particles. The absence of new or shifted absorbance

bands typically associated with terephthalic acid, benzoic acid derivatives, or other thermally induced degradation by-products confirms that the PET macromolecular chains also remained chemically stable within the range of 135°C – 217°C in DMSO [243]. These observations collectively suggest that while cellulose exhibits a markedly higher solubility in DMSO compared to PET, neither material underwent significant thermal degradation during the dissolution process at 150°C. This can be attributed to the DMSO solvent's aprotic, high-boiling, and stabilising nature, which promotes polymer swelling and solvation without facilitating breakdown of the polymer backbone. The spectroscopic evidence thus confirms the preservation of the original chemical structures of both cellulose and PET, further validating the suitability of DMSO as a high-temperature solvent system for textile dissolution studies without compromising polymer integrity.

4.3.1.2 FTIR

Figure 4.15 shows the FTIR spectra of the (a) Cellulose/DMSO (b) PET/DMSO sample, along with the spectra of pure cellulose, pure PET and pure DMSO, to confirm the functional groups presence. The shift broad transmittance band around 3300–3400 cm^{-1} in the Cellulose/DMSO (E7) spectra observed as the O–H stretching, indicating the presence and reformation of hydrogen bonds networks after dissolution [244]. Similarly, peaks near 2900 cm^{-1} are attributed to C–H stretching vibrations of aliphatic groups, which are characteristic of the polysaccharide backbone in cotton [226]. This confirms the presence of cellulose in the sample. In the region between 1460–1410cm^{-1}, a decrease in intensity shows bending vibrations of CH_2 groups, which is known as the "crystallinity band" suggesting a reduction in cellulose crystallinity [245]. The sharp and strong band appearing at around 1050–1070 cm^{-1} corresponds to the S=O stretching vibration and C–O–C stretching, which are distinctive features of DMSO. This confirms that DMSO remains chemically present in the E7 mixture [246]. Additional peaks observed in the range of ~875 cm^{-1}, corresponding to β-glycosidic linkages (C–H bend) region, reflect changes in the glycosidic linkages and the cellulose crystallinity [226].

Meanwhile, Figure 4.15(b) shows the FTIR spectra of the Polyester/DMSO sample, pure polyester and pure DMSO. The pure polyester spectrum displays a shifted peak at ~1725–1710 cm^{-1}, attributed to the C=O stretching (ester carbonyl) group. This

shows the interaction between DMSO associated with the ester functional group within the polyester chain.

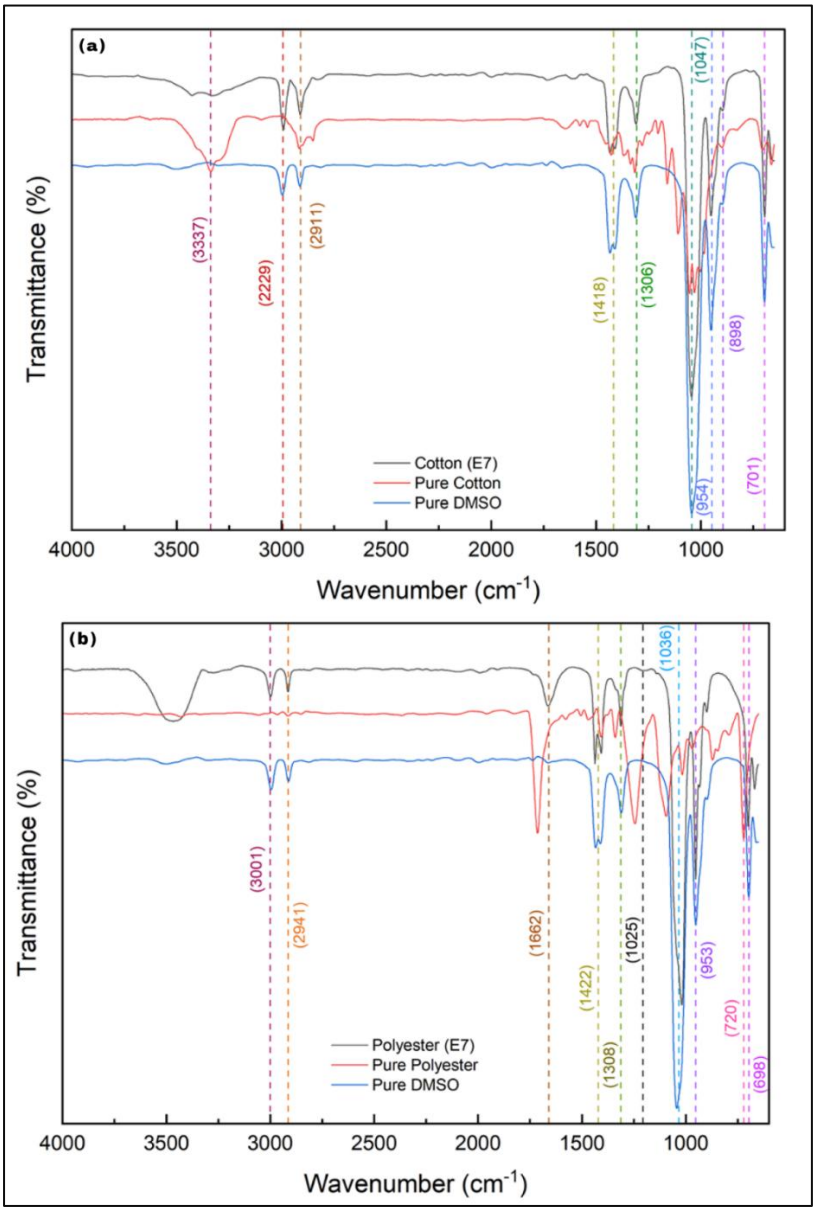

Figure 4.15 FTIR Spectra of (a) Cellulose/DMSO (b) PET/DMSO Sample After Dissolution Process (E7 – 150°C, 4.5mg/ml, 8 Hours)

Additionally, peaks in the range of ~1409–1340 cm^{-1} correspond to aromatic ring vibrations and CH_2 bending and the peaks at ~1310–1250 cm^{-1} are ascribed to C–C–O asymmetric stretching (aromatic ester) [247]. These data strongly suggest the presence of polyesters in the sample. The changes peak at ~1240–1090 cm^{-1} (C–O–C stretching of ester linkages), affirming the presence of polyester's alterations in the ester linkages due to interaction with DMSO [64]. Lastly, the presence peak at ~720 cm^{-1} is a strong absorption corresponding to C–H bending (aromatic) [248]. These peaks are

clearly observable in the sample spectrum, proving there are no modifications or changes in the aromatic ring environment. Overall, the FTIR data confirm that cellulose has been successfully incorporated in DMSO without any significant degradation of functional groups. Thus, it can be concluded that cellulose is present and chemically stable in the DMSO system, validating the solubilisation and compatibility between the two materials. All the characteristic functional groups and skeletal backbones of both cellulose and polyester are preserved, with no significant evidence of degradation, such as the formation of carbonyls in cotton or the cleavage of ester bonds in polyester. This finding is in excellent agreement with the UV-Vis analysis, which also indicated a lack of thermal degradation. The combined results from these orthogonal analytical techniques provide a high degree of confidence that the dissolution method is sufficiently mild to maintain the chemical integrity of the polymers.

4.3.2 Fibre Regeneration Process

Figure 4.16 illustrates the dissolution, precipitation, and regeneration of cotton using dimethyl sulfoxide (DMSO) as the solvent and deionised water as the anti-solvent. In the first stage, Figure 4.16(a), cotton at a concentration of 4.5 mg/ml was dissolved in DMSO at 150 °C for 8 hours. This process produced a homogeneous brown solution, which indicated that the extensive intra- and intermolecular hydrogen bonds within the cellulose network had been disrupted, leading to solubilisation of the cellulose chains.

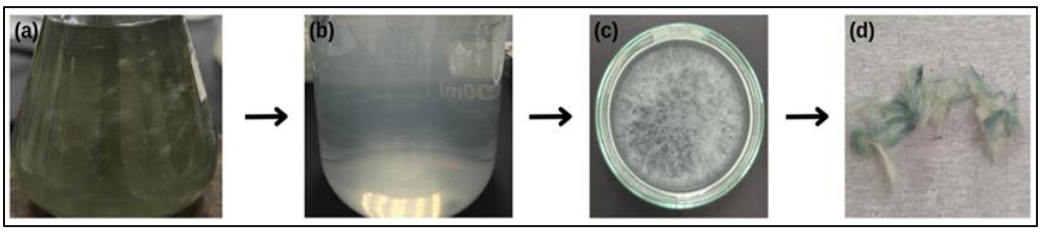

Figure 4.16 (a) The Cotton-DMSO Solution was Cooled Down to 25°C, (b) Add Distilled Water to Achieve a 10:1 Water to Cotton/DMSO Solution Volume Ratio, (c) Left the Mixture for 24 Hours until the Cotton Fibre Fully Precipitated and (d) Regenerated Cotton Fibre (ReC) was Slow Dried at 60°C for Overnight.

In the second stage, Fig 4.16(b), deionised water was added to the solution at a 9:1 ratio relative to the cotton-DMSO mixture, and the system was left undisturbed for 24 hours. The introduction of water displaced DMSO from the solvation shell, which

triggered the reformation of hydrogen bonding among the cellulose chains and promoted aggregation, resulting in visible precipitation. Next, Figure 4.16(c) shows the third stage, which involved the collection of the ReC precipitate, which was dried slowly at 60 °C for 24 hours. The controlled drying condition effectively removed residual solvent while minimising thermal degradation. Finally, Figure 4.16(d) shows the ReC appeared as a fibrous, light-brown material. Although the recovered material resembled natural cotton in appearance, it is expected that changes in crystallinity and morphology occurred because of the solvent–anti-solvent interactions. This dissolution–regeneration sequence confirmed the effectiveness of the DMSO/water system in breaking down and recovering cellulose, thereby demonstrating its potential for cotton recycling applications.

4.3.3 Post-Regeneration

Following regeneration, the solid fibres were subjected to further analysis to assess their thermal, morphological, and structural characteristics. Fourier Transform Infrared Spectroscopy (FTIR), X-ray Diffraction (XRD), Differential Scanning Calorimetry (DSC), and finally, Scanning Electron Microscopy (SEM) analysis was conducted to quantify changes in the thermal transitions, visualisation of the fibre surface morphology, and the crystalline structure to further validate the degree of molecular ordering after regeneration. Together, these multi-technique characterisations provided a comprehensive assessment of the regenerated fibre's quality and its resemblance to the native polymer, confirming the success of the recycling process under the optimised dissolution condition.

4.3.3.1 FTIR

Figure 4.17 shows the FTIR spectra of the regenerated cotton from cotton-only samples (ReC), and regenerated cotton recovered from polycotton (ReM), along with the spectra of pure cotton, pure PET and pure DMSO. Both regenerated fibre (ReC and ReM) shows peak shift broad transmittance band around 3300–3400 cm^{-1}, which is observed as the O–H stretching indicating the presence and reformation of hydrogen bonds networks after regeneration [244]. Similarly, peaks near 2900 cm^{-1} are attributed to C–H stretching vibrations of aliphatic groups, which are characteristic of the

polysaccharide backbone in cotton [226]. Additional peaks observed in the range of ~875 cm^{-1}, corresponding to β-glycosidic linkages (C–H bend) region, reflect changes in the glycosidic linkages and the cellulose crystallinity [226]. However, the FTIR spectra of the ReM sample display an additional shifted peak at ~1725–1710 cm^{-1}, attributed to the C=O stretching (ester carbonyl) group and the peaks at ~1310–1250 cm^{-1} are ascribed to C–O [247]. This shows the interaction between DMSO associated with the ester functional group within the polyester chain, indicating the incomplete removal or trace retention of polyethylene terephthalate (PET) during the dissolution–regeneration process.

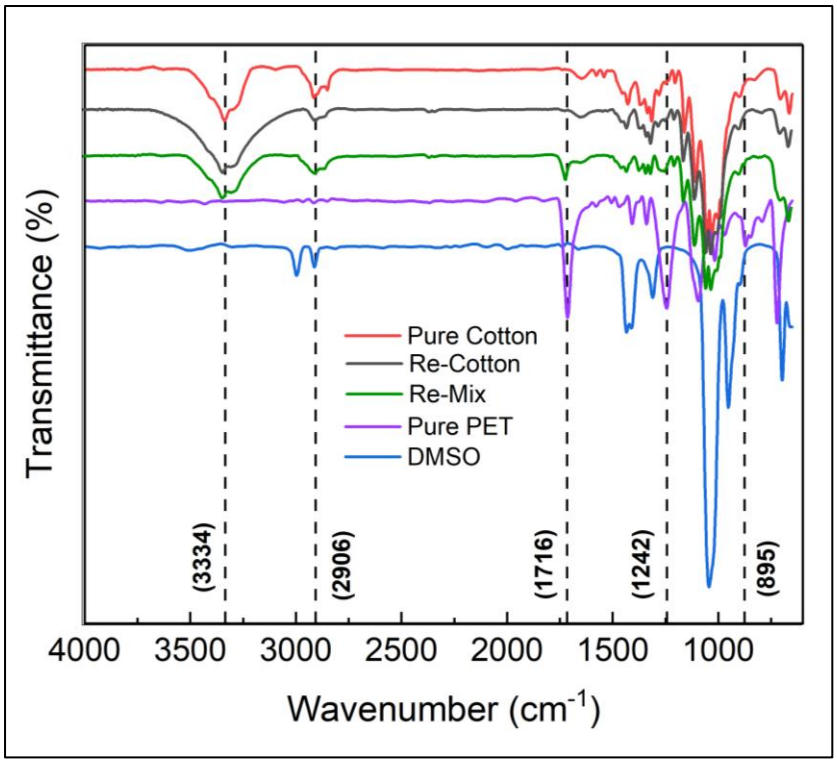

Figure 4.17 FTIR Spectra of Pure Cotton, Pure PET, DMSO, ReC and ReM.

Such traces are consistent with findings by Wu et al., who reported that during solvent-based fractionation, PET fragments may co-precipitate or become entrapped within the ReC matrix due to limited solvent selectivity or partial miscibility [64]. This may lead to slight chemical contamination or physical embedding of PET residues in ReC. Additionally, studies by Rosson et al. observed that DMSO alone has limited efficiency in fully differentiating between cellulose and polyester components in blended textiles without additional selective agents [249]. Thus, the presence of ester-related bands in the regenerated sample confirms that while DMSO facilitates cellulose

recovery, the risk of PET contamination remains, which could affect the purity and downstream application of the recovered cotton fibre. These functional group assignments are summarised in Table 4.7, which provides the detailed wavenumber range, functional group, and source compound (either cellulose, PET, or DMSO).

Table 4.9
The Wavenumber, Functional Group, and its Sources of FTIR Peaks.

Wavenumber (cm^{-1})	Functional Group	Source
~3400 – 3300	O–H stretch (broad, H-bonded)	Cellulose
~2890	C–H stretch (aliphatic)	Cellulose / DMSO
~1725–1710	C=O stretching (ester carbonyl)	Polyester
~1310–1250	C–O stretching	Polyester
~895	C–H bend (β-glycosidic linkage)	Cellulose

4.3.3.2 XRD

Figure 4.18 shows (a) XRD graph of regenerated cotton (ReC) from cotton-DMSO solution via water and (b) RDF graph of interaction cotton in DMSO by MD simulation. The XRD analysis (Figure 4.18(a)) of ReC recovered from Cellulose/DMSO solution displays diffraction peaks at 15.0°, 16.7°, 22.9°, and 34.9°, which match the (1 0 1), (1 1 0), (2 0 0) and (0 0 4) lattice planes reported for native cotton. The prominent reflection at 22.9° corresponds to the (200) crystallographic plane, which matches a calculated d-spacing of approximately 3.87 Å. This d-spacing strongly corresponds to the RDF peak at 3.71 Å observed in the molecular dynamics (MD) simulation (Figure 4.18(b)), indicating periodic interchain packing in cellulose. Peak broadening and a 3–4 % intensity loss relative to the parent fabric indicate reduced lateral crystallite size, yet the persistence of the full peak set confirms that dissolution in DMSO followed by water precipitation preserves the cellulose Iβ polymorph rather than converting it to cellulose II or an amorphous phase. Such agreement between experimental XRD and MD-derived RDF confirms the preservation of cellulose's crystalline domains post-regeneration, consistent with findings by Wei et al., Elf et al. and Zhang et al. [181], [203], [208].

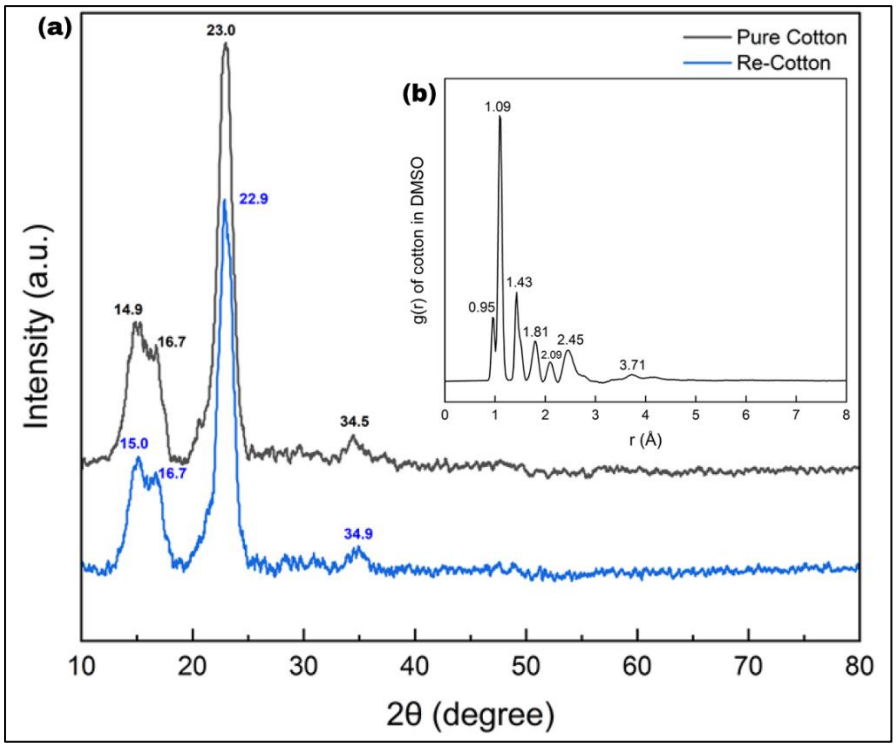

Figure 4.18 (a) XRD Graph of Regenerated Cotton from Cellulose/DMSO Solution via Water and (b) RDF Graph of Interaction Cotton in DMSO by MD Simulation.

Furthermore, the RDF peaks in the 1.81–2.45 Å range represent stable hydrogen bonding between hydroxyl groups, correlating with the (010) and (110) XRD reflections at 14.9° and 16.7°, respectively. These features are hallmarks of ordered cellulose Iβ, reinforcing the structural integrity of ReC. However, at distances beyond ~4.5–5.0 Å, the RDF trend flattens toward unity ($g(r) \approx 1$), indicating a loss of long-range translational order. Ren et al. and Roos et al. also reported that this is consistent with the diminishing XRD intensity beyond 35°, suggesting partial amorphisation of cellulose due to solvent-induced disruption [154], [229]. These results validate the use of molecular dynamics simulation in supporting experimental diffraction data, showing that although some crystalline order is retained, DMSO treatment causes minor loss in long-range cellulose packing while maintaining functional structural integrity suitable for downstream applications. Collectively, experiments and simulations can be concluded that dissolution of cotton fibre using DMSO induces plasticisation of the cellulose fibrils without erasing their fundamental crystalline registry, thereby enabling re-formation of ordered domains upon antisolvent precipitation.

4.3.3.3 TGA-DTG

The TGA-DTG (Figure 4.19) show the thermal transitions curve of pure cotton, pure PET, regenerated cotton from cotton-only samples (ReC), and regenerated cotton recovered from cotton/PET mixtures (ReM). Pure Cotton is used as a baseline to represent the native cellulose to compare the thermal stability with ReC and ReM. Meanwhile, pure PET is also analysed to highlight the distinctly different decomposition behaviour of polyester and to provide a thermal profile that helps identify any remaining PET in ReM samples. Based on Figure 4.19(a), all curves show a small weight drop below 120 °C due to physically bound moisture loss, followed by a major thermal decomposition step occurring between approximately 280 °C and 380 °C, corresponding to the primary degradation of the cellulose backbone [186].

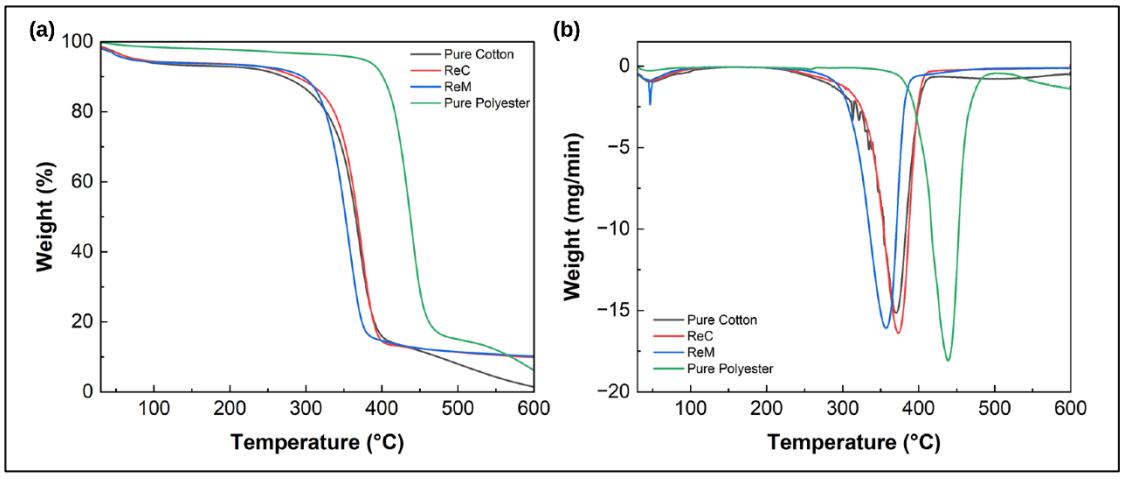

Figure 4.19 TGA-DTG Thermal Transitions Curve of Pure Cotton, Pure PET, Regenerated Cotton from Cotton-Only Samples (ReC), and Regenerated Cotton Recovered from Cotton/PET Mixtures (ReM).

The initial decomposition temperature (T_i) of Pure cotton was observed at around 280 °C, while ReC and ReM exhibited comparable T_i values with only minor shifts, indicating that the dissolution–regeneration process did not significantly alter the onset of cellulose degradation [195]. No obvious difference in T_i between Pure cotton and ReC was observed. However, ReM showed a slight downward shift in T_i, which is attributed to reduced structural regularity and a higher proportion of amorphous domains created during the cotton/PET separation process [250]. The same trend was reflected in the maximum degradation temperatures (T_{max}) shown by the DTG curves (Figure 4.19(b)). T_{max} for Pure cotton occurred at approximately 371 °C, whereas ReC

shifted marginally higher to ~374 °C, and ReM shifted lower to ~357 °C. The relatively small decreases in T_i and T_{max} for the regenerated samples were sufficient to indicate slight thermal destabilisation compared to the original cotton structure. In addition, the residual mass increased for both regenerated samples when compared to Pure cotton, with ReC and ReM each retaining a higher char residue at 600 °C. This increase was attributed to structural rearrangements during regeneration, which may enhance the formation of thermally stable carbon fragments [251]. The absence of a secondary degradation at higher temperatures confirmed that no polyester remained in the regenerated samples. According to thermal behaviour by A. Basch et al. for cellulose-based fibres, the presence of non-cellulosic contaminants or synthetic polymers typically produces additional decomposition peaks at higher temperatures [251], [252]. Therefore, the single-step cellulose degradation observed for both ReC and ReM confirmed the effective removal of PET during processing. The slight reduction in thermal stability for ReM may be explained by partial disruption of the crystalline regions during dissolution and recovery from mixed waste, while the marginally higher T_{max} of ReC suggests that regeneration from pure cotton feeds enhances structural uniformity [253].

4.3.3.4 SEM

Figure 4.20 provides Scanning Electron Microscopy (SEM) images that offer compelling visual evidence of the morphological transformations occurring during the regeneration process of cotton, from both pure recycled cotton and recycled cotton/PET mixture. Figures 4.20 (a-c), representing pure cotton, display characteristic fibrous structures. At lower magnification (a), the material appears as a tangled web of individual fibres. Higher magnifications (b) and (c) reveal the typical flattened, ribbon-like morphology of natural cotton, often exhibiting convolutions or twists along its length. The surface of these fibres appears relatively smooth, consistent with intact primary and secondary cell walls. This morphology underscores the highly ordered, natural cellulose I structure of the original cotton fibres.

In contrast, Figures 4.20 (d-f), illustrating ReC, show a significant alteration in fibre morphology. At lower magnifications (d), the overall fibrous appearance is maintained, but a distinct change becomes evident at higher magnifications (e) and (f). The individual regenerated fibres appear considerably less defined and more irregular

in shape compared to their pure cotton counterparts. The smooth, ribbon-like structure is largely absent, replaced by more cylindrical or amorphous forms. Furthermore, the surfaces of these regenerated fibres appear rougher, with visible signs of aggregation or fusing between individual fibrils, possibly indicating incomplete dissolution or non-uniform coagulation during the regeneration process. This morphology showed preserves the cellulose I rather than converting it to cellulose II during the dissolution and regeneration steps.

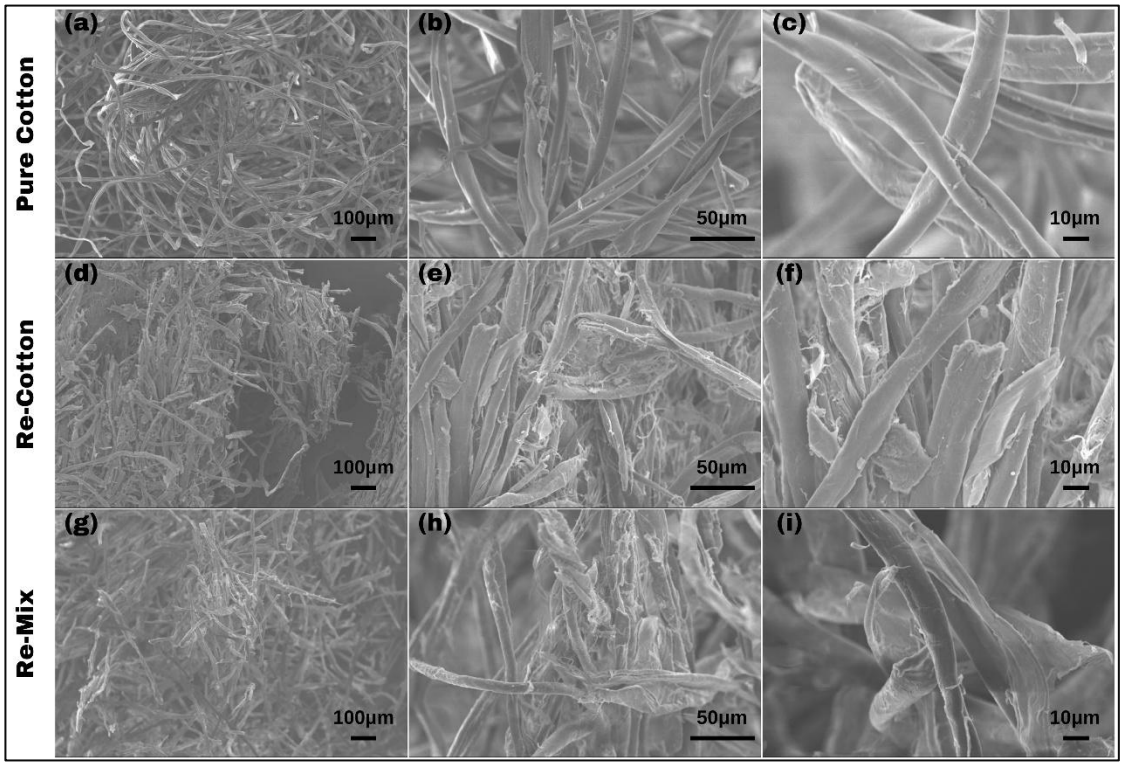

Figure 4.20 SEM Micrographs of (a–c) Pure Cotton, (d–f) Regenerated Cotton (ReC), and (g–i) Regenerated Mixed Fibre (ReM) at increasing Magnifications (100, 500, and 1000 times, Respectively).

Similarly, Figures 4.20 (g-i), depicting the ReM sample, exhibit morphological characteristics like the ReC sample. The low-magnification image (g) again shows a fibrous network. At higher magnifications (h) and (i), the individual fibres display the same loss of the native cotton's characteristic convolutions and ribbon-like structure. They appear irregular, somewhat brittle, and possess a rougher surface texture compared to pure cotton. The visual similarities between the ReC and ReM samples suggest that the regeneration process itself primarily dictates the resulting cellulose morphology, irrespective of the initial presence of PET in the mixture, provided the cotton component undergoes effective dissolution and regeneration. The absence of

clearly identifiable PET remnants in the ReC fibres at these magnifications suggests effective separation or removal of the synthetic component during the process.

In conclusion, the SEM analysis clearly demonstrates that the regeneration process leads to a substantial morphological transformation of cotton fibres. When compared to the well-defined, convoluted, and relatively smooth surface of Pure cotton, both ReC and ReM samples yield regenerated fibres that are generally less uniform in shape, more cylindrical, and possess rougher surfaces. This indicates that while the fibrous nature is retained, the overall quality of the regenerated cellulose fibres, in terms of their distinct morphology and surface smoothness, is visibly diminished compared to the pristine natural cotton fibres. This morphological difference has direct implications for their end-use properties, such as mechanical strength, hand feel, and surface interactions, thereby highlighting the challenges and opportunities in optimising regenerated fibre production for various applications.

CHAPTER 5
CONCLUSION AND RECOMMENDATION

5.1 Conclusion

This study successfully achieved all of its research objectives regarding the dissolution and regeneration of cellulose from textile blends. Firstly, the molecular interactions between polymer (cellulose and PET) chains and DMSO molecules to clarify the solvation mechanisms. Overall, the simulation shows that the DMSO have interacts more with cellulose (cotton) compared to PET (polyester). In terms of temperature and concentration factor, the simulations had predicted that cellulose had the highest interaction at 423K with 4.5mg/ml by considering all thermodynamic properties, such as binding energy. Conversely, PET had a lower interaction with DMSO under the same conditions. The significant difference between the two polymers indicates that there is high possibility for the separation of polycotton at 423K with 4.5mg/ml.

Furthermore, the prediction was supported by an experiment where all parameters that influence dissolution performance were optimised. The effects of temperature, polymer concentration, and dissolution time were analysed to determine conditions that promoted efficient solubilisation while maintaining structural integrity. Based on the result, it proves that the optimum conditions for dissolving cotton in DMSO were 150℃, 4.5mg/ml and 8 hours of dissolution time. The highest dissolution efficiency that was achieved was up to 80%. In contrast, the dissolution of PET shows lower than that of cotton, as the efficiency was less than 20%. The condition was also tested by using a polycotton sample, and it achieved high dissolution efficiency. In addition, the chemical structure of dissolve cotton sample had been analysed, and it shows there is neither an unwanted reaction nor degradation of the chemical structure. This proves that DMSO have high capabilities as a primary solvent in separating cotton from polycotton without any co-solvent.

Finally, the dissolved cotton samples were regenerated using water via the anti-solvent method to assess the possibilities of closed-loop recyclability. The regenerated cotton was characterised to assess its physical and chemical structural transformations.

Overall, the crystallinity, functional group distribution, and morphology of the regenerated cotton were evaluated and found to show no significant changes. The findings confirmed that DMSO facilitated the separation while largely preserving the primary polymer backbone structure.

In conclusion, this work establishes a comprehensive understanding of polymer-DMSO interactions, identifies optimised dissolution conditions, and clarifies the structural integrity of regenerated fibre. Hence, all the objectives of this study were achieved successfully. These findings provide a technical basis for improving solvent-based textile recycling processes, and further studies are needed to enhance solvent recovery efficiency, scalability, and long-term material performance for industrial implementation. However, several key limitations of the current study should be highlighted. This study was conducted within a batch-scale laboratory environment. Therefore, it did not assess the long-term economic viability of the process. In addition, solvent recyclability and the complex dissolution kinetics associated with scaling up the process for multi-component commercial textile waste were not evaluated.

5.2 Recommendation

Based on the findings and limitations identified in this study, several avenues are recommended for future research to advance this technology toward industrial feasibility:

i. Solvent recovery and recyclability should be systematically optimised to minimize waste, lower operational costs, and establish a closed-loop recycling process.
ii. Future work should integrate the current experimental dataset with kinetic and mathematical modelling. This will allow for a deeper optimization of the dissolution mechanisms and facilitate predictable scaling behavior for industrial reactors.
iii. The application of this DMSO-based separation method should be extended to a broader variety of multi-component blended textiles beyond binary polyester-cotton blends to fully assess its adaptability to real-world, post-consumer textile waste.

REFERENCES

Abhiram, G., Bishop, P., Jeyakumar, P., Grafton, M., Davies, C. E., & McCurdy, M. (2023). Formulation and characterization of polyester-lignite composite coated slow-release fertilizers. Journal of Coatings Technology and Research, 20(1), 307–320. https://doi.org/10.1007/s11998-022-00670-6

Abraham, M. J., Murtola, T., Schulz, R., Páll, S., Smith, J. C., Hess, B., & Lindahl, E. (2015). GROMACS: High performance molecular simulations through multi-level parallelism from laptops to supercomputers. SoftwareX, 1–2, 19–25. https://doi.org/10.1016/j.softx.2015.06.001

Acharya, S., Liyanage, S., Parajuli, P., Rumi, S. S., Shamshina, J. L., & Abidi, N. (2021). Utilization of Cellulose to Its Full Potential: A Review on Cellulose Dissolution, Regeneration, and Applications. Polymers, 13(24), 4344. https://doi.org/10.3390/polym13244344

Aghmih, K., Bouftou, A., El Bouchti, M., Boukhriss, A., Gmouh, S., & Majid, S. (2023). Synthesis and application of functionalized ionic liquids-based imidazolium as solvent for cotton fibre cellulose dissolution. Cellulose, 30(3), 1467–1481. https://doi.org/10.1007/s10570-022-04974-z

Ahmed, M. F., Begum, N., & Ali, Md. M. (2024). TEXTILE MERCHANDISING IN THE FAST FASHION ERA: ADAPTING TO RAPID CHANGE IN CONSUMER DEMANDS. Global Mainstream Journal of Business, Economics, Development & Project Management, 3(06), 01–14. https://doi.org/10.62304/jbedpm.v3i06.217

Akhlaghi Bagherjeri, M., Haque, A. N. M. A., Monhemi, H., & Naebe, M. (2024). Dissolution of denim waste in N-methyl morpholine-N-oxide monohydrate for fabrication of regenerated cellulosic film: Experimental and simulation study. Carbohydrate Polymers, 346, 122655. https://doi.org/10.1016/j.carbpol.2024.122655

Akhlaghi Bagherjeri, M., Monhemi, H., Haque, A. N. M. A., & Naebe, M. (2024). Molecular mechanism of cellulose dissolution in N-methyl morpholine-N-oxide: A molecular dynamics simulation study. Carbohydrate Polymers, 323, 121433. https://doi.org/10.1016/j.carbpol.2023.121433

Aksoğan Korkmaz, A., & Toptaş, Y. (2025). Implementation of Taguchi method, ANOVA and regression analyses to enhance char yield by carbonization in

lignite-biomass blended. International Journal of Coal Preparation and Utilization, 45(2), 264–280. https://doi.org/10.1080/19392699.2024.2333825

Alexowsky, C., Bojarska, M., & Ulbricht, M. (2019). Porous poly(vinylidene fluoride) membranes with tailored properties by fast and scalable non-solvent vapor induced phase separation. Journal of Membrane Science, 577, 69–78. https://doi.org/10.1016/j.memsci.2019.01.033

Almeida, A. M., Ramos, M. M. D., & Cadilhe, A. M. (2002). Quantum molecular dynamics simulations of conjugated polymers. Computational Materials Science, 24(1–2), 54–57. https://doi.org/10.1016/S0927-0256(02)00189-1

Anand, A., & Patey, G. N. (2018). Mechanism of Urea Crystal Dissolution in Water from Molecular Dynamics Simulation. Journal of Physical Chemistry B, 122(3), 1213–1222. https://doi.org/10.1021/acs.jpcb.7b07096

Andini, E., Bhalode, P., Gantert, E., Sadula, S., & Vlachos, D. G. (2024). Chemical recycling of mixed textile waste. In Sci. Adv (Vol. 10). https://www.science.org

André, A. D., Teixeira, A. M., & Martins, P. (2024). Influence of DMSO Non-Toxic Solvent on the Mechanical and Chemical Properties of a PVDF Thin Film. Applied Sciences, 14(8), 3356. https://doi.org/10.3390/app14083356

Andrews, J., Gkountouna, O., & Blaisten-Barojas, E. (2022). Forecasting molecular dynamics energetics of polymers in solution from supervised machine learning. Chemical Science, 13(23), 7021–7033. https://doi.org/10.1039/D2SC01216B

Animesh Talapatra, Malhotra Kapish, Choudhury Vinit Ranjan, Vyas Mukul, & Jamal Athar. (2014). Molecular Dynamic Simulation for Nanomechanics of Fiber Reinforced Polymer Nanocomposite Based on Materials Studio. 1(1), 230–235. https://www.researchgate.net/publication/311107196_Molecular_Dynamic_Simulation_for_Nanomechanics_of_Fiber_Reinforced_Polymer_Nanocomposite_Based_on_Materials_Studio

Aulifa, D., Al Shofwan, A., Megantara, S., Fakih, T., & Budiman, A. (2024). Elucidation of Molecular Interactions Between Drug–Polymer in Amorphous Solid Dispersion by a Computational Approach Using Molecular Dynamics Simulations. Advances and Applications in Bioinformatics and Chemistry, Volume 17, 1–19. https://doi.org/10.2147/AABC.S441628

Badar, M. S., Shamsi, S., Ahmed, J., & Alam, Md. A. (2022). Molecular Dynamics Simulations: Concept, Methods, and Applications (pp. 131–151). https://doi.org/10.1007/978-3-030-94651-7_7

Bahraq, A. A., Al-Osta, M. A., Al-Amoudi, O. S. B., Saleh, T. A., & Obot, I. B. (2022). Atomistic simulation of polymer-cement interactions: Progress and research challenges. Construction and Building Materials, 327, 126881. https://doi.org/10.1016/j.conbuildmat.2022.126881

Bakri, M. K. Bin, & Rahman, M. R. (2022). Cellulose interunit linkages and model compounds. In Fundamentals and Recent Advances in Nanocomposites Based on Polymers and Nanocellulose (pp. 41–52). Elsevier. https://doi.org/10.1016/B978-0-323-85771-0.00004-X

Balestra, S. R. G., Vicent-Luna, J. M., Calero, S., Tao, S., & Anta, J. A. (2020). Efficient modelling of ion structure and dynamics in inorganic metal halide perovskites. Journal of Materials Chemistry A, 8(23), 11824–11836. https://doi.org/10.1039/D0TA03200J

Baloyi, R. B., Gbadeyan, O. J., Sithole, B., & Chunilall, V. (2024). Recent advances in recycling technologies for waste textile fabrics: a review. In Textile Research Journal (Vol. 94, Numbers 3–4, pp. 508–529). SAGE Publications Ltd. https://doi.org/10.1177/00405175231210239

Barbosa de Brito, B., Krüger, B., Souza da Silva, L., Marangoni, C., & Cristiane Krause Bierhalz, A. (2025). Regenerated Cellulose Filaments from the Recycling of Textile Cotton Waste Using Ionic Liquids. ACS Omega, 10(19), 19983–19991. https://doi.org/10.1021/acsomega.5c01867

Basch, A., & Lewin, M. (1975). The Influence of Fine Structure on the Flame Retardance of Cellulose. Textile Research Journal, 45(3), 246–250. https://doi.org/10.1177/004051757504500310

Bazooyar, F., Momany, F. A., & Bolton, K. (2012). Validating empirical force fields for molecular-level simulation of cellulose dissolution. Computational and Theoretical Chemistry, 984, 119–127. https://doi.org/10.1016/j.comptc.2012.01.020

Bengtsson, J., Olsson, C., Hedlund, A., Köhnke, T., & Bialik, E. (2017). Understanding the Inhibiting Effect of Small-Molecule Hydrogen Bond Donors on the Solubility of Cellulose in Tetrabutylammonium Acetate/DMSO. The Journal of Physical Chemistry B, 121(50), 11241–11248. https://doi.org/10.1021/acs.jpcb.7b08501

Bering, E., Torstensen, J., Lervik, A., & de Wijn, A. S. (2022). Computational study of the dissolution of cellulose into single chains: the role of the solvent and agitation. Cellulose, 29(3), 1365–1380. https://doi.org/10.1007/s10570-021-04382-9

Boros, K., Nagy, B. E., Tomoiagă, R. B., Tőtős, R., Toșa, M. I., Paizs, C., & Bencze, L. C. (2025). Fine tuning enzyme activity assays for monitoring the enzymatic hydrolysis of PET. Scientific Reports, 15(1), 1877. https://doi.org/10.1038/s41598-024-84177-7

Boschmeier, E., Archodoulaki, V.-M., Schwaighofer, A., Lendl, B., Ipsmiller, W., & Bartl, A. (2023). New separation process for elastane from polyester/elastane and polyamide/elastane textile waste. Resources, Conservation and Recycling, 198, 107215. https://doi.org/10.1016/j.resconrec.2023.107215

Bukhari, M. A., Carrasco-Gallego, R., & Ponce-Cueto, E. (2018). Developing a national programme for textiles and clothing recovery. Waste Management and Research, 36(4), 321–331. https://doi.org/10.1177/0734242x18759190

Bullerjahn, J. T., von Bülow, S., & Hummer, G. (2020). Optimal estimates of self-diffusion coefficients from molecular dynamics simulations. The Journal of Chemical Physics, 153(2). https://doi.org/10.1063/5.0008312

Burkinshaw, S. M. (2024). The roles of elevated temperature and carriers in the dyeing of polyester fibres using disperse dyes: Part 1 fundamental aspects. Coloration Technology, 140(2), 149–207. https://doi.org/10.1111/cote.12715

Cao, R., Long, Y., Li, T., Lv, W., Wu, H., Wang, B., Song, Y., Gao, H., & Nie, Y. (2024). Swelling and dissolution behaviors of cellulose in phosphate-based ionic liquids-H2O binary systems: In-situ observation and molecular dynamics simulation. Journal of Molecular Liquids, 415, 126315. https://doi.org/10.1016/j.molliq.2024.126315

Chai, R., Liu, Y., Liu, Q., & Gu, W. (2021). Experimental and molecular dynamic simulation study on calcite-organic molecule-water interaction mechanism. Journal of Petroleum Science and Engineering, 197, 108114. https://doi.org/10.1016/j.petrol.2020.108114

Chalaris, M., Marinakis, S., & Dellis, D. (2008). Temperature effects on the structure and dynamics of liquid dimethyl sulfoxide: A molecular dynamics study. Fluid Phase Equilibria, 267(1), 47–60. https://doi.org/10.1016/j.fluid.2008.02.019

Chan, T., & Ouyang, D. (2018). Investigating the molecular dissolution process of binary solid dispersions by molecular dynamics simulations. Asian Journal of Pharmaceutical Sciences, 13(3), 248–254. https://doi.org/10.1016/j.ajps.2017.07.011

Chang, C.-J., Kao, Y.-C., Chen, J.-K., Zhang, H.-C., & Wu, S.-Y. (2023). Sustainable waste textile upcycling by selective dye decoloration using ionic liquid and Bi11VO19 photocatalyst. Journal of Industrial and Engineering Chemistry, 124, 412–421. https://doi.org/10.1016/j.jiec.2023.04.035

Chao, P., Zhang, X., Zhang, L., Yang, A., Wang, Y., & Chen, X. (2024). Integration of molecular docking and molecular dynamics simulations with subtractive proteomics approach to identify the novel drug targets and their inhibitors in Streptococcus gallolyticus. Scientific Reports, 14(1), 14755. https://doi.org/10.1038/s41598-024-64769-z

Cheng, X., Ye, H., Guo, C., Pan, L., & Lu, L. (2024). Molecular dynamics simulation of the effects of intermolecular interactions on the diffusion mechanism of 1,2,3-benzotriazole in low density polyethylene. Journal of Polymer Research, 31(4), 109. https://doi.org/10.1007/s10965-024-03961-1

Chmiela, S., Vassilev-Galindo, V., Unke, O. T., Kabylda, A., Sauceda, H. E., Tkatchenko, A., & Müller, K.-R. (2023). Accurate global machine learning force fields for molecules with hundreds of atoms. Science Advances, 9(2). https://doi.org/10.1126/sciadv.adf0873

Ci, Y., Ma, Y., Chen, T., Li, F., & Tang, Y. (2024). Facile dissolution of cellulose by superbase-derived ionic liquid using organic solvents as co-solvents at mild temperatures. Carbohydrate Polymers, 330, 121836. https://doi.org/10.1016/j.carbpol.2024.121836

Cimatu, K. L. A., Ambagaspitiya, T. D., Premadasa, U. I., Adhikari, N. M., Kruse, A., Robertson, E., Guan, S., Rong, L., Advincula, R., & Bythell, B. J. (2022). Polymer-solvent interaction and conformational changes at a molecular level: Implication to solvent-assisted deformation and aggregation at the polymer surface. Journal of Colloid and Interface Science, 616, 221–233. https://doi.org/10.1016/j.jcis.2022.02.006

Claudio, L. (2007). Waste couture: Environmental impact of the clothing industry. Environmental Health Perspectives, 115(9). https://doi.org/10.1289/ehp.115-a449

Crawford, B., & Ismail, A. E. (2020). Insight into Cellulose Dissolution with the Tetrabutylphosphonium Chloride–Water Mixture using Molecular Dynamics Simulations. Polymers, 12(3), 627. https://doi.org/10.3390/polym12030627

Czajczyńska, D., Anguilano, L., Ghazal, H., Krzyżyńska, R., Reynolds, A. J., Spencer, N., & Jouhara, H. (2017). Potential of pyrolysis processes in the waste management sector. In Thermal Science and Engineering Progress (Vol. 3, pp. 171–197). Elsevier Ltd. https://doi.org/10.1016/j.tsep.2017.06.003

Danner, R. P., & High, M. S. (1993). Handbook of Polymer Solution Thermodynamics. Wiley. https://doi.org/10.1002/9780470938232

de Lima, F. P., Alves, C., Gomes-Dias, R., Fernandes, M., Vieira, B., Rodrigues, R., Padrão, J., & Zille, A. (2025). An Eco-friendly Approach for the Separation and Reusage of Pre-consumer Polycotton Textile Waste. Journal of Polymers and the Environment, 33(4), 1847–1863. https://doi.org/10.1007/s10924-025-03500-z

De Silva, R., Wang, X., & Byrne, N. (2014). Recycling textiles: the use of ionic liquids in the separation of cotton polyester blends. RSC Adv., 4(55), 29094–29098. https://doi.org/10.1039/C4RA04306E

Deckers, F., Rasim, K., & Schröder, C. (2022). Molecular dynamics simulation of polypropylene: diffusion and sorption of H2O, H2O2, H2, O2 and determination of the glass transition temperature. Journal of Polymer Research, 29(11), 463. https://doi.org/10.1007/s10965-022-03304-y

Delgado, J. F., Salvay, A. G., Arroyo, S., Bernal, C. R., & Foresti, M. L. (2023). Effect of Dissolution Time on the Development of All-Cellulose Composites Using the NaOH/Urea Solvent System. Polysaccharides, 4(1), 65–77. https://doi.org/10.3390/polysaccharides4010005

Deng, Z., Zhou, G., Fang, T., Fang, K., & Liu, X. (2024). The bidirectional regulation mechanism of NMMO concentration change on cellulose dissolution and regeneration. Cellulose, 31(2), 1205–1222. https://doi.org/10.1007/s10570-023-05673-z

Dignani, M. T., Bioni, T. A., Paixão, T. R. L. C., & El Seoud, O. A. (2020). Cellulose Dissolution in Mixtures of Ionic Liquids and Dimethyl Sulfoxide: A Quantitative Assessment of the Relative Importance of Temperature and Composition of the Binary Solvent. Molecules, 25(24), 5975. https://doi.org/10.3390/molecules25245975

Dong, C., Zheng, W., Wang, L., Zhen, W., & Zhao, L. (2021). Insight into glass transition temperature and mechanical properties of PVA/TRIS functionalized graphene oxide composites by molecular dynamics simulation. Materials & Design, 206, 109770. https://doi.org/10.1016/j.matdes.2021.109770

Du, X., Han, Y., He, X., Lu, Y., Shi, S., & Han, L. (2024). The comparison of cellulose regeneration behavior in different solvents after sulfuric acid treatment. https://doi.org/10.21203/rs.3.rs-4563229/v1

Duman, G. (2021). Preparation of novel porous carbon from hydrothermal pretreated textile wastes: Effects of textile type and activation agent on structural and adsorptive properties. Journal of Water Process Engineering, 43, 102286. https://doi.org/10.1016/J.JWPE.2021.102286

Dzolkifle, N. A. N., & Wan Nawawi, W. M. F. (2024). A review on chitin dissolution as preparation for electrospinning application. International Journal of Biological Macromolecules, 265, 130858. https://doi.org/10.1016/j.ijbiomac.2024.130858

Elf, P., Özeren, H. D., Larsson, P. A., Larsson, A., Wågberg, L., Nilsson, R., Chaiyupatham, P. T., Hedenqvist, M. S., & Nilsson, F. (2023). Molecular Dynamics Simulations of Cellulose and Dialcohol Cellulose under Dry and Moist Conditions. Biomacromolecules, 24(6), 2706–2720. https://doi.org/10.1021/acs.biomac.3c00156

Etale, A., Onyianta, A. J., Turner, S. R., & Eichhorn, S. J. (2023). Cellulose: A Review of Water Interactions, Applications in Composites, and Water Treatment. Chemical Reviews, 123(5), 2016–2048. https://doi.org/10.1021/acs.chemrev.2c00477

Faiz Afzal, M. A., Lehmkemper, K., Sobich, E., Hughes, T. F., Giesen, D. J., Zhang, T., Krauter, C. M., Winget, P., Degenhardt, M., Kyerematen, S. O., Browning, A. R., & Shelley, J. C. (2021). Molecular-Level Examination of Amorphous Solid Dispersion Dissolution. Molecular Pharmaceutics, 18(11), 3999–4014. https://doi.org/10.1021/acs.molpharmaceut.1c00289

Ferchichi, S., Sheibat-Othman, N., Boyron, O., Bonnin, C., Norsic, S., Rey-Bayle, M., & Monteil, V. (2024). In situ dissolved polypropylene prediction by Raman and ATR-IR spectroscopy for its recycling. Analytical Methods, 16(19), 3109–3117. https://doi.org/10.1039/D4AY00667D

Frenkel, D., & Smit, B. (2023). Molecular Dynamics simulations. Understanding Molecular Simulation, 97–124. https://doi.org/10.1016/B978-0-32-390292-2.00012-X

From, M., Larsson, P. T., Andreasson, B., Medronho, B., Svanedal, I., Edlund, H., & Norgren, M. (2020). Tuning the properties of regenerated cellulose: Effects of

polarity and water solubility of the coagulation medium. Carbohydrate Polymers, 236, 116068. https://doi.org/10.1016/j.carbpol.2020.116068

Future Market Insights. (2025). Poly Cotton Fabric Market Growth - Trends & Forecast 2025 to 2035. Future Market Insights. https://www.futuremarketinsights.com/reports/poly-cotton-fabric-market

Gaiduk, A. P., & Galli, G. (2017). Local and Global Effects of Dissolved Sodium Chloride on the Structure of Water. The Journal of Physical Chemistry Letters, 8(7), 1496–1502. https://doi.org/10.1021/acs.jpclett.7b00239

Gao, H.-M., Li, B., Zhang, R., Sun, Z.-Y., & Lu, Z.-Y. (2020). Free energy for inclusion of nanoparticles in solvated polymer brushes from molecular dynamics simulations. The Journal of Chemical Physics, 152(9). https://doi.org/10.1063/5.0002257

Gelpi, J., Hospital, A., Goñi, R., & Orozco, M. (2015). Molecular dynamics simulations: advances and applications. Advances and Applications in Bioinformatics and Chemistry, 37. https://doi.org/10.2147/AABC.S70333

Gkeka, P., Stoltz, G., Barati Farimani, A., Belkacemi, Z., Ceriotti, M., Chodera, J. D., Dinner, A. R., Ferguson, A. L., Maillet, J.-B., Minoux, H., Peter, C., Pietrucci, F., Silveira, A., Tkatchenko, A., Trstanova, Z., Wiewiora, R., & Lelièvre, T. (2020). Machine Learning Force Fields and Coarse-Grained Variables in Molecular Dynamics: Application to Materials and Biological Systems. Journal of Chemical Theory and Computation, 16(8), 4757–4775. https://doi.org/10.1021/acs.jctc.0c00355

Gong, D., Zhang, A., Luo, H., Shi, Y., Zhang, Y., & Tan, L. (2022). Polyhexamethylene biguanide hydrochloride anchored polymeric elastic fibers with robust antibacterial performance. Journal of Applied Polymer Science, 139(7). https://doi.org/10.1002/app.51633

Guo, M., Miao, Y., Su, J., Zhang, X., Zhang, H., Chen, S., Zhang, W., Liu, L., Hou, L., & Fan, W. (2025). The influencing mechanism of thermo-oxidative aging of waste cotton textiles on mechanical properties of their regenerated fibers. International Journal of Biological Macromolecules, 306, 141509. https://doi.org/10.1016/j.ijbiomac.2025.141509

Guo, Y., Wang, W., & Jiang, X. (2023). Molecular Dynamics Study on Mechanical Properties of Cellulose with Water Molecules Diffusion Behavior at Different Oxygen Concentrations. Forests, 14(2), 371. https://doi.org/10.3390/f14020371

Hasija, R., Chaurasia, S., & Gupta, S. (2021). Formulation design, optimization and in vivo evaluation of oral co-encapsulated resveratrol-humic acid colloidal polymeric nanocarriers. Pharmaceutical Development and Technology, 26(9), 953–966. https://doi.org/10.1080/10837450.2021.1966442

Haslinger, S., Hummel, M., Anghelescu-Hakala, A., Määttänen, M., & Sixta, H. (2019). Upcycling of cotton polyester blended textile waste to new man-made cellulose fibers. Waste Management, 97, 88–96. https://doi.org/10.1016/j.wasman.2019.07.040

Hauru, L. K. J., Hummel, M., Nieminen, K., Michud, A., & Sixta, H. (2016). Cellulose regeneration and spinnability from ionic liquids. Soft Matter, 12(5), 1487–1495. https://doi.org/10.1039/C5SM02618K

Hawkins, J. E., Liang, Y., Ries, M. E., & Hine, P. J. (2021). Time temperature superposition of the dissolution of cellulose fibres by the ionic liquid 1-ethyl-3-methylimidazolium acetate with cosolvent dimethyl sulfoxide. Carbohydrate Polymer Technologies and Applications, 2, 100021. https://doi.org/10.1016/j.carpta.2020.100021

He, H., Li, L., Ya, R., Liu, H., Luo, B., Li, Z., & Tian, W. (2024). Molecular dynamics simulation and experimental verification of the effects of vinyl silicone oil viscosity on the mechanical properties of silicone rubber foam. RSC Advances, 14(33), 23840–23852. https://doi.org/10.1039/D4RA04784B

Heinz, H., Lin, T.-J., Kishore Mishra, R., & Emami, F. S. (2013). Thermodynamically Consistent Force Fields for the Assembly of Inorganic, Organic, and Biological Nanostructures: The INTERFACE Force Field. Langmuir, 29(6), 1754–1765. https://doi.org/10.1021/la3038846

Heinze, T. (2015). Cellulose: Structure and Properties (pp. 1–52). https://doi.org/10.1007/12_2015_319

Heiran, R., Ghaderian, A., Reghunadhan, A., Sedaghati, F., Thomas, S., & Haghighi, A. hossein. (2021). Glycolysis: an efficient route for recycling of end of life polyurethane foams. Journal of Polymer Research, 28(1), 22. https://doi.org/10.1007/s10965-020-02383-z

Hou, W., Ling, C., Shi, S., Yan, Z., Zhang, M., Zhang, B., & Dai, J. (2018). Separation and Characterization of Waste Cotton/polyester Blend Fabric with Hydrothermal Method. Fibers and Polymers, 19(4), 742–750. https://doi.org/10.1007/s12221-018-7735-9

Hou, Z., Ju, Y., Zong, Y., Ye, F., & Zhao, K. (2018). Molecular dynamics simulations on the dynamics of two-dimensional rounded squares. Chinese Physics B, 27(8), 088203. https://doi.org/10.1088/1674-1056/27/8/088203

Hsu, H.-P., & Kremer, K. (2017). Detailed analysis of Rouse mode and dynamic scattering function of highly entangled polymer melts in equilibrium. The European Physical Journal Special Topics, 226(4), 693–703. https://doi.org/10.1140/epjst/e2016-60322-5

Hu, H., Xu, Q., Sun, L., Zhu, R., Gao, T., He, Y., Ma, B., Yu, J., & Wang, X. (2023). 1 Rapid Hydrolysis of Waste and Scrap PA6 Textiles to ε-Caprolactam. ACS Applied Polymer Materials, 5(1), 751–763. https://doi.org/10.1021/acsapm.2c01744

Huang, J., Xu, W., Long, Y., Zhu, Y., Chen, S., Duan, W., Ou, J., Wang, H., Dong, C., & Tian, S. (2024). Studies on hydrolysis/alcoholysis/ammonolysis mechanisms of ethylene terephthalate dimer using DFT method. Arabian Journal of Chemistry, 17(4), 105719. https://doi.org/10.1016/j.arabjc.2024.105719

Huang, Y., & Cheng, S. (2021). Chain conformations and phase separation in polymer solutions with varying solvent quality. Journal of Polymer Science, 59(22), 2819–2831. https://doi.org/10.1002/pol.20210526

Huang, Y.-B., Xin, P.-P., Li, J.-X., Shao, Y.-Y., Huang, C.-B., & Pan, H. (2016). Room-Temperature Dissolution and Mechanistic Investigation of Cellulose in a Tetra-Butylammonium Acetate/Dimethyl Sulfoxide System. ACS Sustainable Chemistry & Engineering, 4(4), 2286–2294. https://doi.org/10.1021/acssuschemeng.5b01749

Humbert, M. T., Zhang, Y., & Maginn, E. J. (2019). PyLAT: Python LAMMPS Analysis Tools. Journal of Chemical Information and Modeling, 59(4), 1301–1305. https://doi.org/10.1021/acs.jcim.9b00066

Inakollu, V. S., Geerke, D. P., Rowley, C. N., & Yu, H. (2020). Polarisable force fields: what do they add in biomolecular simulations? Current Opinion in Structural Biology, 61, 182–190. https://doi.org/10.1016/j.sbi.2019.12.012

Islam, M. R., Golovin, K., & Dolez, P. I. (2023). Clothing Thermophysiological Comfort: A Textile Science Perspective. Textiles, 3(4), 353–409. https://doi.org/10.3390/textiles3040024

Jaafari, Z., Avazpour, A., Semiromi, M. A., & Khordad, R. (2025). Theoretical and simulation study of confined oblate hard ellipsoid liquid crystals: NPT, NVT and

extended restricted orientation model. Molecular Physics, 123(18). https://doi.org/10.1080/00268976.2025.2462639

Jadhav, N. R., Gaikwad, V. L., Nair, K. J., & Kadam, H. M. (2009). Glass transition temperature: Basics and application in pharmaceutical sector. In Asian Journal of Pharmaceutics (Vol. 3, Number 2, pp. 82–89). https://doi.org/10.4103/0973-8398.55043

Jaffe, M., Easts, A. J., & Feng, X. (2020). Polyester fibers. In Thermal Analysis of Textiles and Fibers (pp. 133–149). Elsevier. https://doi.org/10.1016/B978-0-08-100572-9.00008-2

Jaillet, L., Artemova, S., & Redon, S. (2017). IM-UFF: Extending the universal force field for interactive molecular modeling. Journal of Molecular Graphics and Modelling, 77, 350–362. https://doi.org/10.1016/j.jmgm.2017.08.023

Jena, K. K., Raju, K. V. S. N., Prathab, B., & Aminabhavi, T. M. (2007). Hyperbranched polyesters: Synthesis, characterization, and molecular simulations. Journal of Physical Chemistry B, 111(30), 8801–8811. https://doi.org/10.1021/jp070513t

Jeong, S. (2023). Investigation of intrinsic characteristics of polymer blends via molecular simulation: a review. Korea-Australia Rheology Journal, 35(4), 249–266. https://doi.org/10.1007/s13367-023-00076-9

Jiang, X., Wang, W., Guo, Y., & Dai, M. (2023). Molecular Dynamics Simulation of the Effect of Low Temperature on the Properties of Lignocellulosic Amorphous Region. Forests, 14(6). https://doi.org/10.3390/f14061208

Johansson, L. (n.d.). On the Mechanical Recycling of Woven Fabrics Improving the Reusable Fibre Yield of Mechanical Methods. Retrieved http://www.teknat.uu.se/student

Juanga-Labayen, J. P., Labayen, I. V., & Yuan, Q. (2022). A Review on Textile Recycling Practices and Challenges. In Textiles (Vol. 2, Number 1, pp. 174–188). Multidisciplinary Digital Publishing Institute (MDPI). https://doi.org/10.3390/textiles2010010

Jung, J., & Sugita, Y. (2020). Group-based evaluation of temperature and pressure for molecular dynamics simulation with a large time step. The Journal of Chemical Physics, 153(23). https://doi.org/10.1063/5.0027873

Jungbluth, M., & Beuermann, S. (2025). Separation of Polycotton for Textile Recycling Using the DBU/DMSO/CO2 Switchable Solvent System. ACS Sustainable

Chemistry & Engineering, 13(11), 4341–4348. https://doi.org/10.1021/acssuschemeng.4c07633

Kalogeras, I. M. (2016). Glass-Transition Phenomena in Polymer Blends. In Encyclopedia of Polymer Blends (pp. 1–134). Wiley. https://doi.org/10.1002/9783527653966.ch1

Kemppainen, J., Gissinger, J. R., Gowtham, S., & Odegard, G. M. (2024). LUNAR: Automated Input Generation and Analysis for Reactive LAMMPS Simulations. Journal of Chemical Information and Modeling, 64(13), 5108–5126. https://doi.org/10.1021/acs.jcim.4c00730

Keppeler, N., Augusto R. Pires, P., Leandro S. Freitas, J., & El Seoud, O. A. (2023). Cellulose dissolution in mixtures of ionic liquids and molecular solvents: The fruitful synergism of experiment and theory. Journal of Molecular Liquids, 386, 122490. https://doi.org/10.1016/j.molliq.2023.122490

Ketema, A., & Worku, A. (2020). Review on Intermolecular Forces between Dyes Used for Polyester Dyeing and Polyester Fiber. Journal of Chemistry, 2020, 1–7. https://doi.org/10.1155/2020/6628404

Khan, R. A. A., Chen, X., Qi, H.-K., Huang, J.-H., & Luo, M.-B. (2021). A novel shift in the glass transition temperature of polymer nanocomposites: a molecular dynamics simulation study. Physical Chemistry Chemical Physics, 23(21), 12216–12225. https://doi.org/10.1039/D1CP00321F

Khan, R. A. A., Qi, H.-K., Huang, J.-H., & Luo, M.-B. (2021). A simulation study on the effect of nanoparticle size on the glass transition temperature of polymer nanocomposites. Soft Matter, 17(35), 8095–8104. https://doi.org/10.1039/D1SM00843A

Khoo, Y. S., Liang, Y. N., Hu, X., & Chew, J. W. (2024). A greener approach for physical separation of polycotton textile waste. Journal of Environmental Chemical Engineering, 12(6), 114281. https://doi.org/10.1016/j.jece.2024.114281

Kirshanov, K., Toms, R., Aliev, G., Naumova, A., Melnikov, P., & Gervald, A. (2022). Recent Developments and Perspectives of Recycled Poly(ethylene terephthalate)-Based Membranes: A Review. Membranes, 12(11), 1105. https://doi.org/10.3390/membranes12111105

Knihs, A. F., Aragão, L. K., Granato, M. A., Bierhalz, A. C. K., & Valle, R. de C. S. C. (2024). Reduction Discoloration of Reactive Dyed Cotton Waste and Chemical

Recycling via Ionic Liquid. Journal of Renewable Materials, 12(9), 1557–1571. https://doi.org/10.32604/jrm.2024.052963

Kostag, M., Pires, P. A. R., & El Seoud, O. A. (2020). Dependence of cellulose dissolution in quaternary ammonium acetates/DMSO on the molecular structure of the electrolyte: use of solvatochromism, micro-calorimetry, and molecular dynamics simulations. Cellulose, 27(7), 3565–3580. https://doi.org/10.1007/s10570-020-03050-8

Krishna, S., Sreedhar, I., & Patel, C. M. (2021a). Molecular dynamics simulation of polyamide-based materials – A review. Computational Materials Science, 200, 110853. https://doi.org/10.1016/j.commatsci.2021.110853

Krishna, S., Sreedhar, I., & Patel, C. M. (2021b). Molecular dynamics simulation of polyamide-based materials – A review. Computational Materials Science, 200, 110853. https://doi.org/10.1016/j.commatsci.2021.110853

Kronberg, S., & Baghaei, B. (2024). Transforming Polycotton Textile Waste into New Bicomponent Fibers: An Investigative Study. Advances in Polymer Technology, 2024(1). https://doi.org/10.1155/2024/5239028

Kutzner, C., Kniep, C., Cherian, A., Nordstrom, L., Grubmüller, H., de Groot, B. L., & Gapsys, V. (2022). GROMACS in the Cloud: A Global Supercomputer to Speed Up Alchemical Drug Design. Journal of Chemical Information and Modeling, 62(7), 1691–1711. https://doi.org/10.1021/acs.jcim.2c00044

Landfield, H., & Wang, M. (2022). Determination of Hydrophobic Polymer Clustering in Concentrated Aqueous Solutions through Single-Particle Tracking Diffusion Studies. Macromolecules, 55(17), 7425–7437. https://doi.org/10.1021/acs.macromol.2c00840

Lee, H. L., Yang, C. L., & Lee, T. (2022). Shaping particle size distribution of a metastable polymorph in additive-assisted reactive crystallization by the Taguchi method. CrystEngComm, 24(40), 7176–7192. https://doi.org/10.1039/D2CE00355D

Lee, I., & Yang, N.-C. (2022). Using Taguchi Method to Determine the Optimum Conditions for Synthesizing Parapyruvate. Molecules, 27(6), 1870. https://doi.org/10.3390/molecules27061870

Lee, S., Goo Lee, J., Lee, H., & Mumby, S. J. (1999). Molecular dynamics simulations of the enthalpy of mixing of poly(vinyl chloride) and aliphatic polyester blends. Polymer, 40(18), 5137–5145. https://doi.org/10.1016/S0032-3861(98)00586-2

Leenders, N., Moerbeek, R. M., Puijk, M. J., Bronkhorst, R. J. A., Bueno Morón, J., van Klink, G. P. M., & Gruter, G.-J. M. (2025). Polycotton waste textile recycling by sequential hydrolysis and glycolysis. Nature Communications, 16(1), 738. https://doi.org/10.1038/s41467-025-55935-6

Leenders, N., van Klink, G. P. M., & Gruter, G.-J. M. (2025). Towards polycotton waste valorisation: depolymerisation of cotton to glucose with polyester preservation. RSC Sustainability, 3(9), 3863–3882. https://doi.org/10.1039/D5SU00230C

Li, G., Zheng, F., Huang, Q., Wang, J., Niu, B., Zhang, Y., & Long, D. (2022). Molecular insight into pyrolysis processes via reactive force field molecular dynamics: A state-of-the-art review. Journal of Analytical and Applied Pyrolysis, 166, 105620. https://doi.org/10.1016/j.jaap.2022.105620

Li, L., Fan, T., Hu, R., Liu, Y., & Lu, M. (2017). Surface micro-dissolution process for embedding carbon nanotubes on cotton fabric as a conductive textile. Cellulose, 24(2), 1121–1128. https://doi.org/10.1007/s10570-016-1160-2

Li, X., Sun, J., Wei, X., Li, L., Jin, H., & Guo, L. (2023). Molecular dynamics study with COMPASS II forcefield on nucleation and growth mechanism of sodium chloride in supercritical water. The Journal of Supercritical Fluids, 202, 106053. https://doi.org/10.1016/j.supflu.2023.106053

Li, Y., Jin, X., Moubarak, E., & Smit, B. (2024). A Refined Set of Universal Force Field Parameters for Some Metal Nodes in Metal–Organic Frameworks. Journal of Chemical Theory and Computation, 20(23), 10540–10552. https://doi.org/10.1021/acs.jctc.4c01113

Lian, X., He, P., Wang, L., Cao, Y., Huang, K., Xu, S., Chen, J., & Li, H. (2022). Purification of MDI Isomers Using Dynamic Falling Film Melt Crystallization: Experiment and Molecular Simulation. ACS Omega, 7(25), 21492–21504. https://doi.org/10.1021/acsomega.2c01021

Liang, Y., Ries, M. E., & Hine, P. J. (2022). Three methods to measure the dissolution activation energy of cellulosic fibres using time-temperature superposition. Carbohydrate Polymers, 291, 119541. https://doi.org/10.1016/j.carbpol.2022.119541

Liebau, J., Laatsch, B. F., Rusnak, J., Gunderson, K., Finke, B., Bargender, K., Narkiewicz-Jodko, A., Weeks, K., Williams, M. T., Shulgina, I., Musier-Forsyth, K., Bhattacharyya, S., & Hati, S. (2024). Polyethylene Glycol Impacts Conformation and Dynamics of Escherichia coli Prolyl-tRNA Synthetase Via

Crowding and Confinement Effects. Biochemistry, 63(13), 1621–1635. https://doi.org/10.1021/acs.biochem.3c00719

Lima, L. F. de, Oliveira, J. O. de, Carneiro, J. N. P., Lima, C. N. F., Coutinho, H. D. M., & Morais-Braga, M. F. B. (2021). Ethnobotanical and antimicrobial activities of the Gossypium (Cotton) genus: A review. Journal of Ethnopharmacology, 279, 114363. https://doi.org/10.1016/j.jep.2021.114363

Lin, L., & Tsuchii, K. (2022). Dissolution behavior of cellulose in a novel cellulose solvent. Carbohydrate Research, 511, 108490. https://doi.org/10.1016/j.carres.2021.108490

Liu, S.-H., Rukmani, S. J., Mohan, M., Yu, Y., Vural, D., Johnson, D. A., Copenhaver, K., Bhagia, S., Lamm, M. E., Li, K., Chen, J., Goswami, M., Smith, M. D., Petridis, L., Ozcan, S., & Smith, J. C. (2024). Molecular-level design of alternative media for energy-saving pilot-scale fibrillation of nanocellulose. Proceedings of the National Academy of Sciences, 121(37). https://doi.org/10.1073/pnas.2405107121

Liu, W., Liu, S., Liu, T., Liu, T., Zhang, J., & Liu, H. (2019). Eco-friendly post-consumer cotton waste recycling for regenerated cellulose fibers. Carbohydrate Polymers, 206, 141–148. https://doi.org/10.1016/j.carbpol.2018.10.046

Long, Y., Li, Y., Cao, R., Qin, C., Wang, B., Wu, H., & Nie, Y. (2024). Molecular insight into the dissolution-degradation process of cellulose bunch in ionic liquids. Journal of Molecular Liquids, 414, 126191. https://doi.org/10.1016/j.molliq.2024.126191

Lu, Y., Jin, G., Xiao, P., Jinshan, Q., & Chao, T. (2021). Cellulose insulation paper with high thermal stability and low polarizability: influence of different substituents on POSS modified cellulose insulating paper. Cellulose, 28(10), 6023–6033. https://doi.org/10.1007/s10570-021-03956-x

Luna, E., Olazabal, I., Roosen, M., Müller, A., Jehanno, C., Ximenis, M., de Meester, S., & Sardon, H. (2024). Towards a better understanding of the cosolvent effect on the low-temperature glycolysis of Polyethylene Terephthalate (PET). Chemical Engineering Journal, 482, 148861. https://doi.org/10.1016/j.cej.2024.148861

Mabesoone, M. F. J., Palmans, A. R. A., & Meijer, E. W. (2020). Solute–Solvent Interactions in Modern Physical Organic Chemistry: Supramolecular Polymers as

a Muse. Journal of the American Chemical Society, 142(47), 19781–19798. https://doi.org/10.1021/jacs.0c09293

Majumdar, A., Shukla, S., Singh, A. A., & Arora, S. (2020). Circular fashion: Properties of fabrics made from mechanically recycled poly-ethylene terephthalate (PET) bottles. Resources, Conservation and Recycling, 161, 104915. https://doi.org/10.1016/J.RESCONREC.2020.104915

Marino, T., Galiano, F., Simone, S., & Figoli, A. (2019). DMSO EVOLTM as novel non-toxic solvent for polyethersulfone membrane preparation. Environmental Science and Pollution Research, 26(15), 14774–14785. https://doi.org/10.1007/s11356-018-3575-9

Melzer, F., Breuer, R., Dahlmann, R., & Hopmann, C. (2024). Calculating diffusion coefficients from molecular dynamics simulations for modelling foam processes of polypropylene: Investigating different process conditions and blowing agents. Journal of Cellular Plastics, 60(2), 97–115. https://doi.org/10.1177/0021955X231225153

Mensah, R. A., Kirton, S. B., Cook, M. T., Styliari, I. D., Hutter, V., & Chau, D. Y. S. (2019). Optimising poly(lactic-co-glycolic acid) microparticle fabrication using a Taguchi orthogonal array design-of-experiment approach. PLOS ONE, 14(9), e0222858. https://doi.org/10.1371/journal.pone.0222858

Meunier, M. (2012). Introduction to materials studio. EPJ Web of Conferences, 30. https://doi.org/10.1051/epjconf/20123004001

Meunier, M., & Robertson, S. (2021). Materials Studio 20th anniversary. Molecular Simulation, 47(7), 537–539. https://doi.org/10.1080/08927022.2021.1892093

Miller-Chou, B. A., & Koenig, J. L. (2003). A review of polymer dissolution. Progress in Polymer Science, 28(8), 1223–1270. https://doi.org/10.1016/S0079-6700(03)00045-5

Mittal, N., Soni, R. K., & Teotia, M. (2025). Innovative approaches to chemical recycling of polyethylene terephthalate waste: Investigating key components and their emerging applications. Journal of Environmental Management, 373, 123595. https://doi.org/10.1016/j.jenvman.2024.123595

Miyata, T., Funahara, Y., Omori, S., & Shinjo, T. (2023). A study on the extension of correlation functions obtained from molecular dynamics simulations by the Ornstein–Zernike theory for modeled molten salts. AIP Advances, 13(11). https://doi.org/10.1063/5.0180366

Mohammadi, M., Davoodi, J., Javanbakht, M., & Rezaei, H. (2018). Glass transition temperature of PMMA/modified alumina nanocomposite: molecular dynamic study. Materials Research Express, 6(3), 035309. https://doi.org/10.1088/2053-1591/aaf6d5

Monteferrante, M., Succi, S., Pisignano, D., & Lauricella, M. (2022). Simulating Polymerization by Boltzmann Inversion Force Field Approach and Dynamical Nonequilibrium Reactive Molecular Dynamics. Polymers, 14(21), 4529. https://doi.org/10.3390/polym14214529

Muhammad Faez Tan, N. U. W., Muhammad, A., Azmi, I. S., Roslan, A., & Abu Bakar, N. F. (2026). Effect of Anti-Solvent in the Regeneration of Cotton from Cotton/DMSO Solution. 189–195. https://doi.org/10.4028/p-B8VlDN

Najib, M., Hammond, R. B., Mahmud, T., & Izumi, T. (2021). Impact of Structural Binding Energies on Dissolution Rates for Single Faceted-Crystals. Crystal Growth & Design, 21(3), 1482–1495. https://doi.org/10.1021/acs.cgd.0c01142

Nazir, M. U., Shaker, K., Nawab, Y., Hamdani, S. T. A., Abdullah, H. M., & Umair, M. (2022). Thermo-physiological Comfort of Woven Fabrics Made from Different Cellulosic Yarns. Journal of Natural Fibers, 19(11), 4050–4062. https://doi.org/10.1080/15440478.2020.1852997

Ndagano, U. N., Cahill, L., Smullen, C., Gaughran, J., & Kelleher, S. M. (2025). The Current State-of-the-Art of the Processes Involved in the Chemical Recycling of Textile Waste. Molecules, 30(2), 299. https://doi.org/10.3390/molecules30020299

Okolie, J. A., Nanda, S., Dalai, A. K., Berruti, F., & Kozinski, J. A. (2020). A review on subcritical and supercritical water gasification of biogenic, polymeric and petroleum wastes to hydrogen-rich synthesis gas. Renewable and Sustainable Energy Reviews, 119, 109546. https://doi.org/10.1016/j.rser.2019.109546

Orlando, C., Prejanò, M., Russo, N., & Marino, T. (2023). On the Role of Temperature in the Depolymerization of PET by FAST-PETase: An Atomistic Point of View on Possible Active Site Pre-Organization and Substrate-Destabilization Effects. ChemBioChem, 24(20). https://doi.org/10.1002/cbic.202300412

Owens, C. E., Du, J., & Sánchez, P. B. (2022). Understanding the Dynamics of Cellulose Dissolved in an Ionic Liquid Solvent Under Shear and Extensional Flows. Biomacromolecules, 23(5), 1958–1969. https://doi.org/10.1021/acs.biomac.1c01623

Pang, J., Mehandzhiyski, A. Y., & Zozoulenko, I. (2023). A computational study of cellulose regeneration: Coarse-grained molecular dynamics simulations. Carbohydrate Polymers, 313, 120853. https://doi.org/10.1016/j.carbpol.2023.120853

Primc, G., & Mozetič, M. (2022). Hydrophobic Recovery of Plasma-Hydrophilized Polyethylene Terephthalate Polymers. Polymers, 14(12), 2496. https://doi.org/10.3390/polym14122496

Pronk, S., Páll, S., Schulz, R., Larsson, P., Bjelkmar, P., Apostolov, R., Shirts, M. R., Smith, J. C., Kasson, P. M., van der Spoel, D., Hess, B., & Lindahl, E. (2013). GROMACS 4.5: a high-throughput and highly parallel open source molecular simulation toolkit. Bioinformatics, 29(7), 845–854. https://doi.org/10.1093/bioinformatics/btt055

Qi, R., Xu, Z., Zhou, Y., Zhang, D., Sun, Z., Chen, W., & Xiong, M. (2021). Clean solid fuel produced from cotton textiles waste through hydrothermal carbonization with FeCl3: Upgrading the fuel quality and combustion characteristics. Energy, 214, 118926. https://doi.org/10.1016/J.ENERGY.2020.118926

Radosinski, L., & Labus, K. (2017). Molecular modeling studies of structural properties of polyvinyl alcohol: a comparative study using INTERFACE force field. Journal of Molecular Modeling, 23(11), 305. https://doi.org/10.1007/s00894-017-3472-z

Raiskio, S., Periyasamy, A., Hummel, M., & Heikkilä, P. (2025). Transforming mechanically recycled cotton and linen from post-consumer textiles into quality ring yarns and knitted fabrics. Waste Management Bulletin, 3(1), 76–86. https://doi.org/10.1016/j.wmb.2024.12.006

Rashid, K. T., Akram, N., Zia, K. M., Usman, M., & Munawar, T. (2024). Novel enrichment in biobased monomers of waterborne polyurethane dispersions as a textile finishing agent for poly-cotton fabrics. International Journal of Biological Macromolecules, 257, 128674. https://doi.org/10.1016/j.ijbiomac.2023.128674

Ren, F., Wang, J., Yu, J., Zhong, C., Xie, F., & Wang, S. (2021). Dissolution of Cellulose in Ionic Liquid–DMSO Mixtures: Roles of DMSO/IL Ratio and the Cation Alkyl Chain Length. ACS Omega, 6(41), 27225–27232. https://doi.org/10.1021/acsomega.1c03954

Reuter, H. (2017). Structural parameters of dimethyl sulfoxide, DMSO, at 100 K, based on a redetermination by use of high-quality single-crystal X-ray data. Acta

Crystallographica Section E Crystallographic Communications, 73(10), 1405–1408. https://doi.org/10.1107/S2056989017012464

Ribeiro, R. S. A., Pohlmann, B. C., Calado, V., Bojorge, N., & Pereira, N. (2019). Production of nanocellulose by enzymatic hydrolysis: Trends and challenges. Engineering in Life Sciences, 19(4), 279–291. https://doi.org/10.1002/elsc.201800158

Ribul, M., Lanot, A., Tommencioni Pisapia, C., Purnell, P., McQueen-Mason, S. J., & Baurley, S. (2021). Mechanical, chemical, biological: Moving towards closed-loop bio-based recycling in a circular economy of sustainable textiles. Journal of Cleaner Production, 326. https://doi.org/10.1016/j.jclepro.2021.129325

Rikiyama, K., Matsunami, A., Yoshida, T., Taniguchi, T., Karatsu, T., Nishitsuji, S., & Aoki, D. (2024). Characterization and ammonolysis behavior of poly(isosorbide carbonate)-based copolymers. Polymer Journal, 56(4), 443–453. https://doi.org/10.1038/s41428-023-00878-2

Roos, E., Gradaus, C., Sebastiani, D., & Brehm, M. (2024). A force field for the solubility of cellulose in DMSO/Ionic liquids. Cellulose, 31(8), 4793–4815. https://doi.org/10.1007/s10570-024-05854-4

Rosson, L., Wang, X., & Byrne, N. (2024). Investigating how the dye colour is impacted when chemically separating polyester-cotton blends. The Journal of The Textile Institute, 115(4), 656–666. https://doi.org/10.1080/00405000.2023.2201977

Saba, H., Yongbo, Y., Jianning, W., Xiaolin, X., Kaijian, W., Yumei, Z., & Huaping, W. (2015). Effect of dimethylsulfoxide on the viscoelastic properties and sol–gel transition of cellulose/ionic liquid solutions. RSC Advances, 5(11), 8318–8322. https://doi.org/10.1039/C4RA14911D

Sakurai, Y., Ito, T., & Nishimoto, M. (2025). Pyrolysis characteristics of blended textile in waste clothing. Journal of the Energy Institute, 120, 102042. https://doi.org/10.1016/j.joei.2025.102042

Salo-Ahen, O. M. H., Alanko, I., Bhadane, R., Bonvin, A. M. J. J., Honorato, R. V., Hossain, S., Juffer, A. H., Kabedev, A., Lahtela-Kakkonen, M., Larsen, A. S., Lescrinier, E., Marimuthu, P., Mirza, M. U., Mustafa, G., Nunes-Alves, A., Pantsar, T., Saadabadi, A., Singaravelu, K., & Vanmeert, M. (2020). Molecular Dynamics Simulations in Drug Discovery and Pharmaceutical Development. Processes, 9(1), 71. https://doi.org/10.3390/pr9010071

Sandin, G., & Peters, G. M. (2018). Environmental impact of textile reuse and recycling – A review. In Journal of Cleaner Production (Vol. 184, pp. 353–365). Elsevier Ltd. https://doi.org/10.1016/j.jclepro.2018.02.266

Sangkhawasi, M., Remsungnen, T., Vangnai, A. S., Poo-arporn, R. P., & Rungrotmongkol, T. (2022). All-Atom Molecular Dynamics Simulations on a Single Chain of PET and PEV Polymers. Polymers, 14(6), 1161. https://doi.org/10.3390/polym14061161

Sankauskaite, A., Stygiene, L., Tumeniene, M. D., Krauledas, S., Jovaišiene, L., & Puodžiuniene, R. (2014). Investigation of Cotton Component Destruction in Cotton/Polyester Blended Textile Waste Materials. Medziagotyra, 20(2), 189–192. https://doi.org/10.5755/j01.ms.20.2.3115

Sasaki, K., & Yamashita, T. (2021). Modification and Validation of the DREIDING Force Field for Molecular Liquid Simulations (DREIDING-UT). Journal of Chemical Information and Modeling, 61(3), 1172–1179. https://doi.org/10.1021/acs.jcim.0c01169

Savin, A. V., & Mazo, M. A. (2020). The COMPASS force field: Validation for carbon nanoribbons. Physica E: Low-Dimensional Systems and Nanostructures, 118, 113937. https://doi.org/10.1016/j.physe.2019.113937

Sayyed, A. J., Deshmukh, N. A., & Pinjari, D. V. (2019). A critical review of manufacturing processes used in regenerated cellulosic fibres: viscose, cellulose acetate, cuprammonium, LiCl/DMAc, ionic liquids, and NMMO based lyocell. Cellulose, 26(5), 2913–2940. https://doi.org/10.1007/s10570-019-02318-y

Schikarski, T., Trzenschiok, H., Avila, M., & Peukert, W. (2023). Impact of solvent properties on the precipitation of active pharmaceutical ingredients. Powder Technology, 415, 118032. https://doi.org/10.1016/j.powtec.2022.118032

Sert, E., Yılmaz, E., & Atalay, F. S. (2019). Chemical Recycling of Polyethlylene Terephthalate by Glycolysis Using Deep Eutectic Solvents. Journal of Polymers and the Environment, 27(12), 2956–2962. https://doi.org/10.1007/s10924-019-01578-w

Sfameni, S., Lawnick, T., Rando, G., Visco, A., Textor, T., & Plutino, M. R. (2023). Super-Hydrophobicity of Polyester Fabrics Driven by Functional Sustainable Fluorine-Free Silane-Based Coatings. Gels, 9(2), 109. https://doi.org/10.3390/gels9020109

Sharma, S., Kumar, P., & Chandra, R. (2019). Applications of BIOVIA Materials Studio, LAMMPS, and GROMACS in Various Fields of Science and Engineering. In Molecular Dynamics Simulation of Nanocomposites Using BIOVIA Materials Studio, Lammps and Gromacs (pp. 329–341). Elsevier. https://doi.org/10.1016/B978-0-12-816954-4.00007-3

Sharma, S., Kumar, P., Chandra, R., Singh, S. P., Mandal, A., & Dondapati, R. S. (2019). Overview of BIOVIA Materials Studio, LAMMPS, and GROMACS. Molecular Dynamics Simulation of Nanocomposites Using BIOVIA Materials Studio, Lammps and Gromacs, 39–100. https://doi.org/10.1016/B978-0-12-816954-4.00002-4

Sheng, C., Wu, G., Sun, X., & Liu, S. (2021). Molecular Dynamics Investigation of the Thermo-Mechanical Properties of the Moisture Invaded and Cross-Linked Epoxy System. Polymers, 14(1), 103. https://doi.org/10.3390/polym14010103

Singh, J., Sung, K., Cooper, T., West, K., & Mont, O. (2019). Challenges and opportunities for scaling up upcycling businesses – The case of textile and wood upcycling businesses in the UK. Resources, Conservation and Recycling, 150, 104439. https://doi.org/10.1016/j.resconrec.2019.104439

Singhal, S., Agarwal, S., & Singhal, N. (2023). Chemical recycling of waste clothes: a smarter approach to sustainable development. Environmental Science and Pollution Research, 30(19), 54448–54469. https://doi.org/10.1007/s11356-023-26438-y

Smelik, A. (2023). Polyester: A Cultural History. Fashion Practice, 15(2), 279–299. https://doi.org/10.1080/17569370.2023.2196158

Steinbach, P. J., & Brooks, B. R. (1994). New spherical-cutoff methods for long-range forces in macromolecular simulation. Journal of Computational Chemistry, 15(7), 667–683. https://doi.org/10.1002/jcc.540150702

Sun, F., Dedong, H., Fei, L., Weiqiang, W., Zhaotao, G., & Zhuo, Z. (2022). Molecular-level investigation of plasticization of polyethylene terephthalate (PET) in supercritical carbon dioxide via molecular dynamics simulation. Royal Society Open Science, 9(8). https://doi.org/10.1098/rsos.220606

Sun, X., Wang, X., Sun, F., Tian, M., Qu, L., Perry, P., Owens, H., & Liu, X. (2023). Textile Waste Fiber Regeneration via a Green Chemistry Approach: A Molecular Strategy for Sustainable Fashion. Advanced Materials, 35(49). https://doi.org/10.1002/adma.202305224

Sun, Y., Yang, T., Ji, H., Zhou, J., Wang, Z., Qian, T., & Yan, C. (2020). Boosting the Optimization of Lithium Metal Batteries by Molecular Dynamics Simulations: A Perspective. Advanced Energy Materials, 10(41). https://doi.org/10.1002/aenm.202002373

Suter, J. L., Müller, W. A., Vassaux, M., Anastasiou, A., Simmons, M., Tilbrook, D., & Coveney, P. V. (2025). Rapid, Accurate and Reproducible Prediction of the Glass Transition Temperature Using Ensemble-Based Molecular Dynamics Simulation. Journal of Chemical Theory and Computation, 21(3), 1405–1421. https://doi.org/10.1021/acs.jctc.4c01364

Szafran, K., Jurak, M., Mroczka, R., & Wiącek, A. E. (2022). Surface Properties of the Polyethylene Terephthalate (PET) Substrate Modified with the Phospholipid-Polypeptide-Antioxidant Films: Design of Functional Biocoatings. Pharmaceutics, 14(12), 2815. https://doi.org/10.3390/pharmaceutics14122815

Tamnanloo, J., & Tsige, M. (2024). All-atom molecular dynamics simulation of solvent diffusion in an unentangled polystyrene film. Soft Matter, 20(26), 5195–5202. https://doi.org/10.1039/D4SM00641K

Tan, S. (Johnathan), Do, D. D., & Nicholson, D. (2020). Consistency of NVT, NPT, μVT and Gibbs (NV2T and NPT) with kinetic Monte Carlo schemes. Chemical Engineering Journal, 401, 126056. https://doi.org/10.1016/j.cej.2020.126056

Tashrifi, Z., Khanaposhtani, M. M., Larijani, B., & Mahdavi, M. (2020). Dimethyl Sulfoxide: Yesterday's Solvent, Today's Reagent. Advanced Synthesis & Catalysis, 362(1), 65–86. https://doi.org/10.1002/adsc.201901021

Textile Exchange. (2021, April). Preferred Fiber & Materials 2020 - Textile Exchange Market Report. Textile Exchange. https://textileexchange.org/app/uploads/2021/04/Textile-Exchange_Preferred-Fiber-Material-Market-Report_2020.pdf

Textile Exchange. (2024, September 26). Materials Market Report 2024 (September Edition). Textile Exchange. https://textileexchange.org/knowledge-center/reports/materials-market-report-2024/

Textile Exchange. (2025, September 18). Materials Market Report 2025 (September Edition). Textile Exchange. https://textileexchange.org/knowledge-center/reports/materials-market-report-2025/

Thompson, A. P., Aktulga, H. M., Berger, R., Bolintineanu, D. S., Brown, W. M., Crozier, P. S., in 't Veld, P. J., Kohlmeyer, A., Moore, S. G., Nguyen, T. D., Shan,

R., Stevens, M. J., Tranchida, J., Trott, C., & Plimpton, S. J. (2022). LAMMPS - a flexible simulation tool for particle-based materials modeling at the atomic, meso, and continuum scales. Computer Physics Communications, 271, 108171. https://doi.org/10.1016/j.cpc.2021.108171

Townsend, P. A. (2024). Adsorption in Action: Molecular Dynamics as a Tool to Study Adsorption at the Surface of Fine Plastic Particles in Aquatic Environments. ACS Omega, 9(5), 5142–5156. https://doi.org/10.1021/acsomega.3c07488

Valdés-Tresanco, M. S., Valdés-Tresanco, M. E., Valiente, P. A., & Moreno, E. (2021). gmx_MMPBSA: A New Tool to Perform End-State Free Energy Calculations with GROMACS. Journal of Chemical Theory and Computation, 17(10), 6281–6291. https://doi.org/10.1021/acs.jctc.1c00645

Validating empirical force fields for molecular-level simulation of cellulose dissolution. (n.d.).

van Gunsteren, W. F., & Mark, A. E. (1998). Validation of molecular dynamics simulation. The Journal of Chemical Physics, 108(15), 6109–6116. https://doi.org/10.1063/1.476021

Vidal, R., Alberola-Borràs, J.-A., Habisreutinger, S. N., Gimeno-Molina, J.-L., Moore, D. T., Schloemer, T. H., Mora-Seró, I., Berry, J. J., & Luther, J. M. (2020). Assessing health and environmental impacts of solvents for producing perovskite solar cells. Nature Sustainability, 4(3), 277–285. https://doi.org/10.1038/s41893-020-00645-8

Vieira, I. H. P., Botelho, E. B., de Souza Gomes, T. J., Kist, R., Caceres, R. A., & Zanchi, F. B. (2023). Visual dynamics: a WEB application for molecular dynamics simulation using GROMACS. BMC Bioinformatics, 24(1), 107. https://doi.org/10.1186/s12859-023-05234-y

Villar, L., Pita, M., González, B., & Sánchez, P. B. (2024). Hydrolytic-Assisted Fractionation of Textile Waste Containing Cotton and Polyester. Fibers and Polymers, 25(7), 2763–2772. https://doi.org/10.1007/s12221-024-00602-8

Villar, L., Schlapp-Hackl, I., Sánchez, P. B., & Hummel, M. (2024). High-Quality Cellulosic Fibers Engineered from Cotton–Elastane Textile Waste. Biomacromolecules, 25(3), 1942–1949. https://doi.org/10.1021/acs.biomac.3c01366

Wan, S., Sinclair, R. C., & Coveney, P. V. (2021). Uncertainty quantification in classical molecular dynamics. Philosophical Transactions of the Royal Society A:

Mathematical, Physical and Engineering Sciences, 379(2197), rsta.2020.0082. https://doi.org/10.1098/rsta.2020.0082

Wang, B., Gao, H., Wu, H., Wu, Y., Ren, B., Liu, X., & Nie, Y. (2024). Diffusion coefficients during regenerated cellulose fibers formation using ionic liquids as solvents: Experimental investigation and molecular dynamics simulation. Chemical Engineering Journal, 488, 151175. https://doi.org/10.1016/j.cej.2024.151175

Wang, J., & Voulgarakis, N. K. (2024). Hierarchically Coupled Ornstein–Uhlenbeck Processes for Transient Anomalous Diffusion. Physics, 6(2), 645–658. https://doi.org/10.3390/physics6020042

Wang, N., Pei, C., Zhong, Y., Zhang, Y., Liu, X., Hou, J., Yuan, Y., & Zhang, R. (2024). Molecular Dynamics Simulation of the Compatibility Between Supercritical Carbon Dioxide and Coating Resins Assisted by Co-Solvents. Materials, 17(24), 6271. https://doi.org/10.3390/ma17246271

Wang, X., Zheng, W., Guo, Z., Nawaz, H., You, T., Li, X., & Xu, F. (2023). Rheological characteristics of novel cellulose/superbase-derived ionic liquid solutions and the coagulation process towards regenerated cellulose films. Green Chemistry, 25(4), 1597–1610. https://doi.org/10.1039/D2GC03278C

Wang, Y. (2010). Fiber and textile waste Utilization. Waste and Biomass Valorization, 1(1), 135–143. https://doi.org/10.1007/s12649-009-9005-y

Wang, Y., Wang, W., Zhang, Z., Xu, L., & Li, P. (2016a). Study of the glass transition temperature and the mechanical properties of PET/modified silica nanocomposite by molecular dynamics simulation. European Polymer Journal, 75, 36–45. https://doi.org/10.1016/j.eurpolymj.2015.11.038

Wang, Y., Wang, W., Zhang, Z., Xu, L., & Li, P. (2016b). Study of the glass transition temperature and the mechanical properties of PET/modified silica nanocomposite by molecular dynamics simulation. European Polymer Journal, 75, 36–45. https://doi.org/10.1016/j.eurpolymj.2015.11.038

Wei, J., Long, Y., Li, T., Gao, H., & Nie, Y. (2024). Exploring hydrogen-bond structures in cellulose during regeneration with anti-solvent through two-dimensional correlation infrared spectroscopy. International Journal of Biological Macromolecules, 267, 131204. https://doi.org/10.1016/j.ijbiomac.2024.131204

Welle, F. (2021). Diffusion Coefficients and Activation Energies of Diffusion of Organic Molecules in Polystyrene below and above Glass Transition Temperature. Polymers, 13(8), 1317. https://doi.org/10.3390/polym13081317

Wilkie, C. A. (1999). TGA/FTIR: an extremely useful technique for studying polymer degradation. Polymer Degradation and Stability, 66(3), 301–306. https://doi.org/10.1016/S0141-3910(99)00054-3

Winterton, N. (2021). The green solvent: a critical perspective. Clean Technologies and Environmental Policy, 23(9), 2499–2522. https://doi.org/10.1007/s10098-021-02188-8

Wojnowska-Baryła, I., Bernat, K., & Zaborowska, M. (2022). Strategies of Recovery and Organic Recycling Used in Textile Waste Management. International Journal of Environmental Research and Public Health, 19(10), 5859. https://doi.org/10.3390/ijerph19105859

Wu, C. (2020). Molecular-weight dependence of simulated glass transition temperature for isolated poly(ethylene oxide) chain. Molecular Simulation, 46(10), 727–735. https://doi.org/10.1080/08927022.2020.1763986

Wu, H., Long, Y., Wang, B., Cao, R., Yang, R., Gao, H., & Nie, Y. (2024). Design and synthesis of novel ionic liquids for the dissolution and separation of waste poly-cotton fabrics. Biomass and Bioenergy, 191, 107444. https://doi.org/10.1016/j.biombioe.2024.107444

Wu, H., Wang, B., Li, T., Wu, Y., Yang, R., Gao, H., & Nie, Y. (2023). Efficient recycle of waste poly-cotton and preparation of cellulose and polyester fibers using the system of ionic liquid and dimethyl sulfoxide. Journal of Molecular Liquids, 388, 122757. https://doi.org/10.1016/j.molliq.2023.122757

Wu, J., Zhong, Y., Kang, H., & Liu, R. (2025). Mechanism of dissolution of cellulose in quaternary ammonium phosphate/dimethyl sulfoxide. Carbohydrate Polymers, 352, 123167. https://doi.org/10.1016/j.carbpol.2024.123167

Wu, W., Fan, B., Zhou, Q., Zhao, Q., Zhong, Y., Xu, H., Wang, J., & Mao, Z. (2024). Distribution of disperse dyes between supercritical CO2 and polyester fibers: A combined molecular dynamics simulation and experimental study. Journal of Cleaner Production, 481, 144162. https://doi.org/10.1016/j.jclepro.2024.144162

Wu, Y., Che, Y., Wei, X., Hu, Q., Xu, J., Guo, B., & Niu, Z. (2024). Nondestructive Recovery of Cotton from Waste Polycotton Textiles by Catalytic Hydrolysis.

ACS Sustainable Chemistry & Engineering, 12(28), 10446–10454. https://doi.org/10.1021/acssuschemeng.4c02547

Xiang, J., Gao, Q., & Wu, A. (2017). The Applications of DMSO. In Solvents as Reagents in Organic Synthesis (pp. 315–353). Wiley. https://doi.org/10.1002/9783527805624.ch7

Xie, R., Weisen, A. R., Lee, Y., Aplan, M. A., Fenton, A. M., Masucci, A. E., Kempe, F., Sommer, M., Pester, C. W., Colby, R. H., & Gomez, E. D. (2020). Glass transition temperature from the chemical structure of conjugated polymers. Nature Communications, 11(1), 893. https://doi.org/10.1038/s41467-020-14656-8

Xiong, R., Zhang, X., Tian, D., Zhou, Z., & Lu, C. (2012). Comparing microcrystalline with spherical nanocrystalline cellulose from waste cotton fabrics. Cellulose, 19(4), 1189–1198. https://doi.org/10.1007/s10570-012-9730-4

Xu, A., Chen, L., Wang, Y., Liu, R., & Niu, W. (2019a). Development of Diallylimidazolium Methoxyacetate/DMSO (DMF/DMA) Solvents for Improving Cellulose Dissolution and Fabricating Porous Material. Polymers, 11(5), 845. https://doi.org/10.3390/polym11050845

Xu, A., Chen, L., Wang, Y., Liu, R., & Niu, W. (2019b). Development of Diallylimidazolium Methoxyacetate/DMSO (DMF/DMA) Solvents for Improving Cellulose Dissolution and Fabricating Porous Material. Polymers, 11(5), 845. https://doi.org/10.3390/polym11050845

Xu, Z., Qi, R., Xiong, M., Zhang, D., Gu, H., & Chen, W. (2021). Conversion of cotton textile waste to clean solid fuel via surfactant-assisted hydrothermal carbonization: Mechanisms and combustion behaviors. Bioresource Technology, 321, 124450. https://doi.org/10.1016/J.BIORTECH.2020.124450

Yamamoto, T., Hussain, M. A., & Yao, S. (2022). Material Property Recovery by Controlling the Melt Memory Effects on Recrystallization and on Crystal Deformation: An Approach by the Molecular Dynamics Simulation for Polyethylene. Polymers, 14(15), 3082. https://doi.org/10.3390/polym14153082

Yan, Z., Lian, J., Li, M., Meng, L., Zhang, Y., Ge, C., & Lu, J. (2020). Deeper insight into hydrolysis mechanisms of polyester/cotton blended fabrics for separation by explicit solvent models. International Journal of Biological Macromolecules, 154, 596–605. https://doi.org/10.1016/j.ijbiomac.2020.03.130

Yang, J., Zhu, Z., Huang, D., & Cao, Q. (2020). Thermodynamic and structural properties of polystyrene/C 60 composites: A molecular dynamics study*. Chinese Physics B, 29(2), 023104. https://doi.org/10.1088/1674-1056/ab6312

Yang, K., Wang, M., Wang, X., Shan, J., Zhang, J., Tian, G., Yang, D., & Ma, J. (2024). Polyester/Cotton-Blended Textile Waste Fiber Separation and Regeneration via a Green Chemistry Approach. ACS Sustainable Chemistry and Engineering, 12(11), 4530–4538. https://doi.org/10.1021/acssuschemeng.3c07707

Yasin, S., Curti, M., Rovero, G., Behary, N., Perwuelz, A., Giraud, S., Migliavacca, G., Chen, G., & Guan, J. (2017). An alternative for the end-of-life phase of flame retardant textile products: Degradation of flame retardant and preliminary settings of energy valorization by gasification. BioResources, 12(3), 5196–5211. https://doi.org/10.15376/biores.12.3.5196-5211

Yong, L., Jian, L., Xian, L., & Bei, W. (2021). Test and analysis of the porosity of cotton fiber assembly. Journal of Engineered Fibers and Fabrics, 16. https://doi.org/10.1177/15589250211024225

Yousef, S., Tatariants, M., Tichonovas, M., Kliucininkas, L., Lukošiūtė, S. I., & Yan, L. (2020). Sustainable green technology for recovery of cotton fibers and polyester from textile waste. Journal of Cleaner Production, 254. https://doi.org/10.1016/j.jclepro.2020.120078

Zhang, F., Wang, H., Zhao, Q., He, J., & Dong, X. (2025). Efficient color management in closed-loop recycling of cotton fabrics by using fiber modification and salt-free dyeing strategy. Journal of Cleaner Production, 491, 144865. https://doi.org/10.1016/j.jclepro.2025.144865

Zhang, J., Tominaga, K., Yamagishi, N., & Gotoh, Y. (2020). Comparison of Regenerated Cellulose Fibers Spun from Ionic Liquid Solutions with Lyocell Fiber. Journal of Fiber Science and Technology, 76(8), 257–266. https://doi.org/10.2115/fiberst.2020-0029

Zhang, L., Wang, P., Yang, Z., Du, F., Li, Z., Wu, C., Fang, A., Xu, X., & Zhou, G. (2020). Molecular dynamics simulation exploration of the interaction between curcumin and myosin combined with the results of spectroscopy techniques. Food Hydrocolloids, 101, 105455. https://doi.org/10.1016/j.foodhyd.2019.105455

Zhang, Q., Mao, J., Liao, Y., Mao, J., Yang, X., Lin, C., Wang, Q., Huang, Z., Xu, T., Liu, B., Xiao, Y., & Zhang, Y. (2022). Salt resistance study and molecular dynamics simulation of hydrophobic-association polymer with internal salt

structure. Journal of Molecular Liquids, 367, 120520. https://doi.org/10.1016/j.molliq.2022.120520

Zhang, T., Zhai, Y., Ma, X., Shen, X., Bai, Y., Zhang, R., Ji, C., & Hong, J. (2021). Towards environmental sustainability: Life cycle assessment-based water footprint analysis on China's cotton production. Journal of Cleaner Production, 313, 127925. https://doi.org/10.1016/j.jclepro.2021.127925

Zhang, X., Zhou, W., Xing, W., Xu, Y., & Zhang, G. (2025a). Efficient Recovery of Waste Cotton Fabrics Using Ionic Liquid Methods. Polymers, 17(7), 900. https://doi.org/10.3390/polym17070900

Zhang, X., Zhou, W., Xing, W., Xu, Y., & Zhang, G. (2025b). Efficient Recovery of Waste Cotton Fabrics Using Ionic Liquid Methods. Polymers, 17(7), 900. https://doi.org/10.3390/polym17070900

Zhang, Y., Wang, Y., Li, Y., & Zhang, Z. (2019). The Mechanical Properties of Poly (Urea-Formaldehyde) Incorporated with Nano-SiO2 by Molecular Dynamics Simulation. Polymers, 11(9), 1447. https://doi.org/10.3390/polym11091447

Zhao, H., Wang, H., Wang, M., Bai, P., Tan, L., Xiong, X., & Zheng, L. (2022). A recyclable anhydrous cotton dyeing technology with low energy consumption and excellent dyeing effects by mixing supercritical carbon dioxide, ethanol, and dimethyl sulfoxide. Journal of Cleaner Production, 367, 133034. https://doi.org/10.1016/j.jclepro.2022.133034

Zheng, J., Wang, D., Zhang, Q., Song, M., Jiao, M., & Zhang, Z. (2022). Molecular Dynamics Simulation and Structure Changes of Polyester in Water and Non-Aqueous Solvents. Materials, 15(6). https://doi.org/10.3390/ma15062148

Zheng, T., Li, T., Shi, J., Wu, T., Zhuang, Z., Xu, J., & Guo, B. (2022). Molecular Insight into the Toughness of Polyureas: A Hybrid All-Atom/Coarse-Grained Molecular Dynamics Study. Macromolecules, 55(8), 3020–3029. https://doi.org/10.1021/acs.macromol.1c02453

Zheng, W., Liu, C., Wei, X., Sun, W., & Zhao, L. (2023). Molecular-level swelling behaviors of poly (ethylene terephthalate) glycolysis using ionic liquids as catalyst. Chemical Engineering Science, 267, 118329. https://doi.org/10.1016/j.ces.2022.118329

Zhenova, A. (2020). Challenges in the development of new green solvents for polymer dissolution. Polymer International, 69(10), 895–901. https://doi.org/10.1002/pi.6072

Zhong-Johnson, E. Z. L., Dong, Z., Canova, C. T., Destro, F., Cañellas, M., Hoffman, M. C., Maréchal, J., Johnson, T. M., Zheng, M., Schlau-Cohen, G. S., Lucas, M. F., Braatz, R. D., Sprenger, K. G., Voigt, C. A., & Sinskey, A. J. (2024). Analysis of Poly(ethylene terephthalate) degradation kinetics of evolved IsPETase variants using a surface crowding model. Journal of Biological Chemistry, 300(3), 105783. https://doi.org/10.1016/j.jbc.2024.105783

Zhou, C., & Wang, Y. (2021a). Recycling of waste cotton fabrics into regenerated cellulose films through three solvent systems: A comparison study. Journal of Applied Polymer Science, 138(48). https://doi.org/10.1002/app.51255

Zhou, C., & Wang, Y. (2021b). Recycling of waste cotton fabrics into regenerated cellulose films through three solvent systems: A comparison study. Journal of Applied Polymer Science, 138(48). https://doi.org/10.1002/app.51255

Zhou, P., Yu, J., Sánchez-Rivera, K. L., Huber, G. W., & Van Lehn, R. C. (2023). Large-scale computational polymer solubility predictions and applications to dissolution-based plastic recycling. Green Chemistry, 25(11), 4402–4414. https://doi.org/10.1039/D3GC00404J

AUTHOR'S PROFILE

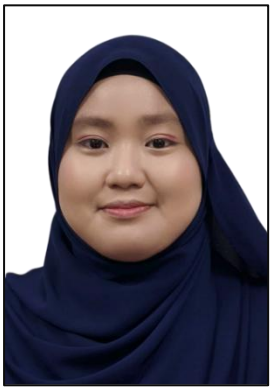

Nur Ummul Waliyyatullah Binti Muhammad Faez Tan graduated with a Diploma in Chemical Engineering from Universiti Teknologi MARA (UiTM) Cawangan Pasir Gudang, Johor in 2020, and later obtained her Bachelor of Chemical Engineering (Environment) with Honours from UiTM Cawangan Permatang Pauh, Penang in 2024. Her academic background interest in multiple areas of chemical engineering, including renewable energy, process safety, and sustainable materials development. Her diploma final year project focused on the production of biofuels as a clean and renewable energy source. During her bachelor degree studies, she concentrated on industrial risk assessment by integrating ALOHA simulation and index-based methodologies to improve safety in chemical processes. Her current research was interest on environmental sustainability specifically textile waste recycling. Through a combination of computational simulation and experimental methodology, her study contributed in understanding fibre dissolution behavior in green solvents, reinforcing the circular economy approach in the textile sector. Waliyyatullah's once achieved a Silver Medal at the Science Invention & Innovation Competition (SIIC) 2024, held at UiTM Permatang Pauh for her bachelor degree project. Her future research interests include green technology, computational modelling, sustainable process engineering, and advanced functional materials.

LIST OF PUBLICATION:

1. Muhammad Faez Tan, N. U. W., Muhammad, A., Azmi, I. S., Roslan, A., & Abu Bakar, N. F. (2026). Effect of Anti-Solvent in the Regeneration of Cotton from Cotton/DMSO Solution. Advances in Science and Technology, 175, 189–195. https://doi.org/10.4028/p-b8vldn
2. Muhammad Faez Tan, N. U. W., Azmawi, F. S., Mohamad, N., Azmi, I. S., Roslan, A., Abu Bakar, N. F., & Muhammad, A. (2026). Sustainability in Textiles: Life Cycle Assessment of Polyester and Cotton Production with Dissolution Recycling Pathways. PaperASIA, 42(1b). https://doi.org/10.59953/paperasia.v42i1b.815

LIST OF CONFERENCES:

1. 4th International Conference on Semiconductor Materials and Technology (ICoSeMT 2025): Preliminary Study of Dissolution Recycled Textile Using Dimethyl Sulfoxide: Effect of Temperature
2. 9th International Conference on Fuel Cell & Hydrogen Technology (ICFCHT 2025): Molecular Dynamics Simulation Study on The Effect of Temperature during Dissolution Cellulose and Polyester (Textile Waste) in Dimethyl Sulfoxide
3. 9th International Conference on Materials Engineering and Applications (ICMEA 2026): Effect of Anti-Solvent in the Regeneration of Cotton from Cotton/DMSO Solution

LIST OF PENDING PUBLICATION:

1. L9 Orthogonal Validation on the Dissolution Behavior of Recycled Cotton and Polyester in Pure DMSO from Molecular Dynamics Simulation Prediction, (WoS, Scopus) – Accepted
2. Molecular Dynamics Simulation Study on The Effect of Temperature during Dissolution Cellulose and Polyester (Textile Waste) in Dimethyl Sulfoxide, Springer Proceedings in Physics (Scopus) – Accepted
3. Molecular Interaction Study for Solvent-Polymer Interactions in Dissolution: A Systematic Review, Structural Chemistry, (WoS, Scopus) – Under Review